

AD-A035 076

SINGER LIBRASCOPE GLENDALE CALIF  
DISPLAY MATERIALS EVALUATION PROGRAM. (U)  
DEC 75 M R SMITH

F/G 9/5

N00173-75-C-0492

NL

UNCLASSIFIED

1 OF 2  
AD-A  
035 076



U.S. DEPARTMENT OF COMMERCE  
National Technical Information Service

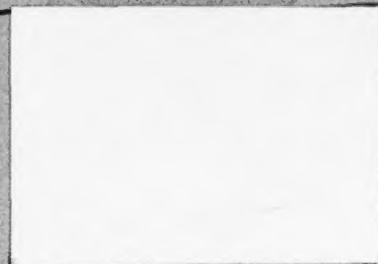
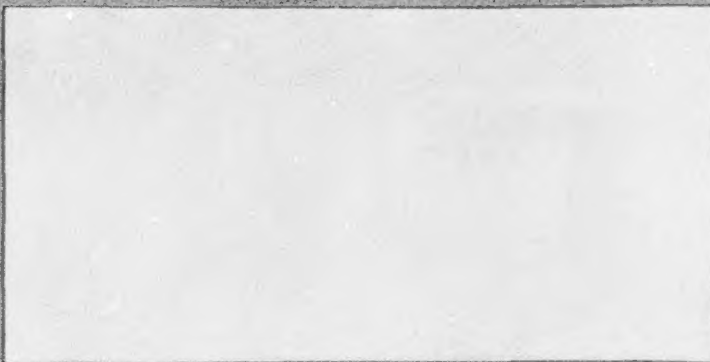
AD-A035 076

DISPLAY MATERIALS EVALUATION PROGRAM

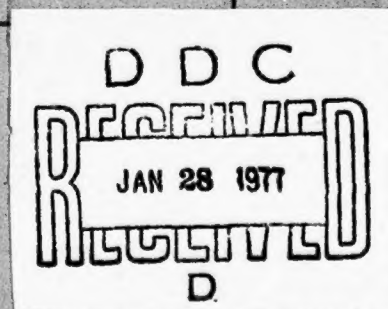
SINGER COMPANY  
GLENDALE, CALIFORNIA

DECEMBER 1975

ADA035076



# LIBRASCOPE DIVISION



**SINGER**  
AEROSPACE & MARINE SYSTEMS

APPROVED FOR PUBLIC RELEASE  
DISTRIBUTION UNLIMITED

*Handwritten signature or initials.*

DISPLAY MATERIALS EVALUATION  
PROGRAM

M. R. Smith, Principal Investigator

Final Report

Contract No. N00173-75-C-0492 *New*

December 1975

**SINGER**  
LIBRASCOPE DIVISION

833 Sonora Ave.  
Glendale, CA 91201

APPROVED FOR PUBLIC RELEASE  
DISTRIBUTION UNLIMITED

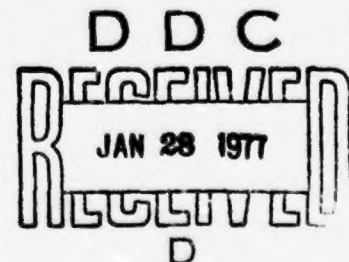


## TABLE OF CONTENTS

1.0	Scope . . . . .	1
1.1	Statement of the Problem . . . . .	1
1.2	Objective . . . . .	1
1.3	Technical Approach . . . . .	2
1.4	Summary of Results . . . . .	2
2.0	Definition and Procedures . . . . .	5
2.1	Display Parameter Definitions . . . . .	5
2.2	Threshold Display Parameters . . . . .	12
2.3	(Not Used)	
2.4	(Not Used)	
2.5	Holographic Terminology . . . . .	17
2.6	Classes of Display Materials . . . . .	18
2.7	Optical Data Processing . . . . .	23
3.0	Materials Survey . . . . .	25
3.1	Introduction . . . . .	25
3.2	Deformable Target Materials . . . . .	28
3.3	Magneto-Optic Materials . . . . .	33
3.4	Liquid Crystals . . . . .	36
3.5	Ferroelectric-Photoconductor (FE-PC) . . . . .	42
3.6	Other FE-PC Crystals . . . . .	46
3.7	Pockels Effect Crystals . . . . .	48
3.8	Thick Ferroelectrics . . . . .	54
3.9	Magnetic Bubbler . . . . .	55
3.10	Metal Films . . . . .	56
3.11	Amorphous Materials . . . . .	56
3.12	Photochromic and Photodichroic Materials . . . . .	57
3.13	Summary . . . . .	61
3.14	Conclusions . . . . .	63
3.15	Appendices . . . . .	63



## TABLE OF CONTENTS (Continued)

4.0	Experimental Measurements in NaF . . . . .	71
4.1	Photodichroism Characteristics . . . . .	71
4.2	Resolution Characteristics . . . . .	71
5.0	Ultra High Resolution Display System Concepts . . . . .	75
5.1	Overall System Description UHRRDS . . . . .	75
5.2	Controller Section (UHRRDC) . . . . .	75
5.3	Recorder-Display Section (UHRRD) . . . . .	96
5.4	Image Uniformity Considerations . . . . .	118
5.5	Recording Gray Level Considerations . . . . .	121

## 1.0 · SCOPE

This document summarizes the results of a research program to evaluate the applicability of available materials for use as the display media in a sonar data signal processing/interactive display system.

### 1.1 DESCRIPTION OF THE PROBLEM

An increasing requirement exists for faster data processing/display systems to handle the vast quantities of data generated from military surveillance and countermeasure activities.

The computer controlled display facilitates optimum human interaction with automated combat, command and control, and military information-handling systems. Increasingly sophisticated requirements and new military concepts necessitate continuously-update, advanced hardware technology to ensure the timely effective evaluation and implementation of these concepts.

The man-machine interface has become increasingly important in the critical need for providing an adequate data display for command and control decision-making processes.

### 1.2 RESEARCH PROGRAM OBJECTIVES

The research program has three principal objectives:

- (1) To evaluate available optical storage and recording materials for use as display media with application to sonar surveillance signal processing/interactive displays.
- (2) To develop preliminary display system concepts for use with sonar surveillance/human operator decision making processes.
- (3) To recommend future materials research and development directions commensurate with future signal processing/display requirements.

### 1.3 TECHNICAL APPROACH

The technical approach for meeting the objectives of the study program was to:

- (1) perform a literature survey to determine currently available optical storage and recording materials in order to evaluate the material characteristics in the context of the defined display requirements and to summarize the appropriate characteristics of the various materials,
- (2) perform an experimental investigation of the display properties of promising and available material candidates,
- (3) and to develop preliminary display system concepts for use with sonar surveillance/human operator decision making processes.

Throughout the study program, the various technical tasks were closely coordinated with ongoing Librascope IR&D programs in the areas of Naval Systems Technology and Display Technology.

### 1.4 TECHNICAL PROGRAM

The technical approach to the research program was carried out through three program tasks:

Task 1, Material Evaluation Study; Task 2, Display Parameters Measurement; and Task 3, Display System Concepts.

The materials were chosen for evaluation in the context of being a potential candidate display material for a B-Format display system which is defined as follows:

- (1) Continuous tone imagery
- (2) 5000 pixels per inch
- (3) up to 4 inches x 4 inches display surface
- (4) ability to superimpose alphanumeric and dynamic cursor information
- (5) permanent and/or selective write and erase



- (6) line scan rate in B- scan mode, .5 to 51/sec
- (7) 8 - 16 grey level dynamic range
- (8) greater than 10:1 contrast ratio
- (9) near instantaneous imagery (less than 5 minutes image processing delay)
- (10) Projection display formats:
  - a) 9" single channel
  - b) optical zoom, multichannel
  - c) rapid sequencing, motion picture frame rates
  - d) holographic display format.

#### Task 1 - Material Evaluation Study

Available optical storage and recording materials were studied to determine their applicability in a "B Format", multichannel display system, as defined previously. A "B Format" is defined as a continuous tone, amplitude modulated recording.

A literature survey was made to determine the characteristics of suitable materials. A compilation and summary was made of the display-oriented characteristics of all appropriate materials which are available in the literature search. The following material characteristics were measured and surveyed:

- a) Resolution
- b) contrast ratio
- c) erasability
- d) fatigue life
- e) spectral sensitivity
- f) spectral transmissivity
- g) reflectivity
- h) image permanence
- i) availability, cost, lead time
- j) diffraction efficiency (applicable to holographic recording materials only)

## Task 2 - Display Parameter Measurements

Na F photodichroic material was selected as a promising write/erase material for the ultrahigh resolution recording display system. Measurements were made on various samples of Na F material to determine the spectral sensitivity, spectral transmissivity, imaging resolution, and other related recording/display oriented parameters.

## Task 3 - Display System Concept

A preliminary display system concept was developed. An ultrahigh resolution recording-display device was devised. The device provides a line scan, waterfall display format of 20,000 pixels per line scan. A projection optical system provides single operator viewing of variable magnification. Annotation and supplementary graphical information is provided on the viewing screen by means of a superimposed graphical CRT.

### 1.5 SUMMARY

Section 2.0 presents definitions of the various terms and parameters used in the data display terminology. A brief discussion of optical display techniques is presented along with a general discussion of classes of display materials.

Section 3.0 presents the results of the display materials survey. Photodichroic material such as Na F and KD\*P electro-optical material appear to be excellent candidates for the present recording-display requirement.

Section 4.0 summarizes the results of experimental measurements which were made with Na F crystal samples.

Section 5.0 describes a system concept for an ultrahigh resolution recording display system with reusable recording material. Many of the critical optical components of the system, such as the projection lenses and the recording lens, have been preliminarily designed. Design summaries are presented.

## 2.0 DEFINITIONS AND PROCEDURES

### 2.1 DISPLAY PARAMETER DEFINITIONS

Various display related parameters and the symbols used to represent them will be defined in this section.

Photometry is the quantitative measurement of radiant flux in relation to its ability to evoke the psychological sensation of brightness (1). Radiometry is the purely physical measure of the radiated power and energy that produces the luminous flux (1). The associated parameters, their standard symbols, and MKS units are listed below:

#### RADIOMETRIC PARAMETERS (1)

<u>Name</u>	<u>Symbol</u>	<u>MKS Units</u>
Radiant energy	U	Joule
Radiant flux	P	Watt
Radiant emittance	W	Watt/m <sup>2</sup>
Radiant intensity	J	Watt/steradian $\omega$
Radiance	N	Watt/ $\omega$ .m <sup>2</sup>
Irradiance	H	att/m <sup>2</sup>

#### PHOTOMETRIC PARAMETERS (1)

<u>Name</u>	<u>Symbol</u>	<u>MKS Units</u>
Luminous energy	Q	Talbot
Luminous flux	F	Lumen
Luminous emittance	L	Lumen/m <sup>2</sup>
Luminous intensity	I	(Lumen/ $\omega$ ) = Candela
Luminance	B	Lumen/ $\omega$ .m <sup>2</sup> = Candela/m <sup>2</sup>
Illuminance	E	(Lumen/m <sup>2</sup> ) = Lux

At 555nm, one watt = 680 lumens

Table 1. Radiometric and Photometric Parameters

- (1) Fundamentals fo Display System Design, Sol Sherr, Wiley, NY, 1970.
- (2) NRL Memo Report 2657, AD767644, Survey of Solid State Reflective/Transmissive Display Media, D. L. Mitchell and L. A. Rauber, September, 1973

Luminous flux (F) is the time rate of flow of light.

Lumen is the units of F. Its dimensions are power.

Luminous energy (Q) is F times time.

Luminous intensity (I) is  $dF/d\omega = F/4\pi$  (for uniform flux).

Candela is the unit of I

Illumination or Illuminance (E) is

where D is the distance from the source,  $I_0$  is its total intensity, F is the flux from  $I_0$  in the solid angle  $\Delta\omega$ , and A is the normal area intersected by  $\Delta\omega$ .

Luminance (B) is a photometric term. It is the ratio of the intensity of a surface A in any direction to the projection of A on a plane normal to that direction

$$B = \frac{dI}{dA \cos \alpha} = \frac{I}{A}$$

$\alpha$  = angle between direction and normal to surface. The second equation follows if the surface follows Lamberts Law,  $I = I_0 \cos \alpha$ .

Brightness is the related psychological perception. It is not the same as luminance B.

Luminous emittance (L) is F per area =  $F/A$  or  $\pi BA$  (where  $F = \omega I = \pi I$  (total) and  $I = BA$ ).

#### Contrast (C)

There are various versions of contrast C. Let:

$B_s$  = luminance of surroundings

$B_o$  = luminance of object

If  $B_s > B_o$ ,

$$C = (B_s - B_o)/B_s$$

If  $B_s < B_o$ ,

$$C = (B_o - B_s)/B_o$$

or in optical transfer function (OTF) use

$$C = (B_o - B_s)/(B_o + B_s)$$

and finally

$$C = \frac{B_{\max} - B_{\min}}{2(B_{\max} + B_{\min})}$$

#### Contrast Ratio (CR)

Contrast ratio (CR) also has two definitions. The most common is:

$$CR = \frac{B_{\max}}{B_{\min}} = \frac{B_s + B_o}{B_s}$$

In Reference (2), several alternate definitions are noted:

$$CR = \frac{R_{on} - R_{off}}{R_{off}}$$

where R is reflectance, T is transmittance and the subscripts refer to on and off states and

$$CR = \frac{T_{on} - T_{off}}{T_{off}}$$

These differ from those above (3) in the use of a minus sign in the numerator.

Ambient illumination conditions affect the actual observed contrast ratio on the viewing screen. The effect of ambient illumination, BA, can be accounted for by redefining equation p6 with an effective surrounding luminance  $B_s'$ , and object illumination  $B_o'$

- (3) R. Kuehn, "Display Requirements for Command and Control Systems", Information Display, 3, No. 6, Nov/Dec 1966, p. 44.



where  $B_s' = B_s + B_A$

and  $B_o' = B_o + B_A$

then the contrast ratio becomes.

$$CR = \frac{B_s' + B_o'}{B_s'}$$

The effect of ambient illumination can be minimized by various techniques, such as shading the viewing screen, using antiglare screens, and using rear projected screens with absorptive outer coatings.

#### Dynamic Range (DR)

Dynamic range (DR) is a measure of the shades of gray possible. It is directly related to CR by

$$DR = \log_2 CR$$

#### Resolution

Resolution is probably the most confusing parameter in display systems with numerous definitions and methods of measurement used.

The optical line pair refers to one dark and one white line of equal width. The luminance profile is considered to be rectangular with a dark line and half a white line on each side.

The CRT spot brightness tends to follow a Gaussian distribution. The line width must thus be specified at a particular luminance level such as half the peak illuminance.

For example, 1000 TV limiting response lines = 416 optical line pairs but not the reverse. The shrinking raster technique = 590 lines (The lines usually merge at 60% of peak illuminance). The MTF or sine wave response gives 800 lines (if the 10% response point is used) or 440 lines (if the 50% point is used). Shrinking raster and TV limiting resolution depend on the characteristics of the observer. Other techniques are more objective. The slit scan method measures line profile directly, MTF measures spatial frequency response which is related to line profile.

Visual acuity (V) is the ability to discriminate fine detail in the field of view. With  $D'$  = a standard viewing distance and D the distance at which the

minimum discernable test object subtends 1 min of arc (a width of 5 nm on the retina)  $V = D'/D$ .

The table below (4) relates these various resolution criteria.

To Convert from to multiply by	TV	10%	TV <sub>50</sub>	Shrink Raster	50% Amp	50% MTF	Opt 1/e	N <sub>e</sub>
TV limiting	-	0.80	0.71	0.59	0.5	0.44	0.42	0.33
10% MTF	1.25	--	0.88	0.74	0.62	0.55	0.52	0.42
TV <sub>50</sub> (3dB)	1.4	1.14	--	0.84	0.71	0.63	0.59	0.47
Shrinking Raster	1.7	1.36	1.2	--	0.85	0.75	0.71	0.56
50% Amplitude	2.0	1.6	1.4	1.17	--	0.88	0.83	0.66
50% MTF	2.26	1.82	1.6	1.33	1.14	--	0.94	0.75
Optical (1/e)	2.4	1.94	1.7	1.4	1.2	1.06	--	0.80
Equivalent passband N Ne	3.0	2.4	2.1	1.77	1.5	1.33	1.25	--

Table 2. Relationship Between Various Resolution Criteria (4).

#### GRAY SCALE

If the maximum luminance  $B_{\max}$  or  $B_{\text{on}}$  (or alternately the transmittance or reflectance) can be adjusted to less than a fixed level, shades of gray or dynamic range for the display can be defined. Shades of gray are defined by various criteria.

Perhaps the most used definition of one gray level is a brightness change in a given area by a factor of  $\sqrt{2}$  from its prior value. The change in dB is then

$$\text{dB} = 10 \log (B_s/B_o)$$

where  $B_s$  and  $B_o$  are the screen highlight and background (brightness respectively). One gray level corresponds to a 1.5 dB brightness change or an optical density change of .15 OD. A given brightness change  $B_s/B_o$  corresponds to N gray levels where

$$\begin{aligned} N = \text{No. of gray levels} &= [10 \log (B_s/B_o)] / 1.5 \\ &= 6.6 \log (B_s/B_o) \end{aligned}$$

- (4) Slocum et al "Airborne Sensor Display Requirements and Approaches", Information Display, 4, No. 6, Nov/Dec 1968, page 45-6.

With contrast C defined as

$$C = (B_s - B_o)/B_o = (B_s/B_o) - 1$$

the number N of gray levels can be related to contrast C by

$$N = 6.6 \log (C + 1)$$

By these definitions, a contrast ratio of 10 corresponds to about 7,  $\sqrt{2}$  gray levels and a contrast ratio of 100 to about 14  $\sqrt{2}$  gray levels.

A more general measure of gray scale is to determine the maximum number of optical density levels that can be resolved in the system and specify the gray scale resolution criteria used. The density range D of a material is related to its CR by  $D = \log_{10} CR$  so that a CR = 10 corresponds to a density range of 1. The minimum gray level step is defined as the minimum resolvable optical density step which is obtainable with the particular recording material. The smallest  $\Delta D$  resolvable depends on the noise level and granularity of the material in a complex statistical fashion that is only well defined for photographic film. To distinguish 8 levels, each will differ by a  $\Delta D = 0.125$  (for 16 levels,  $\Delta D = 0.062$ ).

#### Sensitivity (S)

Sensitivity is the reciprocal of the exposure needed to change the output intensity by some amount (usually 10% or 1/e).

#### Linearity

In general, materials are not linear in output vs. exposure (at a given spatial frequency and modulation level) over their entire dynamic range. The output amplitude A can be related to the exposure E by a power series

$$A = T(a_0 + a_1 E + a_2 E^2 + \dots)$$

where  $T$  is a reference level of output illumination. For an exposure

$$E(x) = E_0 (1 + m \cos fx)$$

we obtain

$$\begin{aligned} A(x) = T [ & a_0 + a_1 E_0 + a_2 E_0^2 (1 + \frac{m^2}{2}) \\ & + m \cos fx (a_1 E_0 + 2a_2 E_0^2) \\ & + \frac{1}{2} a_2 E_0^2 m^2 \cos 2fx + \dots ] \end{aligned}$$

For phase modulation

$$\begin{aligned} A &= T \exp [i \phi(E)] \\ &= T [1 + i \phi(E) - \frac{1}{2} \phi^2(E) + \dots] \end{aligned}$$

If

$$\phi(E) = B_1 E + B_2 E^2 + \dots$$

$$A = T [1 + i B_1 E + (i B_2 + \frac{1}{2} B_1^2) E^2 + \dots]$$

thus, the response is not linear even if  $\phi(E)$  is linear and harmonic response results for  $B_2 = 0$ .

#### Diffraction Efficiency $\eta$

Materials that phase modulate light cannot be characterized by an MTF since the output modulation,  $m$

where

$$m = \frac{B_{\max} - B_{\min}}{B_{\max} + B_{\min}}$$

is zero. For such devices, diffraction efficiency  $\eta$  is used. With a sinusoid input of  $m = 1$ , the ratio of the first order diffracted light to the total light is  $\eta$ . Many devices have no response at zero spatial frequency. For such pass-band response device,  $\eta$  is also used since their MTF is not defined.

For amplitude modulating materials,  $\eta$  can be related to modulation  $m$  by

$$\eta = \frac{m^2}{4(1+m)^2}$$

and to MTF =  $M$  by

$$\eta = \frac{(1 - \sqrt{1 - m^2})^2}{8(1 + m + \sqrt{1 - m^2})^2}$$

For  $M = 1$  (100% modulation),  $\eta = 1/16$ . For small  $M$ ,  $\eta = \frac{m^2}{16}$

Thus, low  $\eta$  materials look much better when MTF rather than  $\eta$  is given.

Conversion from phase modulation to a visible display requires a phase contrast system of some sort.

## 2.2 THRESHOLD DISPLAY PARAMETERS

The threshold display parameters that each candidate display material to be evaluated must satisfy, follow, together with the symbology to be used, the desired definitions of each parameter, the desired accepted measurement technique to be used for each parameter, and some brief discussion of the reasons for each choice.



Resolution =  $R = 200 \text{ lines/mm} = 100 \text{ lp/mm}$ . This threshold value corresponds to a  $5 \mu\text{m}$  spot. This threshold value corresponds to a  $5 \mu\text{m}$  spot. This seems to be a reasonable system parameter that is achievable with laser beam deflections. Higher resolution materials are of course available, but a usable resolution limit of  $500 \text{ lines/mm}$  seems practical from system considerations in a point-by-point deflector. This would correspond to a  $2 \mu\text{m}$  spot.  $R = 200 \text{ lines/mm}$  requires a usable display material area of  $4'' \times 4''$  for a  $20,000 \times 20,000$  point or  $10,000$  line pairs  $\times 20,000$  lines display. This  $4'' \times 4''$  material size coupled with the  $100 \text{ lp/mm}$  are reasonable parameters. Higher resolution materials require less area and hence less laser beam uniting energy smaller projection optics, but a smaller spot size and therefore a lower f-number focus lens. Lower resolution materials conversely require larger area materials with associated greater demands on the laser power and projection systems, but a simplification of the focus lens. The space bandwidth product of the material system is thus provided as a useful overall parameter.

A useful definition for resolution is to specify it at a 50% MTF level ( $CR = 3$ ) and measured by the TV resolution method. In practice, available material data usually includes  $R$  measured at the visibility limit ( $MTF = 0.05 = 5\%$ ). Unless explicitly noted otherwise, it should be assumed that the  $R$  value is given at an  $MTF = 0.05$ . For some materials an MTF curve is available. This is the only recommended way of specifying contrast ratio and resolution.

Space Bandwidth Product =  $SBP = R = 20,000 \text{ lines}$ . See above discussion of  $R$ .

Contrast Ratio =  $CR = 10$ . This is the maximum  $CR$  at low resolution. Its variation with  $R$  (as in an MTF curve) should be provided.  $CR$  is defined as  $I_{\text{max}}/I_{\text{min}}$  where  $I_{\text{max}}$  and  $I_{\text{min}}$  are the maximum and minimum transmitted intensities through an on and off element in the display. It should be measured simultaneously with  $R$ . See shades of gray discussion also.

Dynamic Range =  $DR = \log_2 CR = \log_2 10 = 3.2$

Sensitivity =  $S$ . It is not possible to place a threshold value on  $S$  (units of  $\text{mJ/cm}^2$ ) other than to say that low values of  $S$  are desirable. With a 1 sec line scan time (minimum) and  $20,000$  points/line, the deflected laser beam is on each point for a maximum of  $50 \mu\text{sec}$ .

With a  $5 \times 5 \text{ } \mu\text{m}$  spot and  $50 \text{ } \mu\text{sec}$  dwell time  $T$ , a  $1 \text{ mW}$  focused laser spot corresponds to an incident energy density on the material of  $(1 \text{ mW}) (5 \times 10^{-5} \text{ sec}) / 25 \times 10^{-8} \text{ cm}^2 = 200 \text{ mJ/cm}^2$ . The display material must then have this sensitivity. If  $S$  is larger, a more intense laser must be used at an increased cost.

Additional considerations that must be noted when  $S$  is provided are the write wavelength band  $\lambda_w$  or the range of write wavelengths that can be used. Lasers of sufficient power and in the required wavelength band must be available. Whether the write beam must be polarized or not is an additional consideration since lasers with several lines and with circularly rather than linearly polarized outputs are more powerful. The scan rate of this specific sonar display is usually slow enough and all materials are sensitive enough that this is not a major factor.

Spectral Transmission Region =  $T = \text{Visible}$ . The display material must be transparent in the visible if a readout projection display is to result. If the readout modulation mechanism and the spectral transmission of the material allow for broadband readout light, then projection arc lamps rather than lasers and more brightness in the display are possible. If polarized readout light  $\lambda_R$  is necessary, this further reduces the available light reaching the display screen and requires a more intense and costly projection source as well as a polarizer.

Storage Time =  $T_s = 13 \text{ hours}$ . The  $10,000$  line display at the minimum  $5 \text{ sec/line}$  scan rate requires  $50,000 \text{ sec}$  or over  $13 \text{ hours}$  (worst case) to generate. The material must thus have a storage time of  $13 \text{ hours}$ . Care must be taken that the display material used has a  $T_s = 13 \text{ hrs}$  under readout and not only under dark storage. In practice, the operator may not need to continually view the display for  $13 \text{ hrs}$ , but such a restriction is hard to assess, thus the  $13 \text{ hr}$  threshold parameters was used.

Gray Scale =  $8-16 \text{ levels}$ . If a  $\sqrt{2}$  difference in light level is used as a measure between gray levels, then the display material must have a  $\text{CR} = ?$  for  $8 \text{ gray levels}$  and  $\text{CR} = ?$  for  $16 \text{ gray levels}$ . In general, only the material's  $\text{CR}$  not its gray scale is given. Whether each material offers gray scale potential and if this gray scale is obtained by continuous tone or by half tone methods will be noted. The actual achievable gray scale will be

determined by the users definition of gray level step and by the ultimate granularity and gamma characteristics of the recording media.

Erasability = E. Both total and point-by-point are required. In most materials point-by-point erasure has not been pursued and only its feasibility and the complexity involved will be noted. Time of erasure is not a major consideration, seconds can easily be used. These details are noted where appropriate.

Lifetime =  $T_L$  = 1 year = 400 cycles (or about 1 per day).

Nondestructive Readout = R0 for 13 hours is needed.

Diffraction Efficiency =  $\eta$  should be large. No threshold value is given since it depends on the screen brightness desired, the projection source used, and the display material's transmittance.

Thickness = K is also tabulated for the materials considered. In general, the thinner the material, the better the resolution. This depends on the recording method and modulation mechanism.

Write Method. A point-by-point (P) writing scheme must be used. However, some materials (thick) may require a point-by-point holographic (H) data recording (see Sections 6 and 7). Such a scheme is quite complex (but feasible and similar to one used in a Dupont display ( ) ) and will be avoided where possible.

Voltage Required = V. Most materials will require that a potential V be developed across the display material and subsequently switched. Low voltages, at low frequencies are clearly preferable.

Cycle time =  $T_C$ , Write time =  $T_S$  = 50  $\mu$ sec, Erase time =  $T_E$  = seconds. As noted earlier, the smallest write or dwell time per spot that is expected will be 50  $\mu$ sec and erase times of seconds are clearly acceptable. Cycle time refers to a complete write and erase cycle. In some cases (e.g., liquid crystals) the display material has a long response time before it responds to the incident light energy written on it. Such cases will be noted where they occur.

Support System Complexity = C should be low. This refers to the need for various complexities such as: elaborate temperature control, corona charging, a vacuum environment, susceptibility to damage, precise fabrication steps, elaborate development schemes requiring heating of the material (local or bulk), and other issues such as special material handling, etc.

#### Material Characteristic Summary

The material parameters and their threshold values are summarized in Table 3 below. They will all be provided for the most promising display materials (Sections 9-20). This listing will be followed by other considerations for each material. The most recent state of the art parameters will be provided for each material. Possible future values will be noted in parenthesis and the risks involved in extending these present performance parameters to the threshold levels desired will then be noted.

<u>PARAMETERS</u>	<u>SYMBOL</u>	<u>THRESHOLD LEVEL</u>
Resolution	R	200 lines/mm
Display Material Area	$A = X^2$	16 in <sup>2</sup>
Space Bandwidth Product	SBP = R.X	20,000 lines
Contrast Ratio	CR	10
Sensitivity (1)	S	low
Spectral Transmission	T	visible and broad
Storage Time (2)	$T_S$	13 hours
Erasability	E	point-by-point (P) and total
Lifetime	$T_L$	1 yr, 400 cycles
Nondestructive Readout	RO	for 13 hours
Diffraction Efficiency	$\eta$	high
Support System Complexity	C	low
Thickness	K	low (10 $\mu$ m effective)
Write Method	P or H	(3)
Voltage Required	V	low
Write Times	$T_W$	50 $\mu$ sec

Table 3. Threshold Parameters Required for Display Evaluation

- (1) Specify  $\lambda_w$  and polarized or not
- (2) Under RO
- (3) H = holographic using 2 beams per point, P = direct spot exposure

## 2.5 HOLOGRAPHIC TERMINOLOGY

Many of the materials to be evaluated for the intended display have been used mainly for holographic applications. As noted in Section 7.1, these materials can be classified by whether the recorded imagery results in amplitude or phase modulation of the projected react light. One measure of the effectiveness of these materials is their diffraction efficiency. The maximum theoretical  $\eta$  as a function of the type and class of hologram are listed below (5, 6):

	Amplitude		Phase
Thin	Linear	6.25	33.8
Holograms	Binary	10.13	40.5
Thick	Transmission	3.7	100
Holograms	Reflection	7.2	100

Table 4. Maximum Efficiency  $\eta$  for Various Types of Holograms

As indicated in Table 4, phase holograms and phase modulating materials are more efficient than amplitude modulating materials and dissipate no energy within the material. Materials that exhibit a change in absorption index (e.g., photographic film and photochromics) are examples of amplitude modulation. Photographic film emulsions are typically 6-15  $\mu\text{m}$  thick. When a hologram is formed in green light with two plane waves at an angle  $\theta = 10^\circ$  between beams, fringes occur at  $(\sin \theta)/\lambda = 347$  lines/mm which is approximately a 3  $\mu\text{m}$  line spacing and thus correspond to a surface or thin amplitude hologram. In thick films which exhibit optical density changes, volume amplitude holograms result. Refractive index changes and surface relief effects (deformable materials) are examples of phase modulation materials. The first is a volume effect while the second is a surface phase effect.

- (5) R. J. Collier, C. B. Burckhardt, and L. H. Lin, Optical Holography, NY: Academic Press, 1971.
- (6) E. Ramberg, RCA Rev., 33, 5, March 1972.



## 2.6 CLASSES OF DISPLAY MATERIALS

Various criteria exist for classifying the various display materials to be evaluated. Several of these general remarks on the classes of display materials are included in this section to provide an overview for the second part of this report.

### 2.6.1 Electronic Versus Optical Excitation

The display materials which are being considered in this report can be characterized into two categories by the manner in which information is imposed onto the material. The materials can be either optically addressed by means of a focussed total scene or pixel-by-pixel; or can be electronically addressed by means of charging a surface electrode pattern, and by depositing free charge from an electron beam.

The display materials can be further characterized by the physical manner in which imagery is formed: bulk optical imaging, electronic imaging and bulk optical/electronic imaging. Bulk optical imaging describes the formation of an amplitude or phase image within the bulk of the material as a result of the bulk absorption of radiant optical energy. The image can be formed directly in the medium on a point by point recording or by a total scene recording. The image can also be formed holographically (interferometrically) in the medium on a point-by-point or total scene recording by introducing a separate reference beam.

The total scene image requires the existence of an object transparency (or real object) to be imaged onto the film. Imaging can best be accomplished with incoherent light. Point-by-point recording can readily be accomplished optically by scanning and modulating a focussed laser beam. The laser is an ideal light source for a point recording because of its extremely high brightness. In general, a coherent source should not be used for total scene imaging because of the coherent interference effects throughout the scene which will cause image degradation.

In the holographic recording technique, the image information is encoded with a carrier or reference wave by means of an interference pattern within the display medium. The holographic recording is usually done on a total scene basis; however, a point-by-point holographic recording of an individual pixel can be made.

The second physical imaging classification of display materials is electronic imaging. In this case, the data is recorded as a spatially varying field across the material. This field can be created by applying voltages to a surface electrode pattern, by depositing charge directly on the surface of the material by an electron beam or corona discharges, and by creating electron/hole pairs in a surface photoconductor which diffuse in the presence of an applied external field to produce a surface charge across the display material. The optically addressed surface photoconductor device which produces electronic imaging can also be categorized as an optically addressed device. A photoconductor display material sandwich with a voltage applied across the structure is used in many optically-addressed materials. The incident light beam locally changes the resistivity of the photoconductor or otherwise produces photocarriers in the material and results in a spatially varying electric field across the structural as in the electronically addressed material case. Variations of this scheme using magnetic fields exist. In some cases the resultant fields cause deformations in the material which can subsequently modulate the projected light. These and related aspects are treated in separate subsections to follow.

The difficulty in fabricating an electrode pattern of the required resolution is so severe that such structures are not considered for the present display. Electron-beam addressed materials generally operate at TV rates of 30 frames/sec and  $10^3 \times 10^3$  point resolution. The resolution of presently available devices is thus far below that required in the present display. This resolution is generally limited by the short dwell time (50 nsec for a 1000 spot/line display at a 50  $\mu$ sec line scan rate) of the electron beam on each spot. This necessitates high beam currents and results in larger spot size. The slower (1-5 sec./line) scan rate of this sonar B-scan display can allow for much longer (50-250  $\mu$ sec) spot dwell times and hence less beam current requirements and thus smaller spot sizes.

The limiting resolution of electron beam addressed display materials has not been reached. As the above general remarks indicate, direct electron beam addressed display materials are not unreasonable for this display; however, a valid assessment of their potential would require more effort and major engineering and electron optic considerations beyond the intended scope of this initial survey.

The final category which characterizes the manner in which imagery is created is hybrid bulk optical/electronic imaging. In the devices such as the PROM a localized electronic field is generated across the display material as a result of an applied external electric field and the generation of electron/hole pairs due to bulk optical absorption within the bulk display material. The charged carrier diffuse in the presence of the external field to cause a resultant local electric field across the display material.

The local electric field pattern manifests itself as a image due to the existence of an electro-optic effect, a local material strain, or a local domain formation.

#### 2.6.2 Phase Versus Amplitude Modulation

As shown in Section 6, materials that modulate the phase of the projected light have higher diffraction efficiencies than materials that only modulate the amplitude of the light. When the phase modulation has the form of a surface relief pattern or a deformation pattern on the material, a phase contrast or Schlieren projection system is often needed to produce a visible image. Often the phase modulation is different for different directions of propagation of the light and depends on the orientation of the material. In such cases, the material's birefringence can be used with polarized write and read light to produce modulation that is easily converted to amplitude modulation by use of polarizers.

#### 2.6.3 Resolution in Thick and Thin Materials

One seemingly obvious classification basis for display materials is in terms of their thickness. Only optically excited or addressed materials are considered. If the material is thin (thinner than twice the diffraction limited laser spot size) data can obviously be recorded directly by a deflected and modulated laser beam spot. The diffraction limited spot size to which a laser beam of wavelength  $\lambda$  and diameter  $d$  can be focussed by a lens of focal length  $f$  is given by the diameter of the central airy disc as  $1.22 f \lambda / d$ . More exactly, the minimum focussed laser beam Gaussian spot diameter  $a_0$  over a material of thickness  $t$  occurs when  $t$  equals the beam's confocal parameter. The beam's Gaussian waist now lies in the middle of the material and  $t = (\pi/4) (\eta a_0^2 / \lambda)$ . Packing density increases as  $t$  decreases. For a medium of thickness  $t$  less than this value, the spot size is optics limited

to the beam diameter at the Gaussian waist. If the material possesses a beam power threshold for writing, the written spot size can be less than this Gaussian beam diameter. In general, a limiting spot resolution close to one-half the crystal's thickness can be obtained.

In some materials (e.g., KDP and its isomorphs), the effective crystal thickness can be reduced by cooling the crystal near its Curie point where the ratio of transverse to longitudinal dielectric constant increases dramatically.

In sandwich structures (e.g., a photoconductor on a ferroelectric), the effective thickness of the second layer (material) is reduced by the ratio of the dielectric constants of the layers. In BSO (Bismuth Silicon Oxide), the dielectric constants of the parylene and BSO are 3 and 56, thus a 180  $\mu\text{m}$  thick BSO crystal appears to be 10  $\mu\text{m}$  thick and 5  $\mu\text{m}$  spot resolution should result.

A far more detailed analysis is needed and has not yet been published to explain these resolution effects in sandwich structures such as BSO. One such analysis is included in Appendix A. It indicates that  $d/\epsilon$  ( $d$  is thickness and  $\epsilon$  the dielectric constant) of the layer with the smallest  $d/\epsilon$  value determines resolution. A crude estimate of resolution is approximately  $20/d$ .

#### 2.6.4 Phase Versus Amplitude

Deformable materials (Section 10) exhibit a bandpass frequency response that is unacceptable for the present display. The center frequency varies inversely with the material's thickness. It should be possible to extend the low frequency response of these materials by recording each spot interferometrically. This concept has not been proven however and represents a considerable increase in the complexity of the recording system since two beams must be incident at each recorded spot.

#### 2.6.5 Development Methods

While not a general classification basis for display materials, the method by which the display material is "developed" such that the stored data can modulate read light is of importance. In many cases, a voltage must be applied and/or reversed, etc., between writing and reading (e.g., KDP, BSO, etc.).

In other materials (e.g., photoplastics), heat is used for development. In these latter cases, a dual laser beam recording system must be used. Data would be written with one beam and local heating of the spots to "develop" the material performed by a more intense laser beam. This scheme is again more complex, has received very little attention, and as such, experimental data on it is presently very sketchy and incomplete.

Many of the materials to be considered require heat for recording as well as development and temperature changes with time becoming critical. This heat will again have to be supplied by a focused laser beam which also carries the gray scale information in some cases (e.g., magneto-optic materials). With short laser pulses, the time  $t$  required for the materials temperature to rise can be made arbitrarily short if the laser pulse is much shorter than the material's thermal diffusion time. The main problem will occur in the cooling cycle or decay time. For a Gaussian beam of  $1/e^2$  radius  $r_0$ , the thermal decay time constant (for a 2D thin film material with no backing) is  $r_0^2/4K$ , where  $K$  is the material's thermal diffusivity. For metals,  $t$  is 0.1 - 1.0  $\mu\text{sec}$  for  $r_0 = 1 \mu\text{m}$ . If the material is supported or is thermally thick,  $t = 10^{-9} - 10^{-10}$  sec. See Reference (7).

When larger areas ( $\approx 1\text{mm}^2$ ) are recorded (e.g., 2 D images on holograms not point-by-point recording), the thermal decay time increases accordingly, as does the required energy. To avoid excessive reduction in the thermal modulation depth by thermal diffusion, narrow (in time) laser pulses are needed.

#### 2.6.6 Modulation Mechanisms

The basis on which the display material will be categorized is the modulation mechanism used: deformable, Pockels, ferroelectric, photoconductor-ferroelectric, magneto-optic, electro optic, scattering, etc. This categorization is quite similar to previous distinctions such as development methods, whether surface or volume effects occur, whether phase or amplitude modulation results, etc. It seems reasonable to use this categorization as subdivisions

(7) Michael, et. al., Journal of Applied Physics, 40, 303 (1969)



of the material's thickness. For better presentation of data, certain materials (notably liquid crystals and PLZT) that exhibit many different modulation mechanisms and device structures will be treated in individual sections.

## 2.7 OPTICAL DATA PROCESSING

Since this sonar B-scan multichannel display system can also (with appropriate modifications) function as an optical processor for sonar surveillance signals) a review of coherent optical data processing techniques is included for completeness. The basic optical processor is shown in Figure 1. An input collimated beam of coherent light (uniform in amplitude and phase) illuminates the input plane  $P_0$ . If an optical transparency with amplitude transmittance  $f(x,y)$  is placed in  $P_0$ , the complex light distribution in plane  $P_1$  is (5).

$$F(p,q) = \int_{-\infty}^{\infty} \int_{-\infty}^{\infty} f(x,y) \exp[-i(px + qy)] dx dy$$

where  $p$  and  $q$  are spatial frequency variables. The coordinates  $(\xi, \eta)$  of  $P_1$  are related to  $p$  and  $q$  by

$$\xi = \lambda p f / 2\pi, \quad \eta = \lambda q f / 2\pi$$

where  $f$  is the focal length of  $L_1$ .  $F(p,q)$  is recognized as the 2-D complex transform of  $f(x,y)$ . The second lens  $L_2$  forms the inverse transform of  $F(p,q)$ , in plane  $P_2$ .

Most sonar signal or image processing applications will require the signal or image represented by  $f(x,y)$  to be modified. This can be accomplished

- (5) R. J. Collier, C. B. Burckhardt, and L. H. Lin, Optical Holography, NY: Academic Press, 1971.

easily optically by inserting a second transparency with transmittance  $H(p,q)$  in plane  $P_1$ . The light distribution leaving  $P_1$  is then  $F(p,q) H(p,q)$  and its inverse transform appears in  $P_2$  due to  $L_2$ .

$$r(x,y) = \frac{1}{4\pi^2} \iint_{-\infty}^{\infty} F(p,q) H(p,q) \exp [i(p x + q y)] dp dq$$

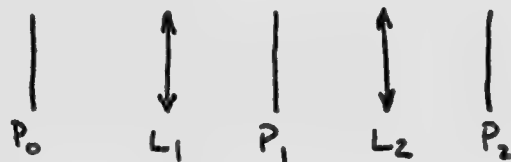


Figure 1. Conventional coherent optical data processor.  $P_0$  = input,  $P_1$  = Fourier transform, and  $P_2$  = correlation or image planes.  $L_1$  and  $L_2$  are spherical lenses.

The real time display materials to be discussed can be used in planes  $P_0$  or  $P_1$ . Only with such materials, can the dimensions of the optical processor be adequately extended to encompass the real-time high data rates possible. Depending on the write and read and erase  $\lambda$ 's, of the materials, the above figure can be modified. A dual image correlator can be used.  $P_1$  can be read in reflex; 1-D or 2-D multiplexing can be incorporated, etc.

When used in coherent light, optical and cosmetic quality are far more important. Material flatness must usually exceed  $\lambda/4$  and scattering effect materials should be avoided, etc.

### 3.0 MATERIALS SURVEY

#### 3.1 INTRODUCTION

The data for this material's evaluation was drawn from many sources. Most are individual articles in journals. Many of the remarks made concerning specific materials and conclusions drawn are based on visits to research labs actively pursuing various materials, from contract reports and from personal experience.

One general source of data and the motivation for much of the material's research work reported on herein has been provided by the mass optical memory programs. However, nearly all of this work utilizes holographic rather than point-by-point storage. The higher packing densities obtainable holographically are the reason for this. Mass optical storage efforts have generally concentrated on volume storage where multiple holograms can be stored in the bulk of a material with again higher  $\eta$  and packing densities. These efforts have been intended for mass digital storage and as a result binary rather than gray scale materials and storage have been pursued. Several general review articles on these materials exist (8-11) and some for displays (2,12-14).

The specific category of electronically addressed materials is also treated in several articles (15-16). The materials to be discussed here are also of interest as optical-to-optical converters in coherent optical data processing.

- (8) D. Chen and O. Tufte, IEEE Spectrum, 10, 26 (1973)
- (9) Fett, IEEE Spectrum,
- (10) Applied Optics, Special Issue, April 1974
- (11) RAC Rev., Special Issue, Vol 33, Nov 1972
- (12) IEEE - ED-20, Nov. 1973
- (13) B. Ellis and A. Walton, Royal Aircraft Estab. Tech Rept. 71009
- (14) A. Agajanian, JSID, 14/2, 76 (1973)
- (15) Drake, Appl. Opt.
- (16) D. Casasent, J.SID, 15/3, 131 (1974)

Several surveys of materials for this application also exist (17-19). Some specific articles surveying materials of one class or type (e.g. ferroelectric single crystals, magneto-optic materials, liquid crystals) also exist and are noted separately in the individual sections. In general, no attempt is made to list every published work on each type of material, rather only the most recent or most comprehensive work. In all cases additional references can be found in the article(s) referred to.

Although some description of each material class or type will be given in the individual sections, several general remarks are included at the outset on some of the basic material types and structures to be treated.

Two major classes of display materials are those that utilize a surface deformation on the material (Section 10) and those that involve a sandwich structure consisting of a sandwich structure with a photoconductor (PC) deposited on a material with electrodes on the outer layers. Several general considerations for these two types of materials are included in this introduction.

The spatial charge or electric field distribution across a deformable material causes modulation when the electrostatically produced deformation forces overcome the material's restoring forces to produce actual deformations in the material.

These deformable materials produce a spatially variable phase modulation of the incident light, where the phase modulation is carried in the material's thickness variations. These devices exhibit a Bessel transfer function for which linear modulation restricts the maximum deformation to 0.2 ( $\eta = 10\%$  values thus result). The amplitude of deformation varies as  $1/\omega_x^2$  (where  $\omega_x$  is the spatial frequency recorded). Compensating filters are thus needed to preserve signal fidelity. A Schlieren projection system is usually used to display the phase modulation. Another feature of most of these materials is their bandpass frequency response. When images are projected onto these materials, a screen grid with a frequency equal to the material's center frequency

- (17) D. Casasent, IEEE Spectrum, to appear
- (18) D. Casasent, Optical Info. Proc., Plenum Press, Chapter to appear
- (19) Lipson, Adv. in Holog., Dekker Pub., Chapter to appear

must be used. In the proposed display, point-by-point addressing must be used. This introduces special problems that can be overcome by writing with two light beams on a point-by-point basis whereby grating patterns are recorded at each point is needed to avoid observing only edge effects. To exhibit storage, some of these materials (e.g. thermoplastics) must be developed by heat, again, by a high energy heating light beam scanning the material (or by a heating current pulse to the entire material). Questions of how long the deposited writing change can remain before the material must be heat developed to produce and freeze in deformations is not known adequately. The point-by-point interferometric addressing scheme has not been proven, nor has high resolution point-by-point heat development. Lifetime of deformable devices is low (1000 cycles) but this may be 3 years in this display application. Cycle times when heat development is used may limit recording speeds. A related IR laser thermo-optic writing scheme used on a liquid crystal and discussed separately seems to be encouraging.

Most of the materials to be discussed are used in a sandwich structure where a photoconductor (PC) is deposited on the material and electrodes on the outer layers. An explanation of the basic operating scheme is thus appropriate. A voltage applied between the electrodes divides across the PC and material. When the PC is locally illuminated, its conductivity increases, its resistance drops, and more of the applied voltage appears across the material (initially most of the applied voltage appeared across the PC). This local spatial voltage distribution across the material can then modulate read light by a variety of electro optic effects. In certain materials to be discussed, strain is used to produce birefringence in materials. In other cases magnetic fields are used. A related factor in these PC sandwich structures (and in all materials) is storage under readout. In general, non-destructive readout (as required in this display) can be achieved by using different wavelengths for writing and reading. Even in this case, the PC usually responds somewhat to both wavelengths. A more viable approach utilizes a blocking layer and readout in reflection, thus achieving non-destructive readout, longer life, and storage. Many variations on these basic ideas and other mechanisms exist.

## 3.2 DEFORMABLE DISPLAY MATERIALS

### 3.2.1.1 Thermoplastic (TP) Recording by Laser (20)

One of the most commonly used deformable target materials is thermoplastic (TP). An 0.4-1.5  $\mu\text{m}$  thick TP on a 2-3  $\mu\text{m}$  thick photoconductor (PC) with a grounded rear transparent electrode is placed on a substrate. The material's thickness is controlled by the rate at which it is pulled from the solution. Fairly reasonable accuracy with 1.5" x 1.5" materials is possible. Thickness cannot be accurately predicted exactly in advance (21). The recording process consists of three steps: (1) charging the TP surface to  $\approx 300\text{V}$ ; (2) exposing the TP to the input write light; (3) recharging; (4) developing the material by heating. Erasure is performed by a longer or more intense heating cycle. A typical cycle (22) is: (1) charge for 25 msec; (2) expose for 100 msec at  $100 \mu\text{J}/\text{cm}^2$ ; (3) develop for 150 msec at 4.5 W or 0.7 J; and (4) reverse charge for 50 msec. Charging is continued during exposure to produce more reproducible  $\eta$  values. Faster cycles and sensitivity to  $5 \mu\text{J}/\text{cm}^2$  is possible but not reliable and reproducible as yet. A 100 msec cycle seems feasible. Erasure requires 450 msec at 4.5 W or 2 J. Resolution is high with a 2000-5000 line/mm center frequency and a  $\pm 200$  line/mm bandwidth.

For the present display, the material must be point-by-point addressed. It does not appear that the material can store the entire pattern before heat development, thus each point or line must be developed separately. This constitutes a major problem since well controlled heat pulses are needed to insure development of the information rather than its erasure and reproducible and reliable results. This heating is usually supplied to the material's rear electrode but could be done with a focused  $\text{CO}_2$  laser, small separate  $1\text{mm}^2$  areas of TP on separate pads spaced by 2mm have been erased by this method with some damage to adjacent points (22). Once written, the material can be read indefinitely. It can only be cycled 1000 times by at 1 display/day this translates to a three year life. The support and monitoring electronic system

(20) T. C. Lee, Applied Optics

(21) Interim Report, Nov. 72, on NAS-8-26808

(22) Final Report, July 74, on NAS 8-26672



is very complex. Controlling times and levels must be done very precisely. Point-by-point writing and local heat development and erasure at the spot sizes needed (5  $\mu$ m) remains to be proven.

As noted earlier, to avoid edge effects only occurring and to thus extend the material's spatial frequency response to zero, each point must be recorded interferometrically with the resultant fringe pattern producing low frequency response. This technique has not been demonstrated, however, and clearly results in a more complex writing scheme.

Other problem areas are the time required to cool the material to room temperature once it has been heat developed. A final item that may preclude reusing the material in this application is the presence of a residual image that grows when a second image is written. This has been observed in some types of TP, especially when the image has been stored for long periods of time. Erasure of such images is also difficult. Parallel plate charging provides for more uniform, reliable, and reproducible results and less damage to the TP than does corona charging. Charging during exposure increases  $\eta$  but also often causes the TP to rupture (23).

A more plausible approach would be the use of commercial GE TP (24) and not re-using the tape. Another alternative that has received little attention is the use of photovoltaic TP (25) that requires no charging. Charging in TP that is point-by-point addressed and developed seems to be another problem area needing attention.

- (23) Credelle and Spong, RCA Rev. 33, 1, 206 (1972)
- (24) Bigelow, Information Display, Sept. 1969, page 49
- (25) Gaynor and Sewell, Photo Science Engineer, 11, 204 (1967)

R 2000 lines/mm (200 lines/mm reasonable)  
 A 1.5 x 1.5 (4 x 4 possible)  
 SBP 7000 lines  
 CR 100:1  
 S 5-10C $\mu$ J/cm<sup>2</sup> (75  $\mu$ J/cm<sup>2</sup> typical)  
 T visible (depends on PC) (400-700 nm)  
 T<sup>S</sup>  $\infty$   
 E yes (local erasure unproven), heat used  
 T<sub>L</sub> 1000 cycles  
 RO yes  
 $\eta$  1-40% (1% norm)  
 C tremendous complexity  
 K 0.5 - 1.5 $\mu$ m  
 W H or 2-D (P unproven), surface relief pattern formed  
 V 300 V charge  
 T<sup>C</sup> 450 msec now (100 msec possible per line)

Table 5. Parameters for Laser Beam Addressed Thermoplastic Display

Risks - local heat development, local 5  $\mu$ m erasure and point-by-point address/development/charge unproven and risky. Residual image problem if reused.

### 3.2.1.2 Thermoplastic (TP) Recording by Electron Beam (26-27)

Electron beam TP recording was developed before TP-PC devices. Here the charge is deposited on the TP target by a scanning electron beam, and heating is achieved by applying a pulse to the rear electrode. RF heating using a reel of TP has also been used. X, Y, or Z axis modulation with the input signal modulating an RF carrier is used. Resolutions of 1800 lines/inch are claimed. The 10  $\mu$ m electron beam spot can probably be reduced since the present display requires 20,000 points/second while the electron beam TP tube addresses  $3 \times 10^7$  points/second. Erasure requires two seconds. Perhaps it can be done by the electron beam locally. In the present tube, the entire

- (26) Glenn, *Journal of Applied Physics*, 30, 12, 1870, Dec. 69  
 (27) Doyle and Glenn, *IEEE-ED-18*, 9, 739, Sept. 71

image is developed and erased at once. Local development may be impossible, but local 1 mil areas have been erased by RF heating in the TP tape system. It is stated that development need not be immediate (26), but it is doubtful if it can be long after writing.

The device cannot be sealed and its lifetime and reproducibility of results are very questionable.

R	70 lines/mm
A	1"x1" (ERIM has fabricated larger 4"x9" targets)
SBP	1800
CR	8
S	electron beam
T	visible
T <sup>S</sup>	?
E	heat used
T <sub>L</sub>	limited
RO	yes
$\eta$	1-10% (1% typical)
C	vacuum, not sealed, electron gun
K	
W	P, surface relief
M	surface relief
V	electron gun
TC	variable by electron gun

Table 6. Parameters for Electron Beam Addressed Thermoplastic Display

- Risks - very research oriented device, many uncertainties
- reproducibility, lifetime very questionable,
  - 4"x4" requires major electron gun changes
  - point-by-point development unproven
  - storage uncertain

(26) Glenn, Journal of Applied Physics, 30, 12, 1870, Dec. 69

### 3.2.2 Oil or Dielectric Material, Electron Beam Writing (28)

The coherent oil film light valve uses a modulated electron beam to produce deformations in an oil or dielectric target. The device does not have the resolution or storage necessary for the multichannel sonar B-scan display, but is worthy of note because of the remarkable engineering achievement it represents. The device is commercially available. Cathode contamination has been solved. (Sealed units have operated over 3000 hours).  $10^3 \times 10^3$  point resolution over 1 in.<sup>2</sup> has been demonstrated. Electronic preprocessing to compensate for the decay of the image as it is written is possible as is electronic distortion correction for phase errors in the oil target. Dynamic range is in excess of 50 dB (perhaps 40 dB linear).

### 3.2.3 Elastomer (E) - PC Material

Xerox (29) has pursued several versions of an E-PC sandwich in which the elastomer layer deforms under an electric field as did the TP in the previous case. The various versions of the device (called a Ruticon) differ in the method by which the initial voltage is applied across the structure. The materials are operated like the PC sandwich structures noted in Section 9 and are optically addressed. They have been used only for holographic recording and direct noncoherent 2-D imaging. Fairly low voltages (40V), good sensitivity (300 ergs/cm<sup>2</sup>) and high  $\eta$  (15%) result but only 40 line/mm resolution even with thin 4.5  $\mu$ m elastomer layers. The most promising structure is the Y-Ruticon which utilizes a flexible metal electrode (opaque) on the side that exhibits the deformations and a transparent electrode on the other side. The opaque electrode provides some isolation between write and read light beams. The stored image is read out in reflection but still there is no storage and the image decays on readout. In addition, lifetime is limited to 10,000 cycles (which is adequate for this application but is typical of the low lifetime of deformable materials. As is the case with many materials, the low resolution and lack of storage makes it unacceptable for this application.

(28) G.E. Tech. Info. Series R75E LS-12, Feb. 1975

(29) Sheridan, IEEE-ED-19, 1003 (1972)

### 3.2.4 Membrane (M) Light Modulator

Another deformable material that was available commercially (Perkins-Elmer) was the membrane light modulator (30-31). Electroded, photoactivated, and electron beam addressed structures have been fabricated. The basic structure consists of small (5-40  $\mu\text{m}$ ) perforations on 50  $\mu\text{m}$  centers on which a thin 0.1  $\mu\text{m}$  gold-coated collodium membrane mirror was deposited. Low voltages (20-40V) were required but only 500x500 point units were fabricated. Photolithographic techniques cannot adequately increase R but more important for this display application was the device's low useful storage of only one second.

### 3.2.5 Deformagraphic Tubes

Many other devices such as the IBM deformagraphic tube have too low of a resolution, no storage, poor lifetime, and are prone to target destruction and are thus not elaborated on. A deformable PLZT structure (Section 3.5) is treated separately.

## 3.3 MAGNETO-OPTIC (MO) MATERIALS

A wide variety of MO materials have been considered for mass optical storage of digital data. These structures consist of thin material layers and one optically addressed. The general writing procedure involves locally heating regions of the material above the material's Curie point by a focused laser beam in the presence of a magnetic field. This thermomagnetic writing causes the magnetization in those written areas to reverse. The MO effects are used to read out these magnetization states in reflection (Kerr effect) or transmission (Faraday effect).

The basis of these MO effects is similar to the more familiar electro-optic EO effects. Linearly polarized read light can be used. It is separated into left and right circularly polarized components. The material's refractive indices for these two components differ and depend on the material's magnetization. (In the EO effect the difference in refractive index for

(30) Preston, IEEE-AES-6, 458 (1970)

(31) Bordogna, et.al. RCA REV. 33, 227 (1972)

orthogonal components of polarized light are different and depend on the electric field across the material). The MO films should be thin enough not to absorb all of the incident light (absorption coefficient  $= \alpha$ ) and thick enough to provide a strong Faraday rotation of the polarization of the input light (Faraday coefficient  $= \theta_F$ ). Film thicknesses are usually less than 1000 Å. If the material's average specific heat is  $C_V$  and a  $\Delta T$  temperature change is required to reach the material's Curie point where magnetization reversal occurs, then  $C_V \Delta T / \alpha$  is the writing energy that must be supplied by a focused laser beam. The signal-to-noise ratio (SNR) is proportional to  $\theta_F / \alpha$  and thus many tradeoffs in CR, R, and S are possible.

MnBi, GdIG, and EuO are the most researched MO materials. GdIG (32) has a compensation temperature near room temperature at which the Gd and iron sublattice magnetizations cancel and where a sharp coercive force peak occurs. Only small  $\Delta T$  values are needed but its  $\alpha$  is 10 times lower than other material's and high energies are needed. Recording has been done on both single crystals (32) and thin films (33) of GdIG. 50 line/mm resolution and 0.08 J/cm<sup>2</sup> sensitivity resulted in the first case with a 100 Oe field, while 300 line/mm = R and S = 0.125 J/cm<sup>2</sup>, with 500 Oe for the film case.

In EuO, the material is heated above its Curie point  $T_C$ . High 3 μm spot resolution and (0.001-0.01 J/cm<sup>2</sup>) sensitivities resulted but the material must be operated at cryogenic temperatures (34).

The most promising material is MnBi (35). It has the largest  $\alpha$  and thus requires the least energy of all MO materials. It has a large  $\theta_F$  and can easily be fabricated with its magnetization normal to the surface. It's  $T_C = 360^\circ\text{C}$  so a large  $\Delta T = 350$  above normal room temperature is needed, but only 10<sup>-2</sup> ergs/cm<sup>2</sup> should be required for a 3 μm spot or 20 μW for 50 μWsec. Heat is dissipated so rapidly because of the large  $\Delta T$  that larger 10<sup>-1</sup> erg/cm<sup>2</sup> sensitivities result in practice. The films are 400-500 Å thick, 5-10 mW pulses for 0.1-1 μsec are used and a 700 Oe field.

- (32) Coeune et.al. IEEE Mag-7, 397 (1971)
- (33) MacDonald and Beck, Journal of Applied Physics, 40, 1429 (1969)
- (34) Ahn, Applied Physics Letter, 17, 347 (1970)
- (35) Chen, Applied Optics, 13, 767 (1974)



All of these materials have low SNR's of about 8 and very poor  $\eta$  values of  $10^{-8}$ - $10^{-4}$  and are only binary devices with only one exception.

Mezrich (35a) states that these devices may not be binary depending on whether temperature or areas are considered. He uses a holographic scheme for recording. Holographic recording using far larger areas than point-by-point recording places severe restrictions on the laser used ( $10^3$  W peak and 10 nsec pulses) that are not obtainable. Even point-by-point writing requires well controlled laser power and duration of pulses at high repetition rates.

To write, the magnetic closure flux and external field determine the direction of magnetization of a heated bit. With the magnetization normal to the film, the closure flux opposes the magnetization direction and no field is needed to write a "1". To erase, an external field  $H_a$  is applied to overcome the demagnetization field  $H_\perp$ , and write a "0". To do this without erasing other areas, the demagnetization field must be less than the coercive force of the medium. To read out data, the easy direction of magnetization must be normal to the plane. This results in smaller domain sizes and higher resolution also. During write or erase, the total field is  $H = H_\perp \pm H_a$  (+ for write, - for erase).  $H_a$  must be larger than  $H_\perp$  for erase, small for convenience, and cover an area longer than 1 bit for practical considerations. The beam heats the selected area within this region. We require the switching field less than the coercive field  $H_c$  to avoid switching surrounding areas.  $H_c$  is proportional to (thickness) $^{-1}$ . A square magnetic hysteresis loop is essential (or one that has less than magnetization constant  $H_c$  independent of  $H_a$  to insure full read-out and no danger of losing remnant polarization).

The one way to obtain analog data is by use of a thermoremanent scheme (36-37). Magnetization changes can occur at  $T < T_c$ . The remnant polarization  $M_R$  after such a thermal heat cycle is reduced from its saturation value  $M_S$ . Under an external field,  $M_R$  can be from  $+M_S$  to  $-M_S$ . ( $M_R$  is the statistical average of + and - domains within the heated spot).  $M_R$  depends strongly on

(35a) Mezrich, Applied Optics, 9, 2275 (1970)

(36) Waring, Journal of Applied Physics, 42, 1763 (1971)

(37) Minnaja, et.al. AIP Conf. Proceeding, 10, 1435 (1973)

the peak T and field and precise control of these is needed to control  $M_R$  reproducibly and thus obtain gray scale. This scheme has been used in MnBi and  $\text{CrO}_2$ .

R	500 lines/mm
A	> 15 cm dia.
SBP	375,000
CR	8
S	10 mJ/cm <sup>2</sup>
T	visible
T <sub>s</sub>	$\infty$
E	yes and local
T <sub>L</sub>	$\infty$
RO	$\infty$
$\eta$	$10^{-1}$ (Kerr) $-10^{-2}$ (Far.)
C	Magnetic field, precise laser
K	400-500 Å
W	P, thin phase
V	Magnetic 700 Oe
T <sub>c</sub>	fast $\mu$ sec

Table 7. Parameters for Magneto-optic Material Display

Risks - Gray scale hard to obtain but possible

- Laser energy, control, pulse width, rep rate not easy (10 MW pulse 0.1-1  $\mu$ sec long at 20K/sec)
- Poor  $\eta$  and CR.

### 3.4 LIQUID CRYSTALS (LC)

Liquid crystal (LC) devices have received enormous consideration as display panel materials in the past eight years. Their low cost, low voltages, etc., are especially attractive features. For the specific display under consideration, there are numerous factors that may preclude the use of LC's. Storage is required, so is selective erasure and 200 line/mm resolution, and a good 10:1 contrast ratio. Another feature of the display is the addressing time; for 20,000 elements per line per 1-5 sec, only 50-500  $\mu$ sec per point dwell times are possible.

The various LC effects and performance will be briefly reviewed first to aid discussion. Over 3000 LC references exist (38), and over 15 electro-optic effects (39) in two LC phases alone; thus the present discussion will be brief by definition.

One of most readable and recent LC display surveys is (40). Several preliminary terms will be defined initially. The basic structure consists of an LC between two electrodes usually with a photoconductor PC layer on one side. For an LC with positive dielectric anisotropy, the molecules align in the direction of the applied field. Molecules in LC's with negative dielectric anisotropy align normal to an applied field. Three major types of LC's exist: nematics (with 1 D ordering with molecules aligned with their long axis parallel); cholesterics (with molecules in a series of nematic like planes with the direction of alignment of the molecules progressively changing between planes); and smectic (with planes of aligned molecules all in the same direction). Two major types of electro-optic effects in LC's are those caused by dielectric forces only or both dielectric and conduction forces. Two conduction induced phenomena (current effects) are the dynamic scattering mode DSM and storage mode SM. Four dielectric effects are: field indirect birefringence FIB or deformation of aligned phases DAP: twisted nematic TN; guest host GH or electronic color switching ECS; and colesteric-to-nematic transition CNT.

The current effects are slow since they require setting a viscous liquid into motion (10 msec). The associated transport of charge produces hydrodynamic instability, low lifetimes, and low contrast ratios. Field effects involve tilting or turning molecules, they are faster (tenths of msec), and provide higher contrast displays. Nematic LC's do not exhibit memory, whereas NLC-CLC (colesteric LC) mixtures do.

FIB devices require a NLC with negative dielectric anisotropy (NDA). With no field, the molecules align normal to the electrodes; with a field, the molecules in the center turn and the LC is birefringent (not linearly with V

(38) Kodak

(39) Flannery, IEEE-ED-20, 941 (1973)

(40) Goodman, RCA Rev, 35, 613 (Dec 1974)

however). NLC's with PDA (positive dielectric anisotropy) are also useful in FIB displays. This mode offers no storage.

The TNE offers wide viewing angle reflection displays. The molecules have a  $45^\circ$  or  $90^\circ$  twist between electrodes with no voltage. With PDA materials, voltages above threshold cause the director (axis of molecules) to untwist and align with the field. Polarized light is needed as in the FIB displays. Its plane of polarization is rotated by the electrically controlled twist angle of the molecules and provides modulation through a polarizer/analyzer. Nonuniformities can be eliminated (reverse tilt and twist) by proper surface preparation and the addition of a cholesteric to the nematic (41-42). In the TNE, there is no storage. It is not clear if storage results in TNE when a CLC is added to the NLC.

The GH effect uses an NLC as a host for a pleochroic dye. The NLC is used to orient the dye while the modulation is due to the dye's absorption spectrum. No storage results, however.

The CNT effect occurs in a CLC with PDA. The cholesteric planes are normal to the cell walls in zero field, the helical axes are randomly oriented and strongly scatter. As the field approaches threshold, the helices unwind and dilate. As the field exceeds threshold, all LC molecules except for surface ones align parallel to the field. This is the homeotropic texture and the nematic phase. The cholesteric scattering structure is not really stable but is metastable (minutes to months). The planar or Grandjean texture is stable. When the field is removed, the fluid returns to the metastable scattering state. Decay from the perpendicular texture (nematic) to the scattering texture (cholesteric) can be retarded by the presence of a field or bias voltage below threshold. It is not clear if storage of hours is possible, however.

The DSM is the most used. The field must be above threshold and below the critical frequency. DSM seems to occur only if the LC is  $\geq 6 \mu\text{m}$  thick, of low  $10^{10}$  ohm-cm resistivity and of NDA. In general, the field for FIB is less

(41) Raynes, Elec. Lett, 9, page 101 (1973)

(42) Raynes, Elec. Lett, 10, page 141 (1974)

than for domain formation. The LC progresses from the undeformed state to the FIB texture to the presence of domains and finally to DSM as the field is increased. No storage results however.

The SM occurs in NLC-CLC mixtures. With no field, the sample is clear; with a dc or low frequency ac field, DSM results, when the field is removed, the forward scattering state remains. Decay time is reported as hours at elevated temperatures which is not adequate. Margerum reports storage for months (43), Haas reports storage for 24 hours (44). Perhaps one was dark storage, another not. The effect of constant readout is not reported.

Several comments on long-life high-contrast LC structures can be made. Ac fields are far superior to dc fields. Ac life of 5-10,000-20,000 hours is reported (45-46). PC coated devices, not electroded ones, must be used for the sonar display. As with all PC sandwich structures, a barrier layer is essential for non destructive RO, storage, and long life. This implies a reflex system. Two different wavelengths for write and read are preferable still. CdS is the most sensitive PC with sensitivities in the  $\mu\text{J}/\text{cm}^2$  range obtained. Typical TNE rise times have been 10 msec and DSM times 200 msec. TNE decay time of 400 msec and DSM decay of 100 msec. For DSM and the field effects, fields can be used to change the decay times. Fast rise times and storage do not seem possible simultaneously.

The only promising LC operational mode utilizes the thermo optic properties of a NLC-CLC mixture (47) or a Smectic LC (48). The smectic LC allows for selective erasure and is thus discussed here. A CBOA, 14 smectic A phase (PDA) LC with special silane surface coupling agents (corning XZ 2-2300) is used. When the sample is cooled slowly from its isotropic state, the smectic texture is non scattering (homeotropic). If cooled rapidly, a scattering and depolarizing smectic texture results. Rapid cooling freezes in this disorder, slow cooling allows the disordered molecules to reorganize to

(43) Margerum, Applied Physics Lett, 17, 51 (1970)

(44) Haas, 1973 SID Digest, page 44

(45) Goodman, J. SID, 13, 121 (1972)

(46) Pohl, 4th LC Conf., paper 144, 1972

(47) Kahn, Applied Physics Lett, 22, 3, page 111, Feb 73

(48) Melchior, Applied Physics Lett, 21, 8 page 392, Oct. 72

a nonscattering state determined by boundary conditions. Crossed polarizers are needed. Thermal erase can be performed locally by scanning the cell at a lower rate than that used to write so that the LC cools slowly and becomes nonscattering. Field assisted erase (35 V at 1.5 kHz) transforms the write beam into an erase beam and erase occurs at write rates. The specs for this one LC display follow. For a 20 mW 1.06  $\mu\text{m}$  IR laser,  $10^4$  points/sec could be written. The limits on writing speed and dwell time per spot are not known. The specified 20,000 points/line in 1-5 sec is only twice the above rate in worst case.

The only problems with the device are the low 50 line/mm LC resolution and only 10:1 contrast that result. These are typical LC specifications. Low contrast seemingly always results. No MTF plot is provided but by normal standards the 10:1 contrast is specified at a low resolution (and probably a  $5^\circ$  half angle) and 50 line/mm resolution is at the visible limit of an MTF of 0.05.

Jacobson (49) has recently fabricated a 2  $\mu\text{m}$  thick hybrid LC cell with 100 line/mm resolution and 100:1 contrast (again not simultaneously obtainable; e.g., contrast is 3:1 at 60 line/mm). This particular LC structure has no storage, but combining this technology with the thermo optic effect should prove rewarding if it is possible. The DMS should be avoided because of the halo effects, noise, and scatter that result by the very nature of the effect.

Several general features of LC display devices are of importance. Storage is possible only in the cholesteric - nematic materials and in the thermo-optic writing on smectic LCs; all use scattering mode. No storage is possible in the field effect. Gray scale can be obtained in both scattering mode and field devices but not with storage. The storage results by snapping the LC chains and is thus a binary or threshold device. Gray scale in the thermo-optic writing results only by varying the laser spot size, thus trading resolution for gray scale. The speed of response of the device also merits several additional words. While 10 msec development is needed, the addressing light beam need not be present for this time rather only the field. The

(49) Jacobson, Optical Engineering, May/June, 1975



duration of the light pulse is determined by the required energy. As the LC thickness is increased, the speed of response drops but the storage time increases (1 sec for 6  $\mu\text{m}$  thickness), and the CR increases. The resolution is mainly determined by surface state spreading at the blocking layer. In excess of 300 lines/mm resolution is possible.

The selective erasure feature of the thermo-optic (TO) effect and low cost of the display make it attractive if low 50 line/inch resolution is acceptable. Resolution can be extended to 100 lines/mm with improved LC fabrication techniques. However, gray scale is possible only by a halftone presentation. This TO LC materials specifications follow:

R	50 lines/mm
A	4x4 cm
SBP	2000 now, 4000 possible
CR	10:1 (half angle probably $5^\circ$ )
S	$\mu\text{J}/\text{cm}^2$ (depends on PC)
T	visible read, IR write, depends on PC
$T_s$	100 hours minimum
E	yes and selectively
$T_L$	not known
RO	not stated, expected to be 100 hours
$\eta$	not stated, expected to be 1-10%
C	IR 1.06 $\mu$ writing at 20mW
K	12 $\mu\text{m}$
W	P, thin phase
V	35 V at 1.5 kHz for erase
$T_c$	$10^4$ points/sec with 20 mW IR laser erase at same rate possible

Table 8. Parameters for Thermo-optic Liquid Crystal Material Display

Risks - low resolution and contrast

- gray scale not confirmed, possible only by larger spots and R loss
- dwell times for write and rise times unclear

Conclusion - 4000 line display with selective erase at low cost seems possible. Never 20,000, however.

### 3.5 PLZT - PC

A wide variety of electro-optic effects in PLZT have received varying degrees of attention as display devices. One of the most recent publications that surveys work in PLZT is Ref. (50).

PLZT consists of a hot pressed mixture of lead lanthanum zirconate titanate ferroelectric ceramic designated PLZT-x/y/z where x is the atomic percent of La and y/z is the ratio of  $\text{PbZrO}_3$  to  $\text{PbTiO}_3$ . Only the most promising structures will be noted. They all consist of a PLZT-PC sandwich between 2 transparent electrodes.

The Ferpic device (51) uses mechanical strain bias applied to the PLZT plate to enable a longitudinal electro-optic effect with memory. (PLZT is normally isotropic in the plane normal to the poling or switching direction). It operates similar to all PC sandwich devices. 220 volts is applied between electrodes, the light pattern is imaged or scanned onto the PLZT and produces a spatially varying transverse field corresponding to the input image intensity. Storage is excellent.

Erasure is achieved by reversing the voltage to -100V and either flooding the ceramic with light or using a scanning beam (this latter method enables selective erasure to occur). Sensitivity is  $\approx 10 \text{ mJ/cm}^2$  for a PVK PC (better results are expected with a CdS PC) 50 line/mm resolution in 50  $\mu\text{m}$  thick plates of 1-2  $\mu\text{m}$  grain size and 15 dB contrast ratios result. Partial switching to states of intermediate polarization between  $\pm P_R$  allows for gray scale images. Lifetime is quoted as  $10^9$  cycles. PLZT is transparent from 400-700 nm. In the above FERPIC system, the image is stored as a spatially varying birefringence in the PLZT. The applied strain bias established a preferred orientation of the polarization while the magnitude of the birefringence is controlled by the applied voltage.

A variation of the FERPIC devices is operated in reflection (52) rather than transmission. In this mode there is less optical loss and problems of the PC responding to the read wavelength do not occur. A reflection layer of metal

(50) Land, Ferroelectrics, 7, 1974

(51) Maldonado, and Meitzler, Proc IEEE, 59, 368-382

(52) Maldonado and Anderson, IEEE, ED-18, 774, 1971

dots was used and poorer resolution resulted than in the transmission device. A 75  $\mu\text{m}$  thick sample gave 100  $\mu\text{sec}$  risetimes with a 2 sec 200mw/cm<sup>2</sup> exposure with 70V applied. Low 6 dB contrast ratio resulted because of a basic 4.5 dB insertion loss and an overall 13.5 dB loss that could easily be reduced to 7.5 dB by a polarizing beam splitter.

A second PLZT-PC device called Cerampic (53) is simpler to fabricate, requires no strain bias, no critical polarization switching to obtain good contrast and gray scale, no polarizer and analyzer with their losses, and can use white light for reading. Numerous breakage and nonuniformity problems occur in strain-biased devices. The Cerampic device uses the longitudinal electro-optic scattering effect. The PLZT is prepoled by applying 450V dc (12 kV/cm) to the plate and flooding the PLZT with light. This aligns all domains in a common direction. To store an image, the voltage polarity is reversed and the image focused or scanned onto the PLZT-PC. This causes partial switching of domains to a lower remnant polarization state. Read light is scattered more in the switched domains. Gray scale is determined by the degree of switching of the domains. The contrast ratio depends on the ceramic preparation technique, the plate thickness and grain size. CR generally increases with plate thickness up to 0.3mm thickness (peak values over 100:1 result). CR increases by 2 orders of magnitude as grain size increases from 1-4.5  $\mu\text{m}$  (probably due to strain relieving domains and reduced light scattering in small grain materials). A 2 $\phi$  angular aperture is mentioned. Resolution was 80 line/mm (40 line pair) in 0.25mm thick plates and decreases as PLZT thickness increases. Insertion loss was 7 dB. A 2msec exposure is mentioned and speed stated to be limited by the PVK PC.

The low contrast that results from scattering mode devices at higher field angles has been a major objection. Another feature of note in all PLZT-PC structures is that the material's sensitivity scales with the PC but is lower than the electrophotographic sensitivity of the PC. In addition, while domain switching can occur in usec times, it is questionable whether enough charge can be transferred through the PC to rapidly switch the high ( $3000 = \epsilon_r$ ) dielectric constant PLZT. Several times  $C_c V_p$  ( $C_c$  is the ceramic's

(53) Smith and Land, Appl. Phys Lett, 20, 169 (15 Feb 1972)

capacitance and  $V_p$  the voltage drop in the PC at the start of exposure) units of charge ( $5-10 \mu\text{C}/\text{cm}^2$ ) must be transported in the PC to alter the ceramic's field and its polarization.

The final PLZT-PC device to be discussed is the Fericon (54). Its structure consists of the PLZT-PC with a transparent electrode and second PC on one side and a flexible metal film on the other side. Its structure and operation are similar to that of the Ruticon. It has storage and selective erasure features that other deformable devices do not. It has less optical insertion loss (3 dB) than scattering mode devices (10 dB) and isolation of the write and read light. 350V is applied and the PC's uniformly illuminated to pole the PLZT to saturation remnance PC normal to the plates. The PC are then exposed with -150V applied. Domains switch to  $P^R=0$  only where the PC is illuminated.

The switched domains produce strains that deform the metal film. Better 50 line pair/mm resolution results with fine grain PLZT and contrast of 7 dB results with white light. Special care is required to fabricate the device. Curvatures apparently always result but these should be capable of being holographically corrected. Spatial frequency response extends down to 8 lines/mm thus holographic recording possibly need not be used point-by-point as is needed in other deformable devices.

Considerable compositional, fabrication, and uniformity problems occur with PLZT. Similar factors may occur in other materials, but PLZT has been so widely used that its true limitations are rather well known (22). EO response of various PLZT plates from one group to the next vary drastically. Large variations in scattered light from group to group and within one disc itself are apparent and due to variations in grain size and chemical composition. Binefringence as a function of strain bias varied locally and batch-to-batch also. CR also varied locally and more drastically batch-to-batch. Plates with consistent response could not be fabricated (batch-to-batch) but within one slug the response was approximately the same. Honeywell plates were used. They were notorious for nonuniformity. Spectrographic analysis

(54) Land and Smith, Appl. Phys Lett, 23, 57 (15 July 1973)

(22) Final report on NAS 8-26671, July 74

confirmed a 3/63/37 not a 7/65/35 composition. Sandia material showed an even lower Lanthanum composition. Electron beam micro-probe analysis of various 7/65/35 PLZT materials from three companies were performed. The results are shown below for a 1  $\mu$ m beam diameter and 9 sample points.

element	Pb	La	Zr	Ti
Honeywell	2.7	5.0	4.6	8.3
Sandia	1.2	2.6	5.1	7.6
Optoceram	2.9	6.5	3.8	4.6

The Sandia material was more uniform in Pb and La, while the Optoceram sample was more uniform in Zr and Ti. Little variation in composition was found when averaged over an area 125 x 125  $\mu$ m while much larger variations result when averaged over a 2  $\mu$ m diameter grain area. Electrical and electro-chemical tests showed similar discrepancies and nonuniformities.

The specifications of all PLZT devices are similar, thus only one table follows. The resolutions listed were in line pairs not lines/mm as noted in the text.

R	80-100 lines/mm
A	1.5 x 1.5" (larger sizes possible)
SBP	3700
CR	7 dB, white light, Fericon 100:1, white light, 2° angle, Cerampic 15 dB, Ferpic
S	10-200 nJ/cm <sup>2</sup> (less if CdS can be used)
T	400-700 nm
T <sup>S</sup>	yes
E	yes, selective, at write rates
T <sub>L</sub>	10 <sup>9</sup> for some
RO	yes
C	high voltage

Table 9. Parameters for Typical PLZT Laser Beam Addressed Display

K	50-250 $\mu\text{m}$
W	P for W and erase
M	scatter, binefringences, and surface relief
V	70-450V positive and negative
Tc	2 msec-2 sec exposures (100 $\mu\text{sec}$ possible)

Table 9. Parameters for Typical PLZT Laser Beam Addressed Display (Continued)

Risks - large material uniformity problems

- 50  $\mu\text{sec}$  rise times questionable
- selective erase possible, not actually done

### 3.6 OTHER FE-PC CRYSTALS

#### 3.6.1 Bismuth Titanate (BTO)

Until 1972 Bismuth titanate (BTO)  $\text{Bi}_4\text{Ti}_3\text{O}_{12}$  received considerable attention. It is a FE with  $T_c = 675^\circ\text{C}$ . Cummins (55) describes four methods of optically reading domains in BTO. The section extinction angle method requires sectioning with the number of elements equal to the number of rows in the display with each cut and polished normal to the b-axis. Severe fabrication problems and limited dimension along the crystal's c-axis make this impractical. Crystal plates with orientation in the ab plane are needed. Several such structures have been considered. The tilted extinction angle method has low and CR because the extinction directions differ by only  $1^\circ$ . Both of the above structures operate in white light. The pure phase mode uses a PC but is applicable only for hologram storage not direct writing and requires coherent read light.

The differential retardation mode (55-57) uses 2 plates and allows operation in white light. Two plates (modulation and compensation) of the same thickness are used. Light propagates parallel to the ac plane at an angle  $\theta$  with the c axis. The modulation plate has binefringences  $\Delta n_1$ , and  $\Delta n_2$ . The

(55) Cummins and Luke, IEEE-ED, -18 761 (1971)

(56) Cummins and Luke, IEEE-SU-19, 125 (1972)

(57) Cummins and Luke, Ferroelectrics, 3, 125 (1972)



compensation plate has only one kind of domain corresponding to either  $\Delta n_1$  or  $\Delta n_2$ . The effective retardation is the difference  $d(\Delta n_1 - \Delta n_2)$ . Contrast for plate thicknesses equal within  $0.3 \mu\text{m}$  yield  $\text{CR} = 28$ . To write an image 300V is applied for 50 msec and the image focused or scanned onto the BTO  $10 \mu\text{sec}$  switching possible. In those regions where it is illuminated, the voltage drops across the crystal and domains switch; in those regions where the crystal is dark, the voltage across the crystal is zero and half the domains take each polarization. Gray scale is possible in regions where the coercive field across the crystal is exceeded, but has not been fully evaluated and appears to be limited (55).

If the voltage is removed, storage is permanent.  $100 \mu\text{m}$  thick crystals yield  $\eta = 12\%$  for  $\sigma = 9.3^\circ$ ,  $\text{CR} = 100:1$  and  $R = 50\text{-}60$  lines/mm.  $37 \mu\text{m}$  thick samples with  $\theta = 8.7^\circ$  yield  $\eta = 5\%$ ,  $\text{CR} = 40:1$  but  $R = 80\text{-}90$  lines/mm. 2 cm BTO crystals are considered feasible now. Severe fabrication difficulties seem to exist in obtaining uniform large (2 cm) samples.

R	= 80-90 lines/mm
A	= $2 \times 2 \text{ cm}^2$
SBP	= 1800
N	= 5%
CR	= 40:1
K	= $37 \mu\text{m}$
S	= $10 \text{ mJ/cm}^2$
Transmission	= 16% (40% with perfect AR coatings)

Table 10. Parameters For BTO Material Display

Risks - large area displays need development of thin film technology

- severe fabrication problems
- switching speed is said to be  $10^{-5}$  sec but not in this mode
- Gray scale not certain, expected to be limited

(55) Cummins and Luke, IEEE-ED, -18 761 (1971)

### 3.6.2 Gadolinium Molybdate (GMO), $\text{Gd}_2(\text{MoO}_4)_3$

GMO has been considered as a light valve by several authors (58-61). It is a FE similar to BTO and KDP. It can be fabricated in large plates, but has 0.1-2 msec switching times that preclude point addressing, it is ferroelastic and exhibits crosstalk that requires the use of 2 plates. A CR = 50 is possible with a  $15^\circ$  aperture angle. 200V is needed during writing. Thickness is quite critical as is orientation.

### 3.6.3 Lead Germanate (PG)

PG is another FE that has been considered for light valve use. Its transmission is only 3.8% and low  $\eta$  results however. Switching time is also long (4 msec with 23 kV/cm and 30 msec with 10 kV/cm) (62). If crystals of this class (point group 3) with larger rotary power (this is the switching mechanism) than  $5.6^\circ/\text{mm}$  can be found, these materials may be useful, 2 crystal plates are again necessary, however.

## 3.7 POCKELS EFFECT CRYSTALS

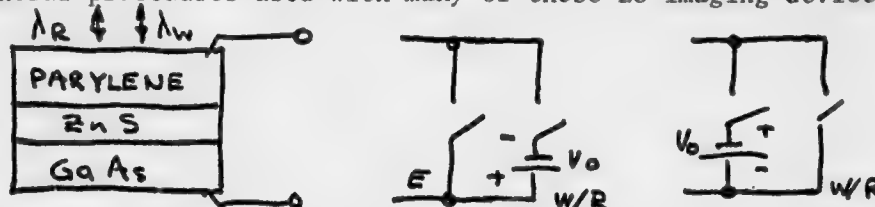
The recording materials that have received the most attention for storage of single images and as optical-to-optical converters are those crystals exhibiting the Pockels effect (linear longitudinal EO effect). They all are generally used in a PC sandwich structure and with readout by reflection.

The resolution of such sandwich structures is considered in Appendix A (see also Section 7.3). The storage time for these various EO materials is considered in Appendix B. The effects of the aperture angle and considerations involving the material's natural birefringence are treated in Appendix C.

- (58) Smith and Burns, Phys. Lett., 28A, 501 (1969)
- (59) Cummins, Ferroelectrics, 1, 11 (1970)
- (60) Kmetz, IEEE, ED-18, 756 (1971)
- (61) Kumada, IEEE, SU-19, 115 (1972)
- (62) Marie and Donjon, Proc IEEE, 61, 942 (1973)

### 3.7.1 Zinc Sulfide

Until 1972, ZnS received attention (63-64) as an image storage material. It is both electro-optic and photoconductive. The sandwich structure used is shown below. Several operating modes are possible and will be discussed to explain the general procedures used with many of these EO imaging devices.



GaAs is opaque, thus W and R must occur from the same side. A dichroic mirror external to the material sandwich separates the W and R light. In the first mode indicated, a voltage  $V_0 C_2 / (C_1 + C_2)$  ( $C_1$  and  $C_2$  are the capacitances of the ZnS and parylene) ( $V_0 = 800V$ ) appears across the ZnS before writing. When illuminated with UV, electron-hole pairs are generated at the ZnS - parylene interface. Electrons flow through the ZnS and decrease the voltage across the ZnS and a negative image appears on RO. Shorting the electrodes erases the image without the need to flood the crystal with light.

For long term storage, the device is primed with  $V_0$  and shorted for writing and reading. With a negative voltage to the GaAs (not a positive one), the electron injecting property of the GaAs-ZnS junction creates a uniform negative charge at the ZnS-parylene interface and erases any prior image. When illuminated with  $\lambda_W$  UV light with the electrodes shorted, the structure is selectively discharged and data stored as a negative. The maximum voltage difference between illuminated and nonilluminated areas is  $V_0 C_2 / (C_1 + C_2)$ . A large  $C_2/C_1$  ratio (i.e., a thin parylene layer) is needed. Reasonable values yield  $C_2/C_1 = 3.4$  and a low 0.1 - 1% modulation efficiency will result. With  $\lambda_W = 340nm$ ,  $S = 10^{-5} J/cm^2$  for CR = 10:1. Transit time is negligible ( $10^{-10}$  sec).

(63) Oliver et al, Appl Phys Lett, 17, 10, 416 (1970)

(64) Oliver and Buchan, IEEE, ED-18, 769 (1971)

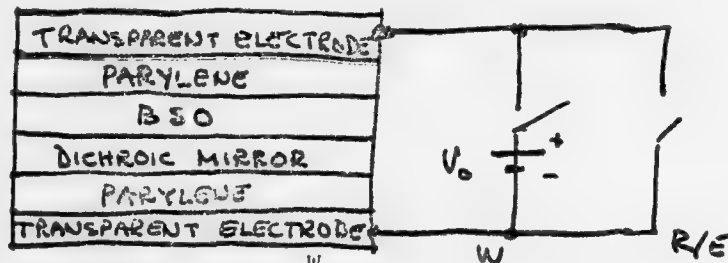
The discharge time constant is (see Appendix B)

$$\tau_D = \tau \left[ \frac{C_1 + C_2}{C_1} \right] = 4.4 \tau = 6 \text{ min}$$

Dark storage of 100 hrs has been observed and RO for 1 hour is possible indicating that the actual value of  $\rho$  for ZnS is  $10^3$  times the value quoted. ZnS is not insensitive to  $\lambda_R$  light. With  $2 \text{ J/cm}^2$  exposures at 633 nm, CR drops to 2:1. Resolution is 85 line pairs/mm = 190 lines/mm even in thick 300  $\mu\text{m}$  samples because the charge layer is localized at the interface. The low  $\eta = 10^{-2} - 10^{-3}\%$  and low storage time of 1 hour under RO are major drawbacks.

### 3.7.2 Bismuth Silicon Oxide (BSO), $\text{Bi}_{12}\text{SiO}_{20}$ (65-66)

BSO is both electro-optic and photoconductive and has a far larger efficiency than does ZnS and a lower half-wave voltage (4KV vs. 13KV). It can be grown in large and thick crystals. An asymmetric structure with parylene on both sides of the BSO with a dichroic mirror on one side for reflex operation allows the induced birefringence to double and cancels the material's optical activity. The mirror transmits the blue or UV.  $\lambda^W$  light (the photosensitivity of BSO peaks between 400-450 nm). At the peak at 420 nm,  $S = 2 \times 10^{-5}$  to  $2 \times 10^{-6} \text{ J/cm}^2$  and depends on the  $\lambda^W$  intensity.



BSO strongly absorbs blue,  $\lambda^W$  light generates electron hole pairs very close to the illuminated surface of the crystal (bottom). With a negative voltage present there during write, the electrons can propagate through the

(65) Vohl et al, IEEE, ED-20, 1032 (1973)

(66) Feinleib and Oliver, Appl Opt., 11, 2752 (1972)

BSO and decrease the voltage across it. If read with  $V^0$  present, a negative image results. If read with  $V^0$  shorted, a positive results since a voltage exists across the BSO only in exposed regions. The holes are essentially immobile and photoconductivity is due to electrons. Thus, to erase the reading side is flooded with UV or blue light. Selective erasure is possible. BSO is sensitive in the visible and low RO energies of  $10^{-4}$  J/cm<sup>2</sup> must be used. An ac bias can decrease RO sensitivity problems. The image decays at a rate (Appendix B).

$$\tau_D = \tau \left\{ \frac{C_1 + C_2}{C_1} \right\} = 3.8 \tau = 15 \text{ min}$$

Dark storage of 2 hours has been observed. However under low  $0.4 \mu\text{W/cm}^2$  633 nm read light, the image decays with  $\tau \approx 20$  min. Cooling the crystal could improve storage time.

The CR between zero and infinite exposure is  $10^4$ . The measurement method used is somewhat questionable however. The MTF is measured by imaging sinusoidal patterns from a Michelson interferometer onto the BSO. The intensity of various diffracted orders are then measured on RO with a He-Ne laser. An aperture much larger than the transform spot was used to measure integrated background noise. Dividing these measured SNR levels by the ratio of aperture size to spot size provides a measure of SNR. SNR values in excess of  $10^5$  at spatial frequencies beyond 100 lines/mm resulted from this method. In earlier work (65) a 50:1 CR resulted after along 40 msec exposure and 1000:1 after voltage decay was complete.

Some fabrication problems exist with the dichroic mirror layer used in reflex BSO devices and with the  $\text{In}_2\text{O}_3$  electrodes. These have been largely overcome but not eliminated.

Bismuth germanium oxide BGO has been operated quite similar to ZnS and BSO but in less depth and with less promising results.

(65) Vohl et al, IEEE, ED-20 1032 (1973)

The resolution obtainable in BSO and similar PC sandwich structures is analyzed in Appendix A.

### 3.7.3 Potassium Dihydrogen Phosphate (KDP) and its Isomorphs

KDP is probably the most widely available EO material exhibiting the Pockels effect and available in large size platelets. Its most common and promising isomorph is potassium dideuterium phosphate (DKDP). Because of their large half-wave voltages at which full  $\pi/2$  phase modulation occurs ( $\approx 7000\text{V}$  for KDP and  $\approx 3500\text{V}$  for DKDP), the crystals are used at their Curie point ( $T_C$ ) where half wave voltages of several hundred volts occur. The very low ( $-150^\circ\text{C}$ ) Curie point for KDP makes it less attractive than DKDP with its higher ( $-55^\circ\text{C}$ ) Curie point that can be reached by Peltier Cells. The temperature dependence of  $\epsilon$ ,  $e$ , and the storage time constant for DKDP as a function of deuteration level is presented in appendix B.

KDP and DKDP have both been successfully electron beam addressed (62, 69). Relatively thick  $250\text{ }\mu\text{m}$  target crystals of DKDP (because of its lower  $T_C = -55^\circ\text{C}$ ) are used. However, the effective crystal thickness is reduced by  $\sqrt{\epsilon_1/\epsilon_3}$  (Appendix B) where  $\epsilon_1$  and  $\epsilon_3$  are the material's transverse and longitudinal dielectric constants. Since  $\epsilon_3$  increases dramatically near  $T_C$  ( $\epsilon_1$  is relatively constant with temperature), the material's effective crystal thickness is greatly reduced and 10 line/mm resolution results. Electron beam addressed DKDP materials have demonstrated  $1000 \times 1000$  point resolution,  $5\text{ }\mu\text{sec}$  rise times, and a complete write and erase cycle of all  $10^6$  points in 30 msec. As shown in Appendix B, the useful storage of DKDP is only a few hours (1-2). KDP would exhibit for longer storage adequate for the intended display (68) but operation at its lower ( $-150^\circ\text{C}$ )  $T_C$  value would result in a much more complex design.

The solution is to control the deuteration level of the DKDP. This is easily accomplished in the crystal growth. As shown in Appendix B, a 72% deuteration level corresponds to a reasonable  $-78^\circ\text{C} = T_C$  level and a 1 day

(62) Marie and Donjon, Proc IEEE, 61, 942 (1973)

(69) Casasent and Sterling, IEEE, TC-24, 348 (1975)

(68) Casasent, IEEE, ED-20, (1973)

storage time. New developments such as  $\lambda/15$  flatness and 25  $\mu\text{m}$  thick DKDP plates that are now possible could increase the resolution to 100 lines/mm. As noted earlier 20,000 point per line electron gun systems have been fabricated (for writing in 1-D on photographic film) and may make such an approach feasible in time. The required electron beam current to write full half-wave voltage in a 1 mil spot in 50  $\mu\text{sec}$  is approximately 50  $\mu\text{A}$ . (Casasent, thesis). The transfer function for output  $I$  vs input  $I_0$  intensity is related to the voltage  $V$  across the crystal by

$$I = I_0 \sin^2(\pi V/K)$$

where  $K$  is the half-wave voltage. The relation is linear for small  $V$  and over a limited region 20-80% of the  $\sin^2$  curve. Gamma correction is easily possible because of the known transfer function and hence linearity should not be a problem.

A more promising DKDP structure (67) consists of a PC-DKDP sandwich. A Se photoconductor is used since DKDP is not photoconductive. The Se-DKDP is sandwiched between electrodes, written from one side and read from the other in reflection. The material's sensitivity is low (100 ergs/cm<sup>2</sup>) its response time (30  $\mu\text{sec}$ ) and erase time (300  $\mu\text{sec}$ ) are also adequate for the intended display. The required operating voltages are much lower (80V) than for BSO. The validity of extrapolating the  $\epsilon$  and Curie constant dependence to  $T_C$  as done in Appendix B may not be valid. But, Marie (62) has demonstrated 150 lines/mm resolution at  $-50^\circ\text{C}$  in a 170  $\mu\text{m}$  thick DKDP-PC structure. The resolution in DKDP improves both because of the variation in  $\epsilon_3$  with temperature causing the lines of force to localize and not spread and because of the PC sandwich structure, (Appendix A). Extrapolating the data of Appendix B to a 25  $\mu\text{m}$  thick DKDP plate, a 7.5  $\mu\text{m}$  thickness should result at  $T_C$  and 3.75  $\mu\text{m}$  spot sizes or 200 lines/mm resolution easily. Control of the deuteration level (Appendix B) can provide adequate storage time. CR values

- (67) J. Donjon, et al, IEEE-ED-20, 1037 (1973)  
 (62) Marie and Donjon, Proc IEEE, 61, 942 (1973)



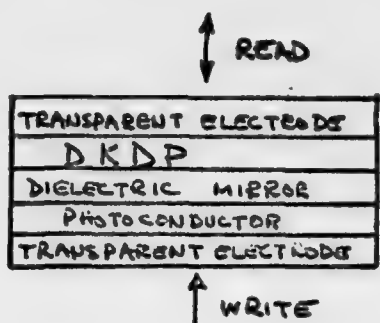


Figure . Optically Addressed DKDP Material Sandwich Structure

of 100:1 have been obtained and large 3" x 3" DKDP plates are possible. This material structure seems most promising and should be more fully pursued.

### 3.8 THICK FERROELECTRICS

This class of FE is characterized by strontium barium nobate (SNB) (70), Lithium niobate (71), and similar materials. In these materials, the writing light directly produces storage rather than generating carriers in the PC thus increasing the conductivity of the PC and switching the voltage across the FE, as in the prior FE-PC sandwich structures.

These thick materials are primarily used for high efficiency and multiple volume phase holograms. The photocarriers are generated in the bulk of the material by absorption of the input write light. These carriers then diffuse

(70) T. Inagaki, et. al., Appl. Opt., 13, 814 (1974)

(71) D. Staebler and W. Phillips, Appl. Opt., 13, 788 (1974)

R	150 lines/mm
A	2" x 2" (3" x 3" possible)
SBP	12,000 lines
CR	100:1
S	100 erg/cm <sup>2</sup>
$\lambda$	visible
T <sub>S</sub>	2 hrs - 1 day (function of deuteration)
$\Sigma$	yes, selective, and total
T <sub>L</sub>	$\infty$
RO	yes
C	80V
K	25-250 $\mu$ m
W	P
V	80V
T <sub>C</sub>	10 $\mu$ sec/point, 300 $\mu$ sec erase

Table 12. Parameters for Laser Addressed DKDP Material Display

or drift to regions of lower light intensity where they are trapped. The fields created by these carriers correspond to the input illumination and locally modulate the material's index of refraction causing modulation of linearly polarized read light. The material's modulation mechanism does not appear to lend itself to point by point addressing. More important, for storage the image must be fixed thermally (LNB) or by applying a field 0.5 sec after exposure (SBN) or by recording at elevated temperature (LNB). Erasure (using heat) of one entire image out of many stored ones has been demonstrated. Erasure is apparently not complete however. Fe doping has allowed great control over S, E and RO.

### 3.9 MAGNETIC BUBBLES

Magnetic bubbles are single magnetic domains (1-20  $\mu$ m) in a thin ferro-magnetic crystal that are mobile in a magnetic field and whose magnetization can be controlled by a magnetic bias field. These materials have been suggested as displays. In this mode, polarizers are needed and readout is by the Faraday effect. With present materials, low rotations, contrast, and

efficiency result. Small sample size (one inch), slow speeds (8 KHz), and questions of gray scale make these materials even less attractive. (72)

### 3.10 METAL FILMS

A concentrated scanned laser beam at  $10^6$  spots/sec has been successfully used to store images on this ( $500\text{\AA}$ ) Bismuth films (73). Spot sizes of  $5\text{ }\mu\text{m}$  were used. 8-10 gray levels were obtained with short (20 nsec) laser pulses in which the image was recorded as an array of discrete holes with the intensity of the laser pulses controlling the size of the holes and the area written linearly with pulse height. The video image data modulated a 450 MHz RF signal with dc bias used to control modulation depth and gray scale.

By raising the temperature of the Bismuth to its vaporization point recording as half tone images is affected but obviously recycling is very hard. Experiments (31) have shown however, that a contained cell can be made in which the material is evaporated between two close proximity surfaces and thus redistributed during recording. Image erasure by exposure to a uniform light pulse that would redistribute the film and cycling for a limited (5-10) number of cycles has been shown. It is not unreasonable that cycle lifetime can be extended, however the limit is not clearly defined.

### 3.11 AMORPHOUS MATERIALS

A variety of amorphous semiconductor materials have been considered for storage and display use. The basic operation of all materials is similar. One bit at a time is stored by illumination with laser pulses of various peak powers and durations. These laser supplied heat pulses switch the state of the thin ( $500\text{\AA}$ ) films from the amorphous to the crystalline state. These two phases have different absorption and reflections and may be optically detected.

Chalcogenide (74) is a typical amorphous material for which  $S = 50 - 150\text{ }\mu\text{J}/\mu\text{m}^2$  or less. Unsymmetric spots (e.g.,  $1 \times 15\text{ }\mu$ ) result

(72) Onyshkeoych et al., RCA. Rev., 35, 216 (June 1974)

(73) D. Maydan, Bell Sys. Tech. J., 50, 1761 (1971)

(31) Bordogna, et.al. RCA REV. 33, 227 (1972)

(74) A. Smith, Appl. Opt., 13, 795 (1974) and other papers in this issue

R = 200 - 1000 lines/mm  
 A = 15 x 15 mm  
 SBP = 3000 now  
 CR = 8 - 10 gray levels  
 S = 50 - 60 mJ/cm<sup>2</sup>  
 T = visible  
 T<sub>s</sub> = yes  
 E = not selective, erasure hard  
 T<sub>2</sub> ?  
 RO = yes  
 K = 500 Å  
 W = P  
 V = none  
 Tc = 10 cycles, 10<sup>6</sup> spots/sec

Table 13. Parameters For Laser Addressed Thin Metal Film Display

Risks - maximum size unclear  
 - no selective erasure  
 - 10 cycle life (possibly more)

however, (500 lines/mm). Power levels and pulse durations are quite critical but erasure is possible. The degree of crystallization is a measure of gray scale. Optical contrast is only 2:1 while electrical contrast is 10:1 or 100:1. To obtain high contrast, a mechanical (dry stripping) or chemical etching step is needed (0.5 sec). Individual spots can be addressed in nsec times however. (75)

### 3.12 PHOTOCHROMIC (PC) AND PHOTODICHROIC (PD) MATERIALS

Color center defects can be intentionally introduced into many of the alkali halides. These color centers have specific absorption spectra, which when properly chosen exhibit two separate bands, one in the UV and the other in the visible (usually). When illuminated in the UV band (write band), the

(75) S. Ovshinsky and P. Klose, J. SID 13/4 (1972) p. 189

crystal's absorption in the visible (read band) changes as centers of one type switch to another. By proper illumination in the second band, the centers can be reconverted. The advantages of this material as a display are its ultra-high resolution, essentially diffraction limited. It is a thick material however, ( $\leq 0.1\text{mm}$ ) although ion implanted samples  $10\text{ }\mu\text{m}$  thick have recently been fabricated (of low color center concentration however). Its classic disadvantages are poor S, write and read light restricted to specific wavelength bands, decay, fatigue and temperature control. For this application,  $S = 200\text{--}300\text{ mJ/cm}^2$  is possible now and adequate since  $1\text{ }\mu\text{m}$  spots will be used. Room temperature crystals also exist now. Contrast, has been improved by use of an extinction writing scheme. Use of the dichroism of higher order color centers with a preferred dipole moment direction (i.e., photodichroic rather than photochromic effects) has overcome most of the prior material disadvantages.

One example (76) of a photochromic of high promise is salicylideneaniline. It is written on near  $380\text{ nm}$  and read near  $480\text{ nm}$ . A stored image has a life of 30 hours (dark storage). Crystals have been used for 3 years with no fatigue. Maximum  $\eta$  is only 0.7% but  $R = 3300\text{ lines/mm}$  (measured holographically). This resolution is typical of all PC and PD materials. CR can exceed 10,000 with extinction writing. Operation for over  $5 \times 10^4$  cycles with no degradation and 30 nsec response have been reported. Gray scale is present and adequate (78). The material's resistance to constant RO (not dark storage) is not explicitly noted, but low power levels must be used. Care must be taken in writing not to heat the material since it melts at  $50^\circ\text{C}$ .

Use of the dichroism of higher order centers such as the M and  $M_A$  centers particularly in NaF are of more importance (77). The modulation is now dependent on the polarization of the read and write light. Fatigue and other crystal parameters improve remarkably when the photodichroic nature of the centers is used. Although present samples are only  $1'' \times 1''$ , large PD materials of

(76) D.S. Lo, Appl. Opt., 13, 861 (1974)

(78) D. Casasent & F. Caimi, to be published

(77) I. Schneider, Appl. Opt., 10, 980 (1971)

excellent quality have been fabricated for laser windows. The wavelength and polarization for the write/read/erase (and alignment) steps are noted in the table below. The write wavelength  $\lambda_R$  is about 500 nm.  $P_0$  and  $P_1$  refer to orthogonal polarization directions.

<u>Operation</u>	<u>Wavelength</u>	<u>Polarization</u>	<u>Results</u>
Alignment	$\lambda_W$	$P_0$	All centers in state 0
Write	$\lambda_W$	$P_1$	Light (dark) areas in state 1 (0)
Read	$\lambda_R$	$P_0$	Output is replica of input
	$\lambda_R$	$P_1$	Output is inverse of input
Erase	$\lambda_W$	$P_0$	All centers in state 0

A new suppressive writing procedure (78) whereby coherent UV is not needed for writing and a coherent focused and scanned UV beam is not needed, has been developed. The only change in the above table is the write operation which now becomes:

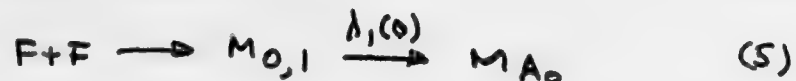
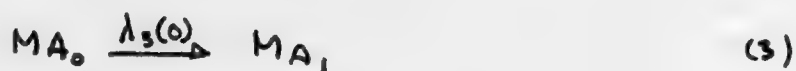
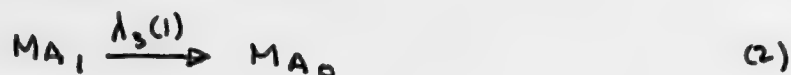
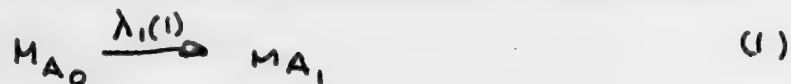
Write	$\lambda_W, \lambda_R$ (information on $\lambda_R$ beam)	$P_1$	$\lambda_R$ and $\lambda_W$ areas in state 0
-------	--	-------	--

In this case, the crystal is flooded with broadband  $\lambda_W$  light during write as well as read. The amounts of  $\lambda_W$  and  $\lambda_R$  light are determined from the material's (NaF) H-D curves (79). The  $\lambda_R$  beam is now modulated with the data to be written (not the UV beam at  $\lambda_W$ ). The centers present in those areas of the crystal when both the  $\lambda_R$  and  $\lambda_W$  light are present in the proper (not equal) amounts, the centers maintain a preferred dipole moment in direction 0

(78) E. Casasent & F. Caimi, to be published

(79) D. Casasent & F. Caimi, to be published

(no change). Those dark areas of the image or data to be recorded (where there is no  $\lambda_R$  light) switch to state 1. These states can easily be detected by polarizers. In our actual experimental system,  $\lambda_R = \lambda_3 = 506$  nm was polarized at  $45^\circ$  to the directions of states 1 and 0. We also distinguish the effects of  $\lambda_W$  light at  $\lambda_1 = 340$  nm and  $\lambda_2 = 310$  nm. The following transition equations explain the processes occurring in the crystal.



Equations (2) and (3) result because the  $\lambda_3$  light is polarized at  $45^\circ$  to the  $\lambda_1$  light. The transitions in (4) and (5) are observed as a loss in  $M_A$  centers (this loss is retrievable however) and a growth in the F band. Eq. (5) expresses the subsequent recovery of the M centers by  $\lambda_1$  light by aggregation. Eqns (1) and (3) produce  $M_{A_1}$  centers that contribute to the reaction in (2) and the  $M_{A_0}$  centers produced in (2) enter the transitions in (4) and (5). Basically,  $\lambda_W$  write light converts  $M_0$  centers to  $M_1$  centers, while  $\lambda_3$  light (where present) converts them back to  $M_0$  centers. The effects of  $\lambda_W$  are thus suppressed by  $\lambda_R$ .



Tabulated data for NaF at room temperature follow:

R	over 2000 lines/mm
A	1 x 1 cm <sup>2</sup> now
SBP	20,000
CR	60 minimum
DR	6 minimum
S	150-400 mJ/cm <sup>2</sup>
T	write $\leq$ 320nm, read $\leq$ 500nm
$T_L = T_C = T_S$	10 <sup>6</sup>
E	yes
RO	yes, but limited
$\eta$	1%
K	0.1mm, 10 $\mu$ m ion implanted
W	P or H, phase
V	no

Table 14. Parameters for Photocidhroic Display

Risks - reproducibility and RO fatigue need more testing  
 - size not yet above 1"

This material was chosen for initial tests because it was readily available and because thin samples of adequate concentration of M centers can be fabricated. Coloration by well controlled and lower energy particles can yield lower depths of coloration and hence effectively thinner crystals that can be recorded on by a conventional scanned, modulated, and focused laser beam.

The material's sensitivity is not as low as others. Its size, resistance to RO fatigue, and reproducibility of data are other issues of concern.

### 3.13 SUMMARY

The results of the materials study Part 2 (Sections 10-20) are summarized below.

TP - Heat development by second laser beam and interferometric writing with two laser beams are required. Too complex of a system and too many unproven points exist. Conclusion: Rejection.

Other Deformable Materials - No storage. Conclusion: Rejection.

MO - Gray scale possible only in thermoremanent writing which has received little attention. Precise laser power, amplitude, and duration needed because of thermomagnetic writing. Diffraction efficiencies are very poor. Conclusion: Rejection.

LC - Thermo-optic writing is most feasible method but gray scale is possible only by a half-tone image and resolution is low. Conclusion: Possible but reject compared to others.

PLZT - All have too low an R and CR and 100  $\mu$ sec rise times. The strain bias mode of the Ferpac has severe fabrication and uniformity problems as does the Cerampic and Fericon. The Fericon is the most feasible if nonuniformities are optically (holographically) or otherwise connected. Conclusion: Rejection.

BTO - Very severe fabrication problems and limited gray scale. Conclusion: Rejection.

GMO - Slow 0.1-2 msec response. Conclusion: Rejection.

PG - Slow 4 msec response. Conclusion: Rejection.

Zns - RO of only 1 hour and low  $\eta = 10^{-3}\%$ . Conclusion: Rejection.

BSO - RO of only 15 min. Conclusion: Rejection.

DKDP - PC structure is promising. Conclusion: Test it.

- Electron beam addressed possible. Conclusion: More analysis needed, PC-DKDP more promising at present.

Thick FE - Not point-by-point writing. Conclusion: Rejection

Bubbles - Slow, questionable gray scale, rather undeveloped. Conclusion: Rejection for now.

Metal Film - Limited life. Conclusion: Rejection.

Amorphous - Low CR. Conclusion: Rejection.

PD - NaF merits attention to thin layers, fatigue on RO, reproducibility and cycle lifetime. Conclusion: Test it.

### 3.14 CONCLUSIONS

Deformable materials - Poor: Thermoplastics are the most promising but methods of point-by-point heat development and carrier (low spatial frequency) recording must be developed, reproducibility is questionable, latent image problems occur, and the support control and monitoring system is quite complex.

Magneto Optic - Good: Thermoremanent writing on  $M_n B_i$  and  $CrO_2$  is the most promising scheme but low  $\eta = 10^{-2}\%$  and CR of 8:1 should be expected. This method has only received limited attention and may require considerable development.

Liquid Crystal - Good: Thermo-optic recording coupled with new 2  $\mu m$  thick LC technology may be acceptable, with 5-10,000 line resolution maximum with some development. Speed of response, storage, SNR, gray scale, and similar questions remain. None seem really major but will require development, but not necessarily breakthroughs.

PLZT - Poor: Material problems, but can possibly holographically correct.

KDP - Possible with  $-78^\circ C$  operation of PC-DKDP.

Bi Films - Poor: Not yet easily recyclable.

Photodichroic - Good: Reproducibility and fatigue questionable. Thin samples necessary.

### 3.15 APPENDICES

#### 3.15.1 Resolution in Thick E-O Materials

The resolution in a simple thin recording material is approximately half the material's thickness. The resolution in thicker materials and more complex sandwich structures is more difficult to vigorously predict.

For the case of electron beam addressed KDP and DKDP (Section 15.3) the resolution as a function of temperature is well understood (68) (See Appendix B). The effective crystal thickness has been shown (68) to decrease by a factor of  $\sqrt{\epsilon_1 / \epsilon_3}$ .

The resolution of sandwich structures is definitely higher than one-half the thickness. With two layers of  $\epsilon_a$  and  $\epsilon_b$ , the effective thickness of the modulating material seems to be reduced by about  $\epsilon_a / \epsilon_b$  (Section 7.3). The actual analysis is more complex and follows shortly. First however, several more qualitative arguments to explain the increased resolution in BSO are advanced to provide some insight into the process that occurs in the structure.

Because of the electrostatic field present in BSO during writing, the photo-generated carriers seem to be transported along lines of force normal to the crystal faces with little or no lateral spreading. Photogenerated carriers of opposite polarity are separated and trapped in two thin layers at the two BSO-parylene interfaces creating an electrostatic image pattern. The effect of readout resolution can also be seen by realizing that the thickness of the crystal is so large compared to the insulating layers (parylene) that the problem reduces to a planar charge distribution separated from a ground plane by the thickness of the parylene. The voltage drop across the EO crystal equals the potential difference of each interface layer relative to the grounded electrodes (at signal ground). Thus the interface potential distribution corresponds to the interface charge distribution as long as the parylene is thinner than the minimum spatial resolution in the stored image pattern.

In a carrier diffusion analysis, the photogenerated ion-electron pairs (only electrons are mobile) drift. Some electrons drift as far as the crystal's surfaces where their charge accumulates. Most are trapped in the bulk of the crystal. The front region (that was illuminated and where the electrons were created) is depleted and becomes positive. The inner regions of the crystal (where the electrons are trapped) becomes negative. The field

(68) Casasent, IEEE, ED-20, (1973)

created by this charge separation opposes further electron drift and the photoconductivity drops on further exposure. Resolution is also observed to increase with exposure, probably again due to a nonuniform exposure throughout the crystal's thickness. Most of the exposed light is absorbed in the front of the crystal and the field there decays to zero. The back surface is then a thin crystal (with better resolution) but receives only part of the light (with poorer sensitivity).

A more rigorous analysis (Lipson, Recyclable Incoherent-to-Coherent Image Converters, Chap. in Advances in Holography, M. Dekker Publisher, N.Y. to Appear, 1976) follows.

The field distribution in a crystal slice is usually determined by a surface charge distribution. The field is read out optically in transmission (one pass) or reflection (two passes) by a light beam whose phase is varied by the E-O effect in the crystal. The total phase shift of the read beam is the integral of the E-O effect along the light path in the crystal. For a linear E-O effect the phase shift on each pass is

$$d\phi = \int \alpha E ds = \alpha dV$$

where  $dV$  is the voltage difference between the light's entrance and exit points and  $\alpha$  is a constant. The shift  $d\phi$  depends only on the voltage difference  $dV$ .

A surface charge distribution of spatial frequency  $K$  produces an electric field distribution in the medium that decays (A) exponentially with depth with characteristic distance  $(1/K)$ . High spatial frequency signals thus modify only the crystal surface. This occurs because

$$V(x,y) = \cos Kx \exp(\pm Ky)$$

is a solution of Laplace's equation in this case.

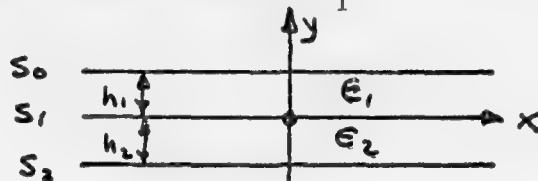
The effects of this field fringing on the MTF of a thick E-O crystal exist (B) but are unpublished. The analysis follows. The two-layer sandwich

- (A) J.D. Jackson. Classical Electrodynamics, Wiley, N.Y., 1962, Chap 2.  
 (B) Itek Tech. Rept. 71-5236-03, 1971

structure below and geometry are assumed. Surfaces  $S_0$  and  $S_2$  are assumed to be at ground (signal ground) and a sinusoidal charge distribution

$$\sigma(x) = \sigma_0 (1 + \cos Kx) / 2$$

is assumed to exist at surface  $S_1$ .



Assuming a linear superposition of solutions of the prior form of  $V(x, y)$  in each layer and appropriate boundary conditions ( $S_0 = S_2 = 0$ ,  $S_1 = \sigma(x)$  above), the potentials  $V_1$  in the top layer and  $V_2$  in the bottom layer are

$$V_1(x, y) = \cos Kx [a \sinh K(y - h_1)] + c(y - h_1)$$

$$V_2(x, y) = \cos Kx [b \sinh K(y + h_2)] + d(y + h_2)$$

At  $y = 0$  (layer  $S_1$ )

$$\epsilon_1 (dV_1/dy) - \epsilon_2 (dV_2/dy) = \sigma(x)$$

$$V_1(x, 0) = V_2(x, 0) = V(x, 0)$$

from which  $V(x, 0)$  at layer  $S_1$  is

$$V(x, 0) = -\frac{1}{2} \sigma \left[ \frac{1}{(\epsilon_1/h_1) + \epsilon_2/h_2} + \frac{1}{K(\epsilon_1 \coth K h_1 + \epsilon_2 \coth K h_2)} \right]$$

The normalized MTF is defined by

$$MTF = \frac{m(\text{out at } K)}{m(\text{in at } K)} \bigg/ \frac{m(\text{out at } K=0)}{m(\text{in at } K=0)}$$

where  $m(\text{out})$  and  $m(\text{in})$  are the input and output modulation. Assume  $\sigma$  is directly related to the input (with no  $K$  terms) and since  $d\phi = \alpha dV$  depends only on the voltage difference between crystal faces, we obtain

$$MTF = \frac{(\epsilon_1/h_1) + (\epsilon_2/h_2)}{K(\epsilon_1 \coth K h_1 + \epsilon_2 \coth K h_2)}$$

### 3.15.2 Storage Time of FE Materials

The intrinsic time constant of the materials to be evaluated is determined by their relative dielectric constant  $\Sigma_c$  and resistivity  $\rho_c$  where the subscript c denotes the c or optic axis of the crystal

$$\tau = \epsilon_c \rho_c / 36\pi \times 10^{11}$$

These parameters for various materials are listed below. For KDP and its isomorphs several values at different temperatures and deuteration levels are given.

	KDP	DKDP	DKDP	DKDP
% Deuteration	0	98	98	72
Temperature °C	20	20	-52	-78
$\Sigma_c$	21	54	600	600
$\rho_c$ (r-cm)	$4 \times 10^{10}$	$4 \times 10^{10}$	$4.5 \times 10^{13}$	$2 \times 10^{15}$
T(sec)	0.08	0.2	2400	$10^4$
	Zns	ZnSe	BGO	BSO
$\Sigma_c$	9	9	40	56
$\rho_c$ (r-cm)	$10^{14}$	$10^{10}$	$8 \times 10^{10}$	$5 \times 10^{13}$
T(sec)	80	0.008	0.28	250

Table 11.  $\Sigma$ ,  $\rho$ , and T Values For Various Ferroelectrics

These values are theoretical. In practice larger discharge time T values result because of the capacitances of the various dielectric layers present in the actual device structures used. The Curie point of DKDP drops as the deuteration level increases and its storage time and resolution increase.

Other features of the second group of ferroelectric-photoconductive materials are that BGO and BSO are optically active ( $22^\circ/\text{mm}$ ) so that thin plates or compensation canceling schemes must be used. In all cases, non-destructive RO requires that write ( $\lambda_w$ ) and read ( $\lambda_R$ ) light be different.  $\lambda_R$  must not fall within the high photosensitive spectral region of the material. This will reduce write and read interaction. A sharp PC band



edge is needed (but not sufficient as we will see).  $\lambda_W$  is usually in the blue or UV and  $\lambda_R$  in the red or visible.

The discharge time constant  $\tau = \epsilon \epsilon_0$  for KDP and its isomorphs increases as temperature  $T$  approaches the Curie point  $T_c = -50^\circ\text{C}$  for DKDP and  $-150^\circ\text{C}$  for KDP. Resolution also increases as  $T$  approaches  $T_c$ . Resistivity (longitudinal  $\rho_3$  and transverse  $\rho_1$ ) for KDP varies with  $T$  as

$$\text{Log}_{10} \rho_3 = 1.27 + 2740/T \quad \Omega\text{-cm}$$

$$\text{Log}_{10} \rho_1 = 1.85 + 2740/T \quad \Omega\text{-cm}$$

The dielectric constant has a Curie-Weiss dependence

$$\epsilon_3 = 4.5 + 3122/(T - T_c)$$

The transverse  $\tau_1$  and longitudinal  $\tau_3$  time constants for stored charge for clamped KDP and DKDP plates as a function of temperature follow (68).

KDP	T	=	25°C	0°C	-50°C	-150°C
$\tau_3$	in sec		0.056	0.44	110	$4.6 \times 10^{13}$
$\tau_1$	in sec		0.053	0.32	38	$9.7 \times 10^{10}$
DKDP	T	=	25°C	0°C	-25°C	-50°C
$\tau_3$	in sec		0.11	1.1	20	2700
$\tau_1$	in sec		0.07	0.4	3.5	60

Pure or lightly deuterated KDP should thus be capable of the required storage time. The only associated problem is maintaining the low  $-150^\circ\text{C}$  operating temperatures.

The material may be electron beam or optically addressed point-by-point. The crystal's thickness  $d$  affects resolution. However, the effective thickness  $d^* = d/\sqrt{\epsilon_3/\epsilon_1}$  also varies with  $T$ . Present materials are 10 mils and 170  $\mu\text{m}$  thick. New technology can produce 25  $\mu\text{m}$  thick crystals. While

(68) Casasent, IEEE, ED-20, (1973)

$\sqrt{\epsilon_3/\epsilon_1} = 1$  at  $25^\circ\text{C}$ , it increases greatly as  $T$  decreases, thus reducing the crystal's effective thickness and thus increasing its potential resolution. The crystal's thickness is reduced by the factors below as functions of temperature.

KDP at T	=	$25^\circ\text{C}$	$0^\circ\text{C}$	$-50^\circ\text{C}$	$-150^\circ\text{C}$
$d^1/d$ ratio		1.41	1.26	1.23	0.3
DKDP at T	=	$25^\circ\text{C}$	$0^\circ\text{C}$	$-25^\circ\text{C}$	$-50^\circ\text{C}$
$d^1/d$ ratio		1.17	1.0	0.75	0.3

A 72% deuteration level would result in  $T_c = -78^\circ\text{C}$  and a storage time of over one day.

### 3.15.3 Natural Birefringence Effects

Many crystals are uniaxial with no field and have a natural birefringence. The CR is thus dependent on the aperture angle of the light beam. A general derivation for the effects of a light ray making an angle  $\theta$  with the crystal's  $a$  axis (the  $c$  axis is the optic axis of modulation). With an angle of incidence  $i$ , the indices of refraction are  $\eta_0$  and

$$\eta' = \eta_0 + \left( \frac{\eta_e^2 - \eta_0^2}{2\eta_e^2\eta_0} \right) \sin^2 i$$

An input polarizer is used. Light in the crystal divides into components proportional to  $\cos \theta$  and  $\sin \theta$  that propagate at velocities dependent on  $\eta_0$  and  $\eta^1$ . After a length  $d$  of crystal, the components have a phase shift.

$$\psi = \frac{2\pi d}{\lambda} \left( \frac{\eta_e^2 - \eta_0^2}{2\eta_e^2\eta_0} \right) \sin^2 i$$

The crossed output polarizer transmits part of each component proportional to  $\pm \cos \theta \sin \theta$  with  $\eta^e$  and  $\eta_0$  respectively or

$$T = \sin^2 2\theta \sin^2 \left( \frac{\psi}{2} \right)$$

With  $\psi$  and  $i$  small,

$$T = \left( \frac{\pi d}{\lambda} \right)^2 \left( \frac{n_e^2 - n_o^2}{2 n_e^2 n_o} \right)^2 i^4 \sin^2 2\theta$$

With the input light constant in a cone apex angle  $\alpha$ , the average transmittance is

$$\overline{T} = \left( \frac{\pi d}{\lambda} \right)^2 \left[ \frac{n_e^2 - n_o^2}{2 n_e^2 n_o} \right]^2 \frac{\alpha^4}{96}$$

Using DKDP values with  $d = 0.25\text{mm}$  and  $\lambda = 550\text{nm}$

$$\overline{T} = 27\alpha^4$$

With  $\alpha = 8^\circ$  aperture angle,  $\overline{T} = 0.01$ . The maximum linear transmittance is 0.75 and  $CR = 75$  then. This effect can be compensated for by better collimated light and better alignment or by use of a compensated crystal plate.

The modulation efficiency  $\eta$  drops (62) if the aperture angle exceeds  $20^\circ$ . Below  $15^\circ$ , the effect is negligible. Below  $20^\circ$ , it is acceptable.

(62) Marie and Donjon, Proc IEEE, 61, 942 (1973)

#### 4.0 EXPERIMENTAL MEASUREMENTS IN NaF

Measurements of display oriented properties of NaF crystal samples were made.

##### 4.1 PHOTODICHROISM CHARACTERISTICS

NaF samples were exposed to UV radiation at 350.7 and 356.4 nm from a krypton ion laser equally polarized along the  $[011]$  and  $[0\bar{1}1]$ , crystallographic axis. After exposure to a 2 cm diameter 70 mw beam for 1800 sec, the spectral absorptivity of the sample was measured. The results are shown in Figure 4.1 in the curve marked (1, 11). The absorption spectra indicates a maximum at 520 nm and a spectral bandwidth of approximately 40 nm.

The sample was subsequently exposed with the polarized UV laser beam along the  $[011]$  crystal direction, and the resulting absorption spectrum is shown on Figure 4.1 in the curve marked (11). The absorption spectrum for oppositely polarized viewing light is described in the curve marked  $\perp$ . The useful display characteristics result from the difference in absorption characteristics for 11 and  $\perp$  polarized viewing light.

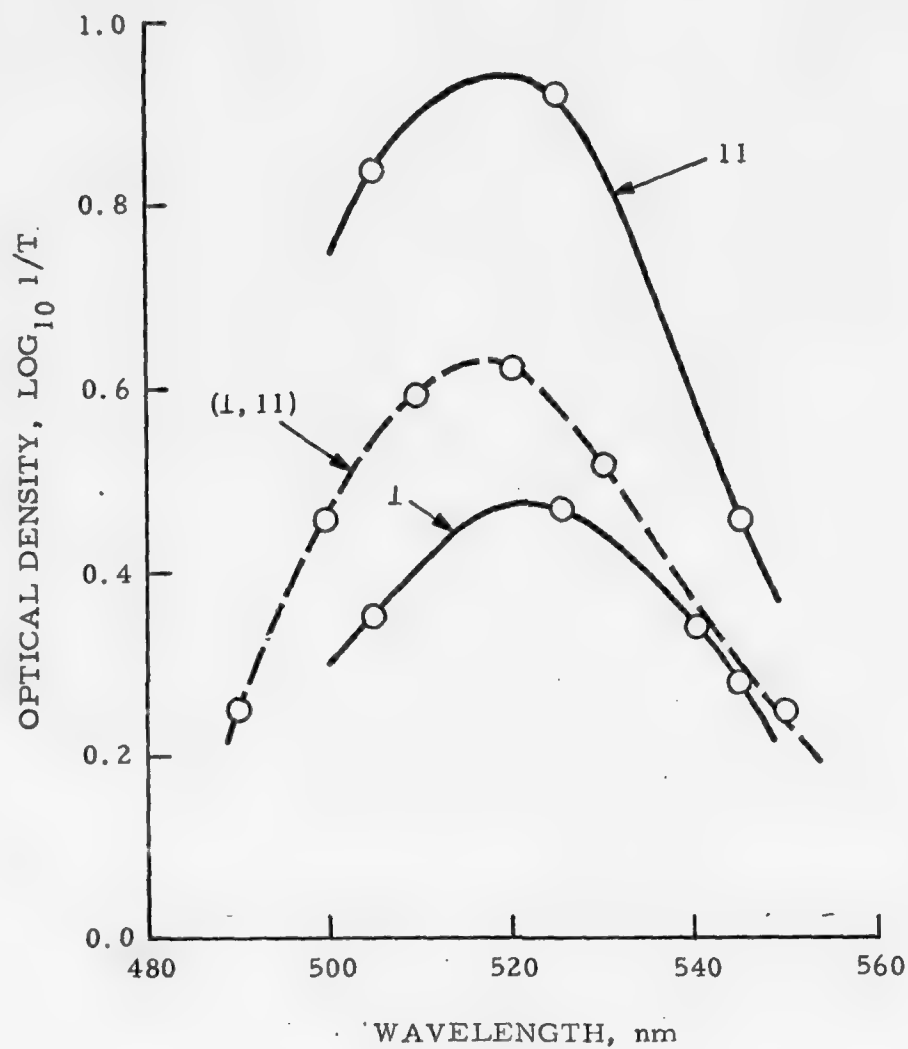
The NaF dichroism in the measured sample exhibited a decay as a result of exposure to the viewing light. Figure 4.2 shows the results of the decay measurement. The NaF sample was exposed to UV laser light polarized along the  $[011]$  direction, and the absorptivity at 505 nm wavelength polarized in the  $[011]$  and  $[0\bar{1}1]$  direction was measured as a function of exposure duration to the 505 nm viewing light.

##### 4.2 RESOLUTION CHARACTERISTICS

A 1 mm thick NaF crystal was contact printed using a bar pattern resolution test chart and a randomly polarized incoherent UV light source. The resulting imagery was observed between crossed polarizer with a microscope.

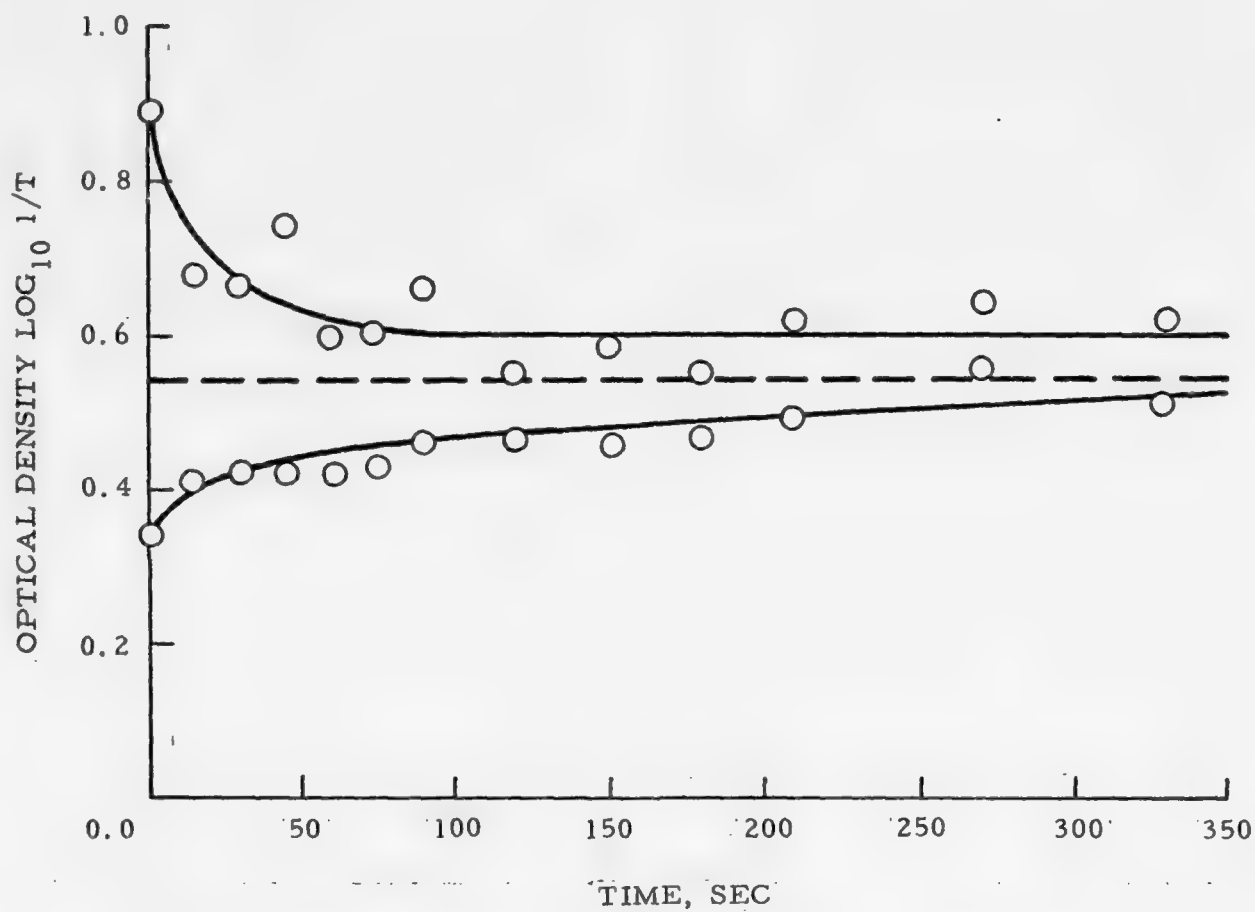
For low exposures, the limiting resolution of the imagery was in excess of 100 lp/mm.

For longer exposure to the UV imaging source, the limiting resolution decreased by an order of magnitude.



#### ABSORPTION SPECTRA IN NaF CRYSTAL

- 11, Sample exposed to UV light polarized along  $[011]$  direction and measured with  $[011]$  polarized light
- 1, Measured with  $[0\bar{1}1]$  polarized light
- (1, 11) Exposed to randomly polarized UV and measured with  $[011]$  and  $[0\bar{1}1]$  polarized light.



Decay of Dichroism as a Result of Exposure to Viewing Light

These results were observed because the image depth within the NaF sample is a function of the total incident exposure intensity. For exposure formed an image only near the surface of the contact printed sample and effectively behaved as a thin sample of NaF. Longer exposures apparently produce an image with a greater depth extent within the crystal, which causes a loss of resolution.



## 5.0 ULTRA HIGH RESOLUTION DISPLAY SYSTEM CONCEPTS

### 5.1 OVERALL SYSTEM DESCRIPTION - ULTRA HIGH RESOLUTION RECORDER - DISPLAY SYSTEM (UHRRDS)

5.1.1 The following system concept describes an ultrahigh resolution recording-display device (UHRRDS). The device receives a digital data bit stream organized in a line-at-a-time format and converts this data into a high resolution grey tone pictorial image on a viewing screen.

The UHRRDS is comprised of a controller section (UHRRDC) and a recording-display section (UHRRD). The normal data input to the UHRRDS comes from a digital tape recorder (DTR). The controller section provides a reference clock signal to synchronize the DTR with the scanning mirror.

### 5.2 CONTROLLER SECTION (UHRRDC)

The UHRRDC accepts serial data from the DTR or an equivalent digital data source and processes these data to produce the required parallel data output which is then fed to the video D/A converter of the recorder section.

#### 5.2.1 Input Logic - General Description

The input logic and buffers encompass that portion of the UHRRDC related to accepting the data from the DTR and storing the data until it is required by the output. The input logic has been divided into seven units, each of which is discussed in some detail on the following pages.

- All clocks for this portion of the UHRRDC are based on the DTR furnished input clock.
- All buffers are made up of RAMs. The prime reason for not using shift registers is that static shift registers are too slow, and dynamic shift registers require periodic refreshing when the system is operated at the lower bit rates.

- All RAMs are bipolar. This eliminates the interfacing problems associated with using mixed TTL and MOS technology; accommodates the high data rates with a minimum of parallelism; and simplifies packaging by having only 16-pin IC packages with the standard pins assigned to VCC and ground.
- All logic is straightforward, using primarily MSI and LSI TTL integrated circuits.

#### 5.2.1.1 Input Registers

There are two input registers as shown in the diagram:

- 32-bit Serial-to-Parallel Conversion Register
- 8-bit Buffer Register

The Serial-to-Parallel Conversion Register is 32-bits long and operates at rates from 500 kHz to 20 MHz. All 32 bit parallel outputs from this register are connected to the Frame Synchronization logic (see Page 2-10); and 8-bits to the Buffer Register described below.

The 8-bit Buffer Register serves two purposes:

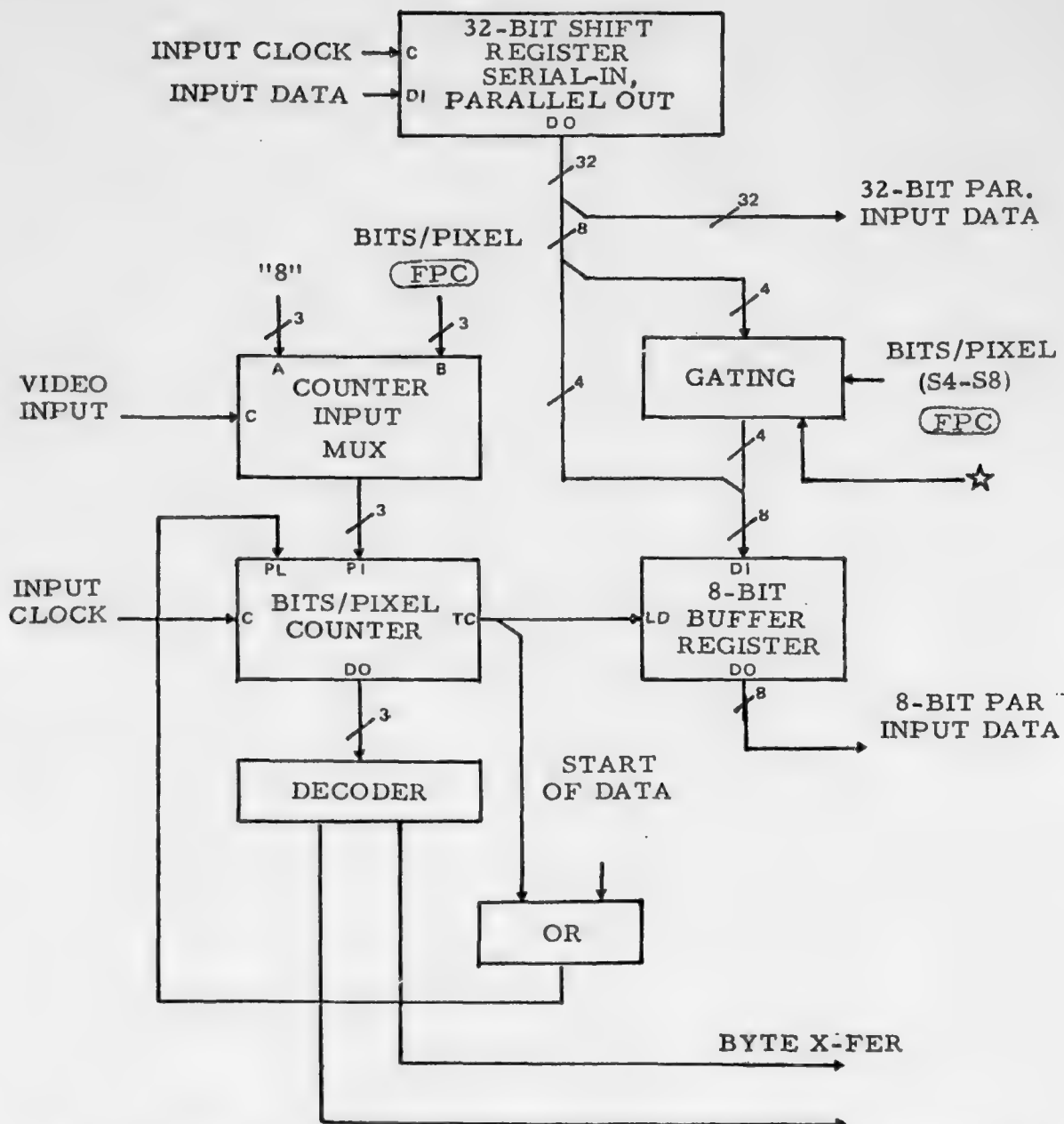
- Holding the data steady for a minimum of 200 ns, thus allowing the use of slower logic from this point on.
- Breaking up the input bytes into pixels by means of gating as shown in the diagram.

The input register logic is shown in the diagram. In order to translate from bytes to pixels, the buffer is loaded every 4, 5, 6, 7 or 8 bit times. This is controlled by the Bits/Pixel counter and the associated counter input multiplexer. The Bits/Pixel counter is set on the front panel control (FPC). The decoder on the output of the counter generates the controls for the loading of the data into the Tick Mark, Annotation, and Video Data Buffers.

#### 5.2.1.2 Central Input Controls

The central input control circuitry primarily handles the proper routing of all incoming data. It generates the following signals:

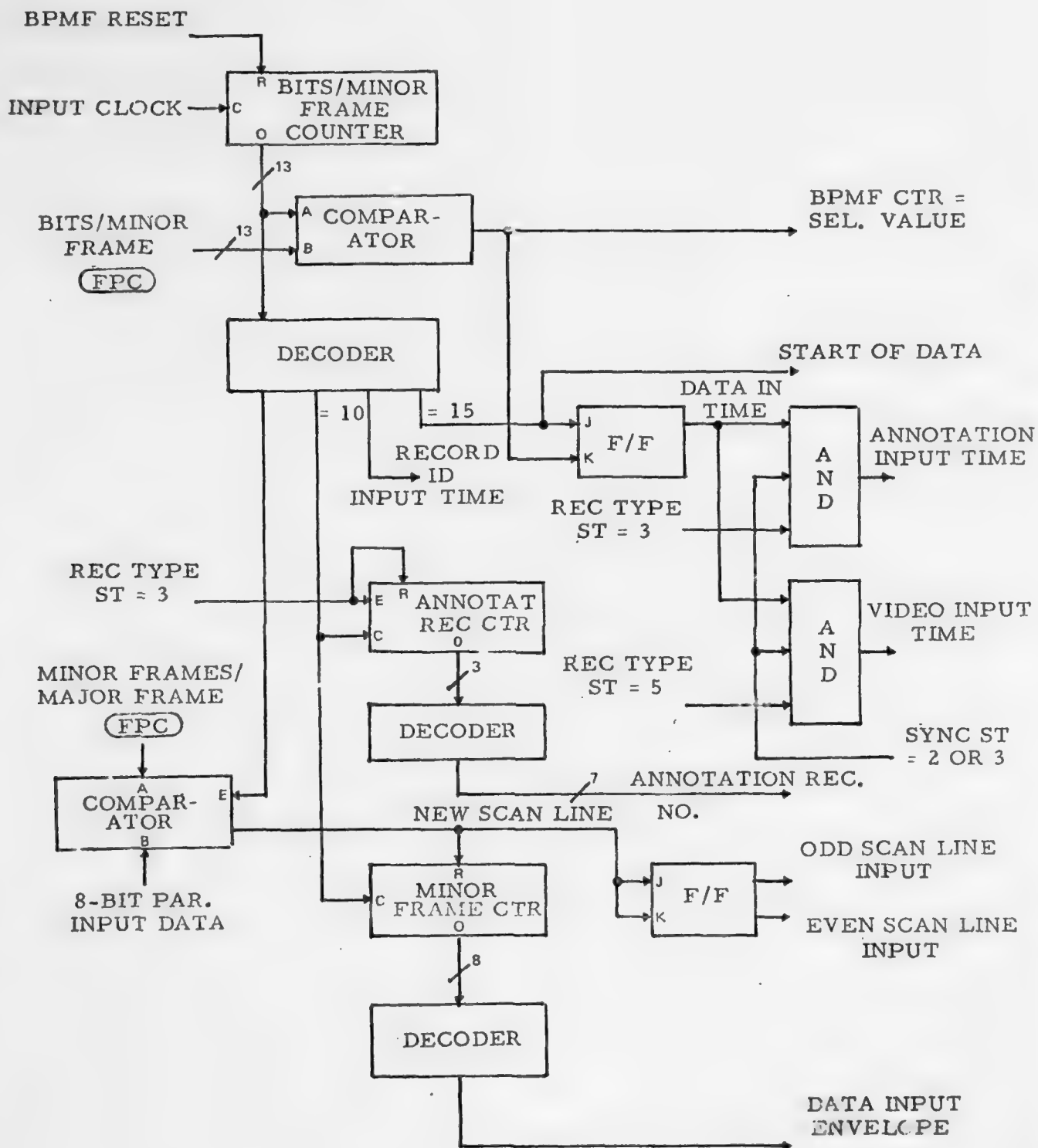
- Bits/Minor Frame Counter = selected value
- Start of Data
- Video Input



- ★  $B5 = D5 \cdot (S5 + S6 + S7 + S8) + \text{VIDEO IN}$   
 $B6 = D6 \cdot (S6 + S7 + S8) + \text{VIDEO IN}$   
 $B7 = D7 \cdot (S7 + S8) + \text{VIDEO IN}$   
 $B8 = D8 \cdot S8 + \text{VIDEO IN}$

BYTE WRITE ENABLE

INPUT REGISTERS



CENTRAL INPUT CONTROLS

- Record ID Input
- Odd vs. Even Scan Line Input
- Data Input Envelope

The method for generating these signals are straightforward, as shown in the diagram.

#### 5.2.1.3 Frame Synchronization

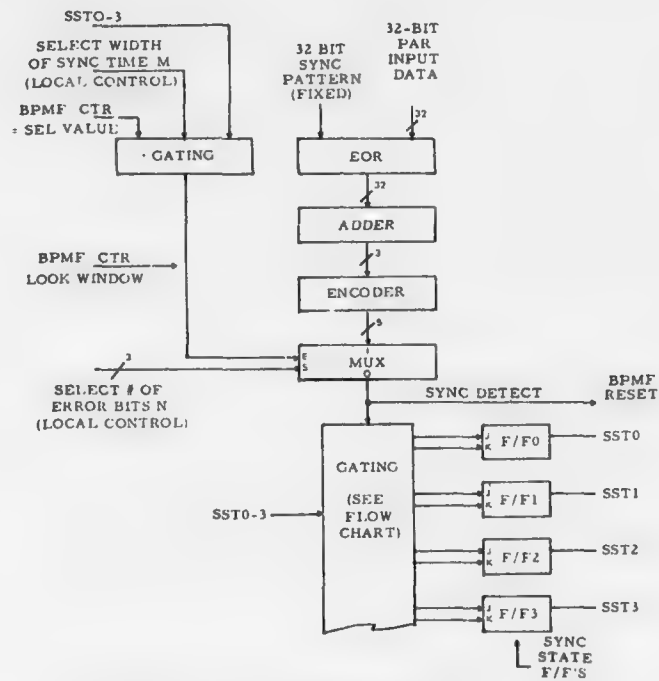
One of the most critical areas of the system is to have a method of establishing sync correctly and maintaining same in spite of occasional noise bursts in the incoming data. The flow chart shows the proposed synchronization process.

Initially, the system is in a search-for-sync state; then, upon detecting a correct 32-bit sync pattern, a trial-acquire state is entered. After seeing a second sync pattern at the correct interval, the in-sync state is entered.

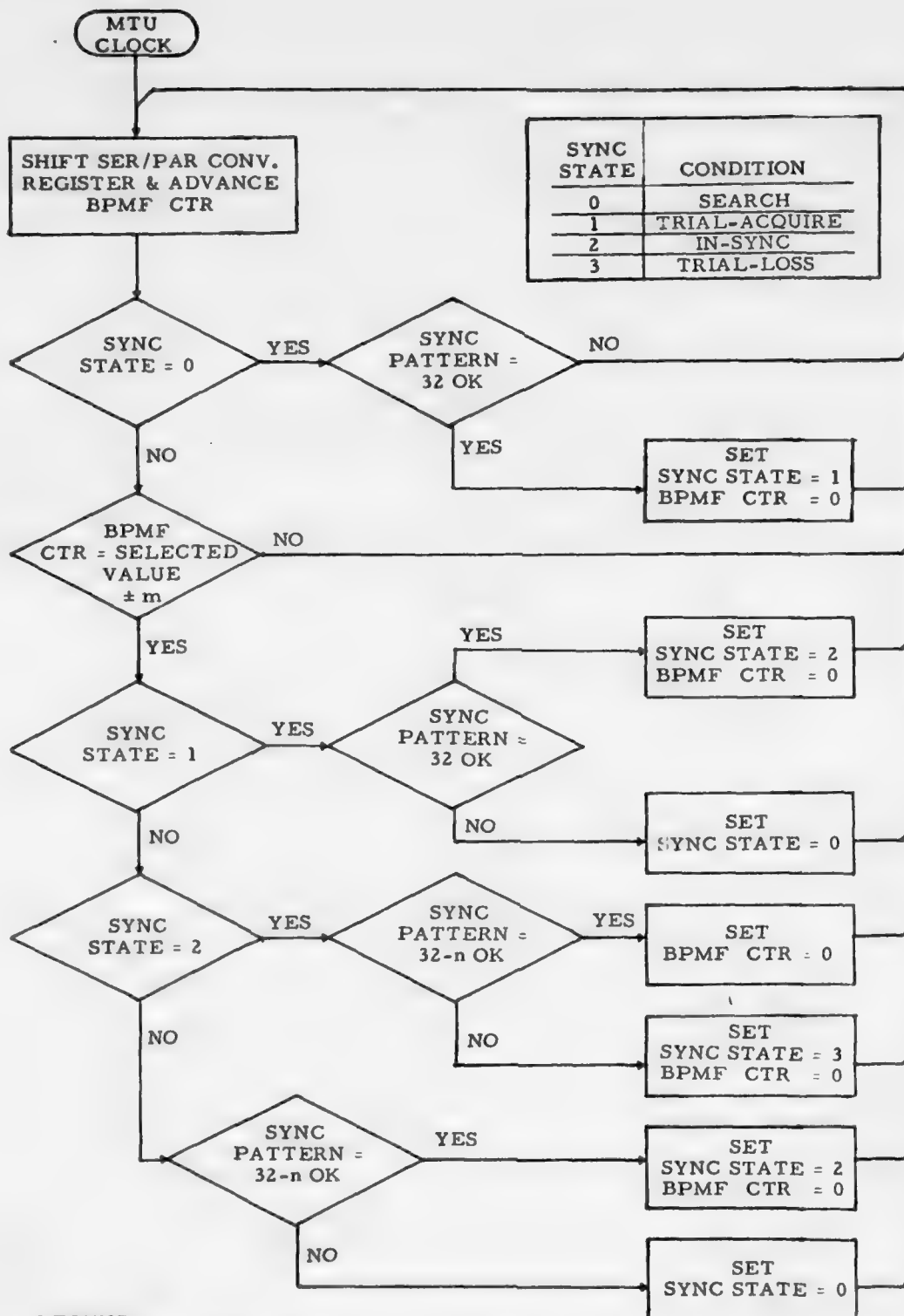
Thereafter, a selected number of bits (m) in error at "Sync Time" will not cause a loss of sync, but will be ignored. "Sync Time" is the time at which the next sync pattern should occur based on the selected number of bits per minor frame. However, to protect against the loss of sync due to the accidental dropping of clock pulses by the HDDR, "Sync Time" is widened by a selected number of bits (n). The selection of how many bits m and n are allowed to be in error is based on manual switch settings. The switches will be mounted on the logic (not the control) panel and will allow setting at 0, 1, 2, 3 or 4. They will not be under operator control since they are not expected to be frequently changed. The recommended setting of these switches are  $m = n = 1$ .

If more than the selected number of bits are in error during "Sync Time," a trial-loss state will be entered. A second incorrect sync pattern at "Sync Time" will cause the search state to be re-entered.

The above algorithm is consistent with having a 32-bit sync word and a tape error rate of less than 1 in  $10^6$ . It assures syncing correctly within the first part of the preamble filler, and to have a worst-case probability of loss of sync in less than one out of  $8 \times 10^{12}$  scan lines for n set equal to 1.



FRAME SYNCHRONIZATION LOGIC



FRAME SYNCHRONIZATION FLOW CHART



#### 5.2.1.5 Video Data Buffer (VDB)

The video data is fully double buffered, i.e., one scan line is stored in one buffer, the next in the other, etc., as shown in the diagram. This has three major advantages:

- The controls of input vs. output are much simpler and more straightforward.
- The rate at which the memory circuits have to operate is reduced by a factor of two since the same RAM IC is not required to accommodate a read cycle between the two write cycles, or a write cycle between two read cycles.
- The tolerances on the PLL controlling the HDDR servo are greatly relaxed.

The video data is stored in the form of two pixels/word. An 8-bit Auxiliary Input Buffer Register is required as shown in the diagram. The multiplexing required on the buffer output to return to single pixels in sequence is provided by the video Data Buffer Output circuit.

The reason for this is that the "worst-case" pixel output rate can be 17.5 mHz, thus allowing approximately 55 ns to read the data out of the memory; this is marginal in terms of proven IC RAMs at the present time. By storing two pixels in parallel, the rate is reduced to 8.75 mHz, thus allowing over 110 ns per read cycle which is easily achievable.

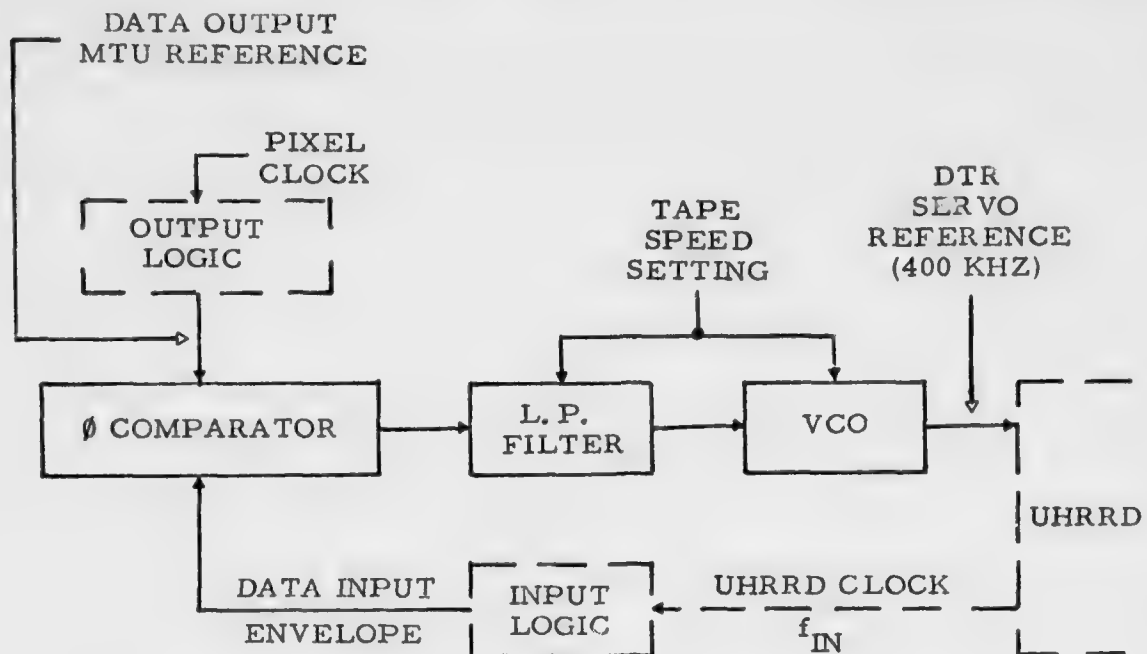
#### 5.2.1.5 Reference Frequency for DTR Servo

While it would be simplest to slave the entire recording system to the DTR the specification for the Ampex FR-2014 magnetic tape transport precludes this approach. Specifically, Ampex quotes the following:

Tape Speed Accuracy:  $\pm 0.15\%$  maximum error, long term, with input power variations from 105 to 125 volts AC, 47-63 Hz.

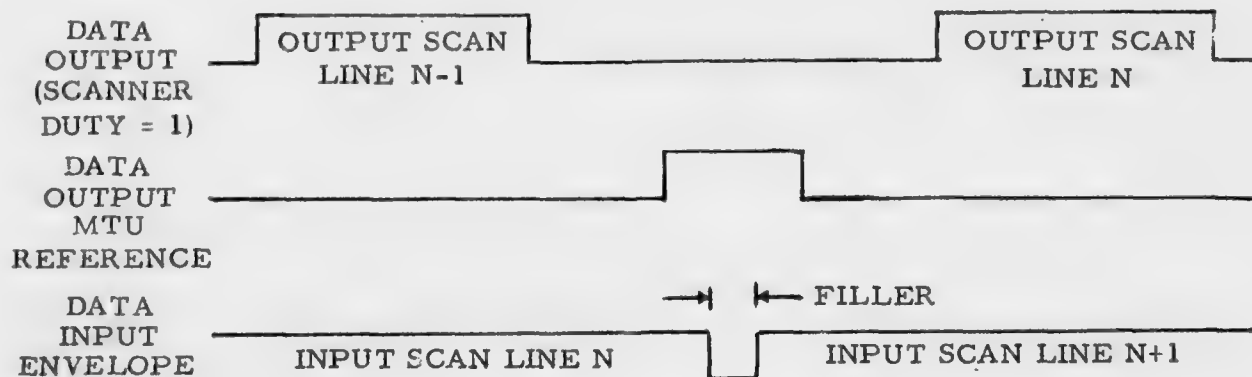
Thus, there is a problem in terms of the scanner motor being part of a very stiff servo loop to insure high mirror rotational stability. If the magnetic tape speed and hence the clock rate varied by as much as 0.15% in the region from 0.005 Hz to 0.5 Hz, the scan motor cannot follow these variations, and thus the HRFRC would be required to have a very large buffer to accommodate the speed differential between input and output.





ONE SCAN PERIOD =  
1/350 SEC

24°      48°



REFERENCE FREQUENCY FOR DTR SERVO

The best way to solve the problem appears to be one of slaving the magnetic tape unit to a very stable frequency. This is readily accomplished with a simple PLL as shown in the diagram. Note that this approach assures a long term tape speed accuracy which permits operation with double buffering (two scan lines) of the video data. This approach also means that there are no restrictions on the stiffness on the scanner motor servo. And the FR-2000 series instrumentation recorders are equipped to accept an external capstan servo 400 kHz reference frequency, so no special modifications are required. (Refer to Ampex Manual #1802512-01, FR-2000A Recorder/Reproducer, Section 4.2-13 and 4.6-6).

### 5.2.2 Output Logic

#### 5.2.2.1 Radiometric Loop-Up Table and Buffer

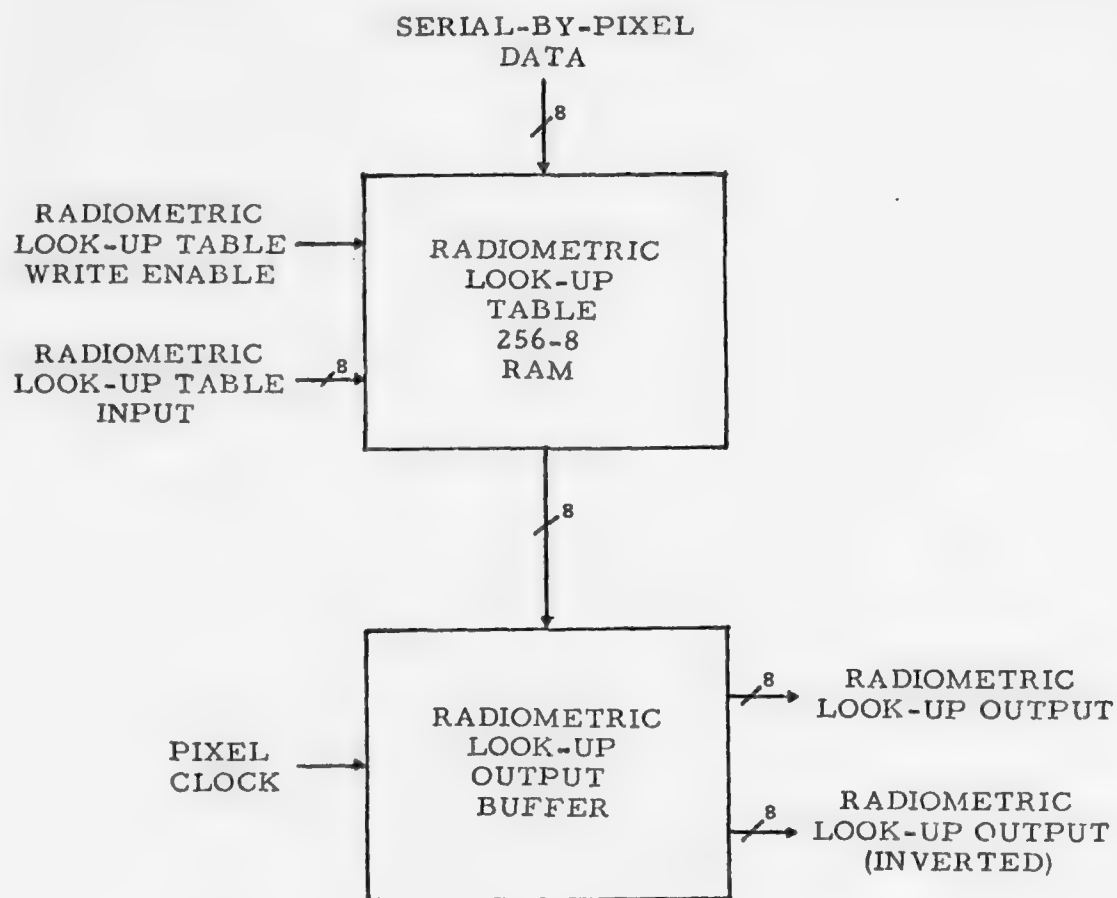
Prior to the data being sent to the HRFRC, a radiometric calibration takes place on each pixel. This is performed by means of a RAM arranged in the form of a look-up table. Since up to four film recorders may be driven from one HRFRC, and each may need a different radiometric correction, four separate RAMs are provided. Each is  $256 \times 8$  arrangement, providing for both an 8-bit input and an 8-bit output, as shown in the diagram. (The reasons for using a  $256 \times 8$  rather than a  $256 \times 6$  RAM are discussed in Section 4 under Image Density Characteristics).

The look-up tables will be loaded from a perforated tape reader; the contents of the table can be readily displayed for verification purposes. The RAM input and output is arranged to give an adequate timing margin at the maximum 17.5 mHz pixel clock rate.

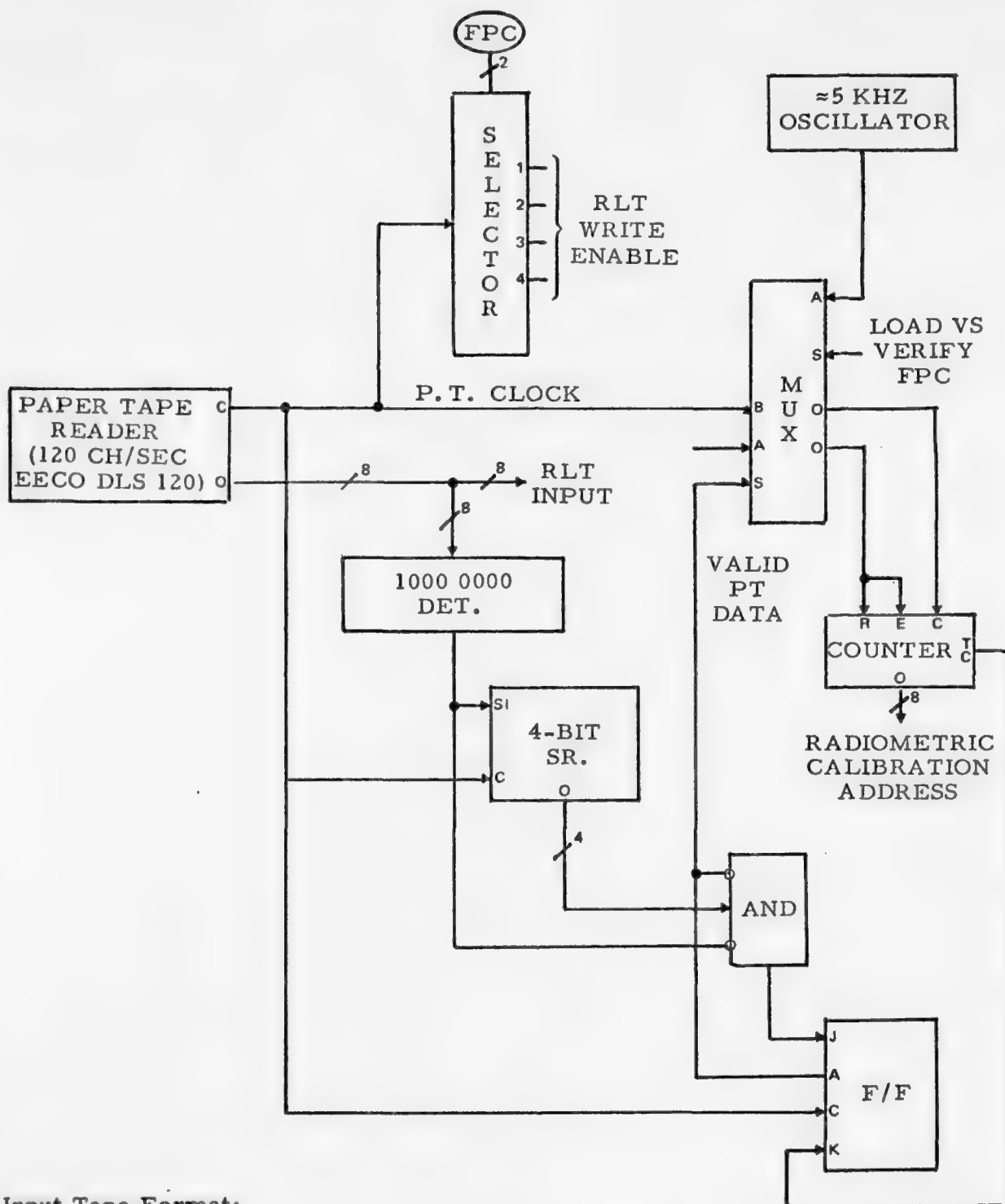
A perforated tape, prepared externally, will be used to load each radiometric look-up table. The format of the tape and the logic for transferring the data into the proper location of the RAM are shown in the diagram.

Verification of the contents of the look-up table is handled as follows: (refer also to diagram). Circuitry is provided so that the RAM addresses are continuously incremented at a slow rate of about 5 mHz; hence, a cycle through the entire RAM address locations takes about 50 ms.

By converting the RAM address and the RAM output in two separate D/A converters, an X-Y plot can be displayed on either a commercial oscilloscope or a pen and paper X-Y recorder. This results in a rapid check that the RAM has been loaded properly.



RADIOMETRIC LOOK-UP TABLE AND BUFFER



#### Input Tape Format:

Four (4) or more 1000 0000 (80<sub>HEX</sub>) patterns followed by a single 0100 0000 (40<sub>HEX</sub>) precede the actual data. Thereafter, 256 characters of data follow for loading sequentially in RAM locations 0 through 255. Thereafter, four (4) or more 0100 0000 (40<sub>HEX</sub>) patterns shall complete the tape.

#### RADIOMETRIC LOOK-UP TABLE (RLT) LOADING AND VERIFICATION

The combined time for both loading and verifying the contents of each radiometric look-up table will take less than one minute.

Since verification of the data in the look-up table is relatively simple, no elaborate parity or check-sum schemes will be employed on the perforated tape.

#### 5.2.2.2 Video Data Buffer (VDB) Output

The Video Data Buffer Output primarily provides transfer buffering.

Each line of video data is stored in one of two 18K × 16 RAM buffers (i. e., VDBA or VDBB). As indicated on Page 2-18, the buffer addressing is shared between the input phase and the output phase.

For the output phase, the address counter controls are as follows:

Control Logic VDBA Address Counter:

Reset = (Video Out) · (Output Line Counter = Odd) · (Start of Line)

Count = (Video Out) · (Output Line Counter = Odd) · (Pixel Clock)

Control Logic VDBB Address Counter:

Reset = (Video Out) · (Output Line Counter = Even) · (Start of Line)

Count = (Video Out) · (Output Line Counter = Even) · (Pixel Clock)

To keep the memory speed down, each video buffer is organized 16 bits wide as discussed on Page 2-18. Thus, two pixels are read out of the memory in parallel.

The logic shown in the diagram buffers the video to permit proper ordering in the Output Collector Multiplexer (see Page 2-44). Note that the Video Data Buffers are unloaded only on alternate pixel clocks.

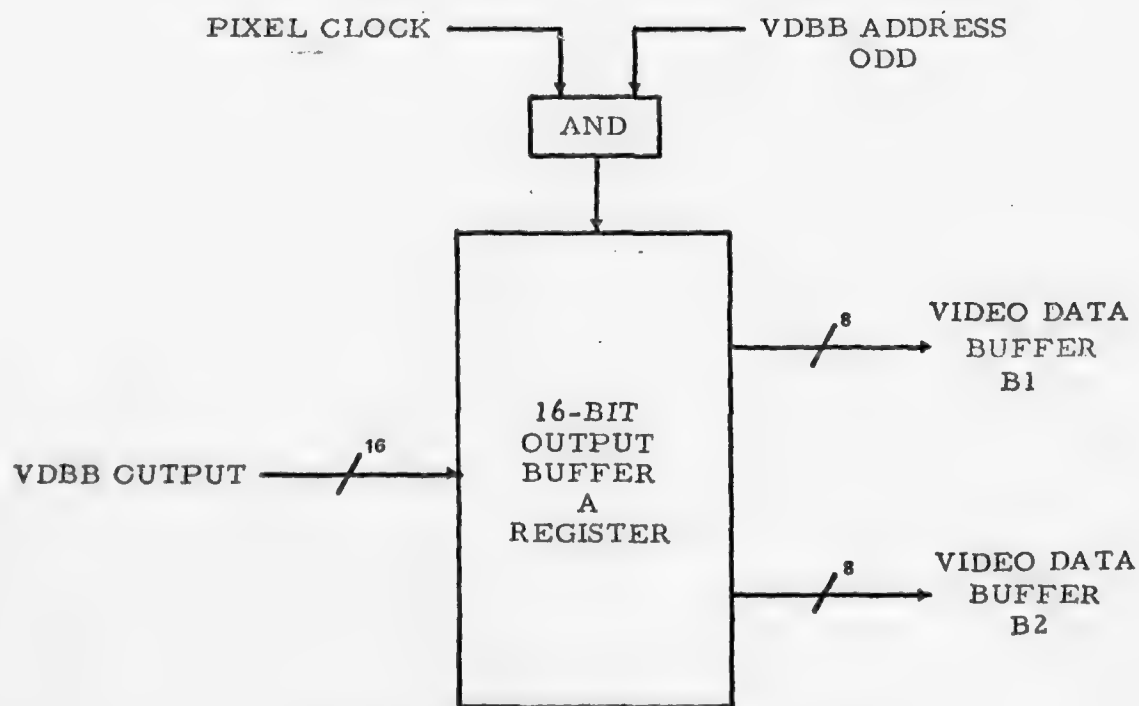
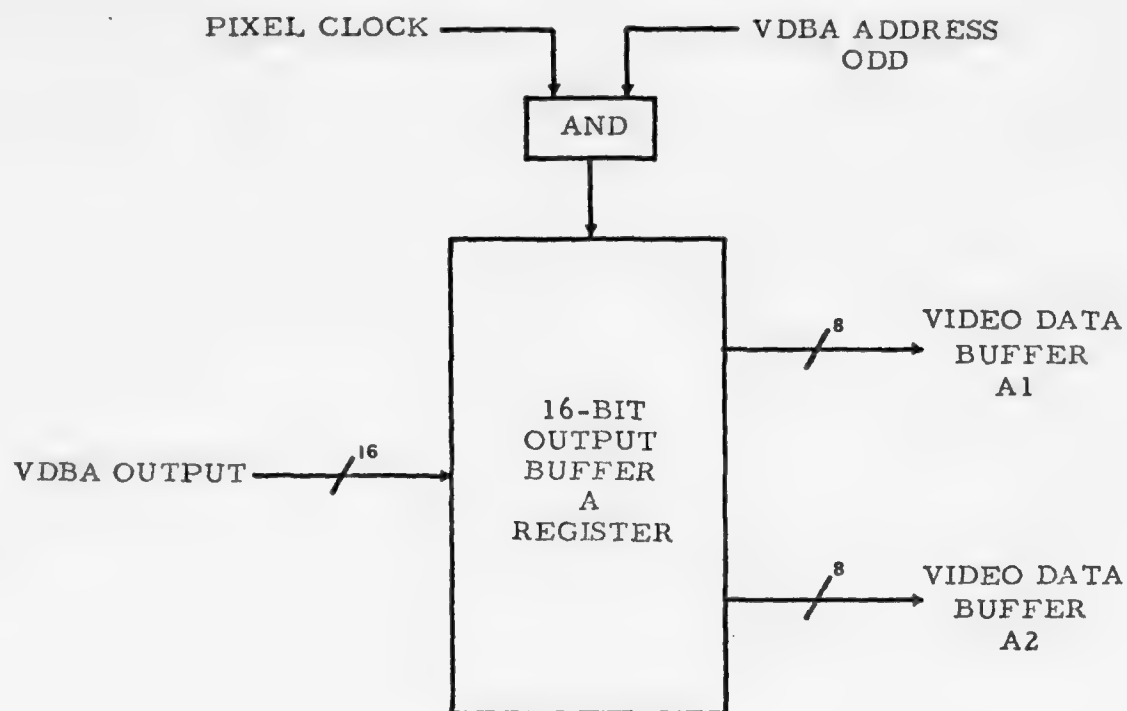
#### 5.2.2.3 Pixel Clock and Scanner Reference Output

The pixel clock is generated from the scanner motor tachometer. One output pulse is provided from the scanner mirror servo system for each pixel location during the synchronized line scan. In this manner, the pixel clock is directly related to the scanner mirror position and reproducibility and accuracy is excellent.

#### 5.2.2.4 Platten Drive Output

A signal to increment the platten drive screw is also derived from the scanner mirror tachometer therefore assuring an accurate relationship between the platten advance and the line scan.





VIDEO DATA BUFFER OUTPUT LOGIC

#### 5.2.2.5 Data Output to UHRRD

The output video data to the HRFR can be calibrated or bypassed by the radiometric table and can be presented normal or intensity inverted.

There are two choices to be made prior to outputting the video data to the film recorders:

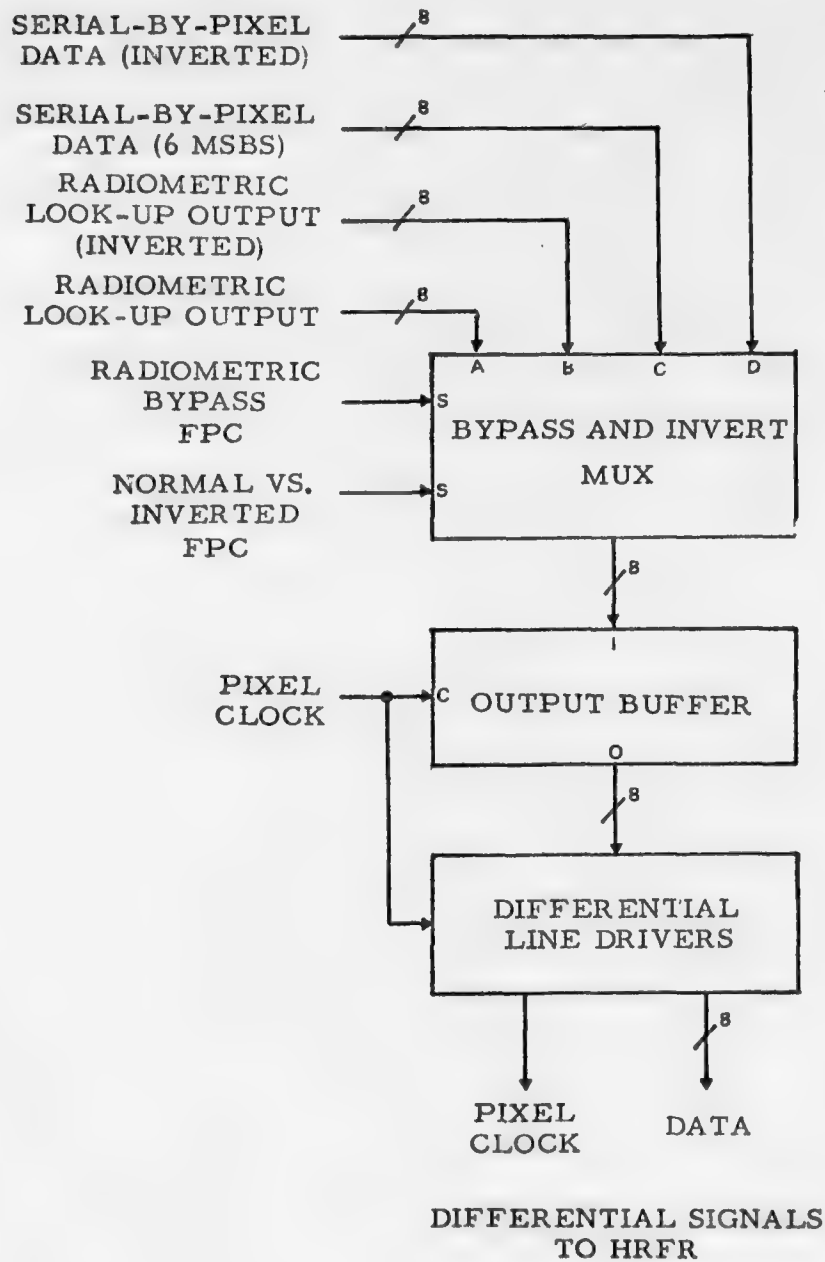
- Is the radiometric data to be bypassed?
- Is the data to be inverted?

Both of these choices are made by operator switch settings.

Using a 4:1 multiplexer, the proper data is selected as shown in the diagram. An output buffer is used to eliminate any skew between the 8-bits of data prior to the transmission to the HRFR.

Differential line drivers will be employed to send the data and clock to each HRFR via twisted-pair lines. The maximum allowable cable length will be 60' between the HRFR and any one HRFR.

Four Data Output circuits will be provided.



DATA OUTPUT TO UHRRD LOGIC  
(ONE PER HRFR)

AD-A035 076

SINGER LIBRASCOPE GLENDALE CALIF  
DISPLAY MATERIALS EVALUATION PROGRAM. (U)  
DEC 75 M R SMITH

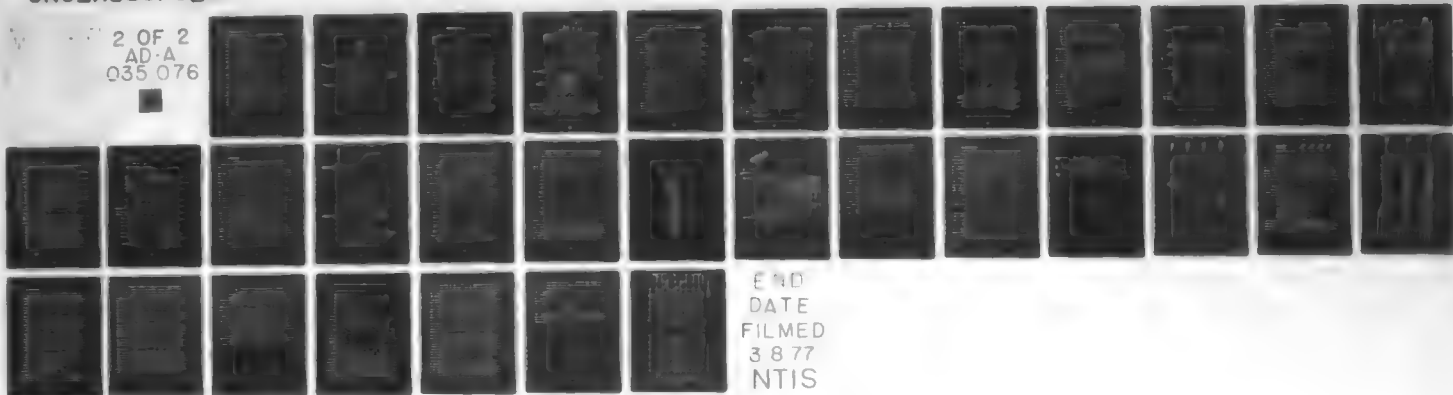
F/6 9/5

N00173-75-C-0492

NL

UNCLASSIFIED

2 OF 2  
AD-A  
035 076



### 5.2.3 Internal Test Pattern Generation

#### 5.2.3.1 Resolution Target Generation

Horizontal and Vertical Resolution Targets are generated to provide inputs for image resolution measurements.

Each image in the band-sequential mode will include resolution targets. The resolution targets will consist of bar patterns in both the horizontal and vertical direction. For each direction, there will be four frequencies corresponding to:

- Maximum resolution system is set up for
- 1/2 Maximum resolution system is set up for
- 1/4 Maximum resolution system is set up for
- 1/8 Maximum resolution system is set up for

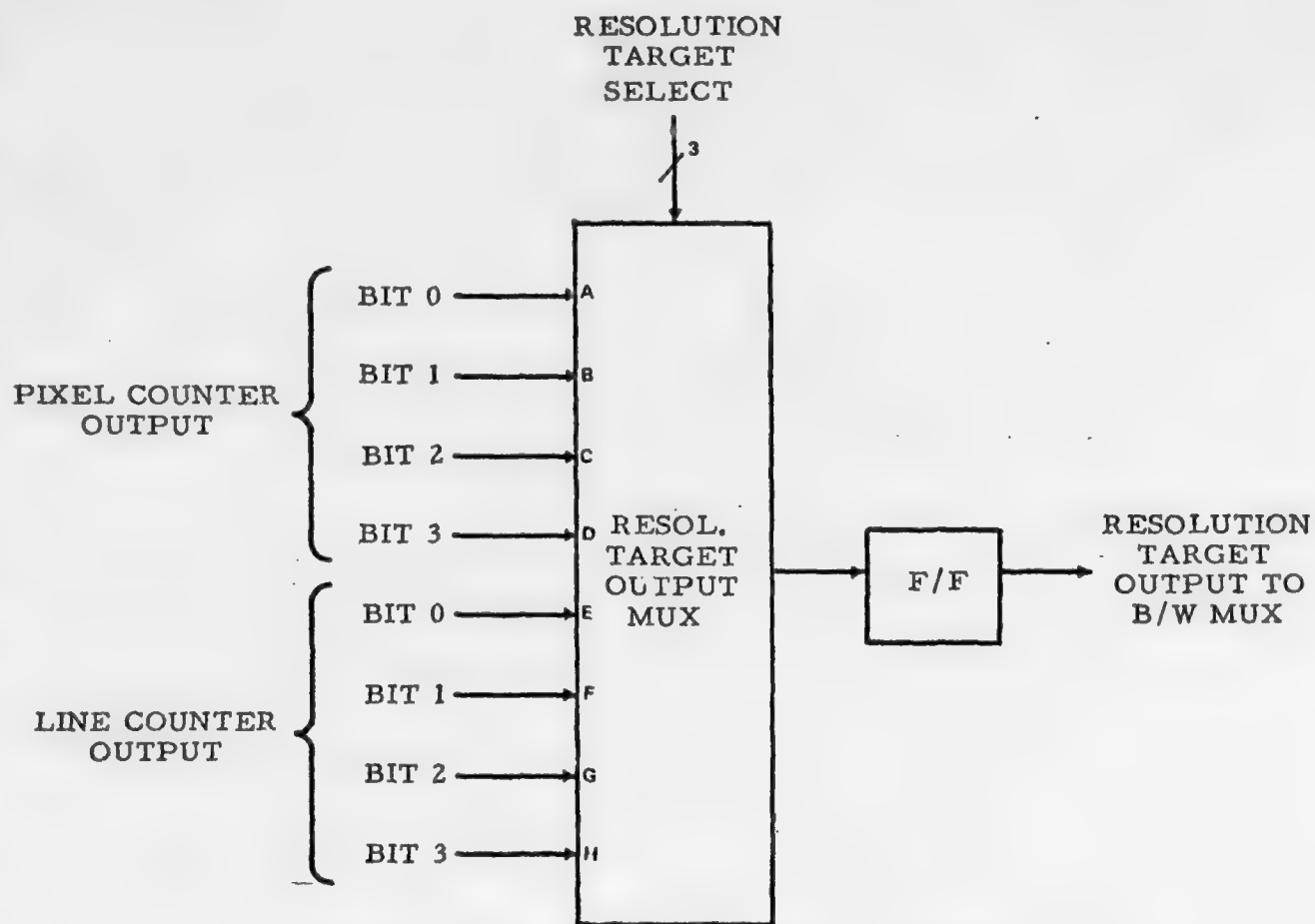
The logic for implementing the resolution targets is shown in the diagram. As can be seen, it essentially consists of a simple multiplexer selecting appropriate counter outputs.

#### 5.2.3.2 Gray Scale Generation

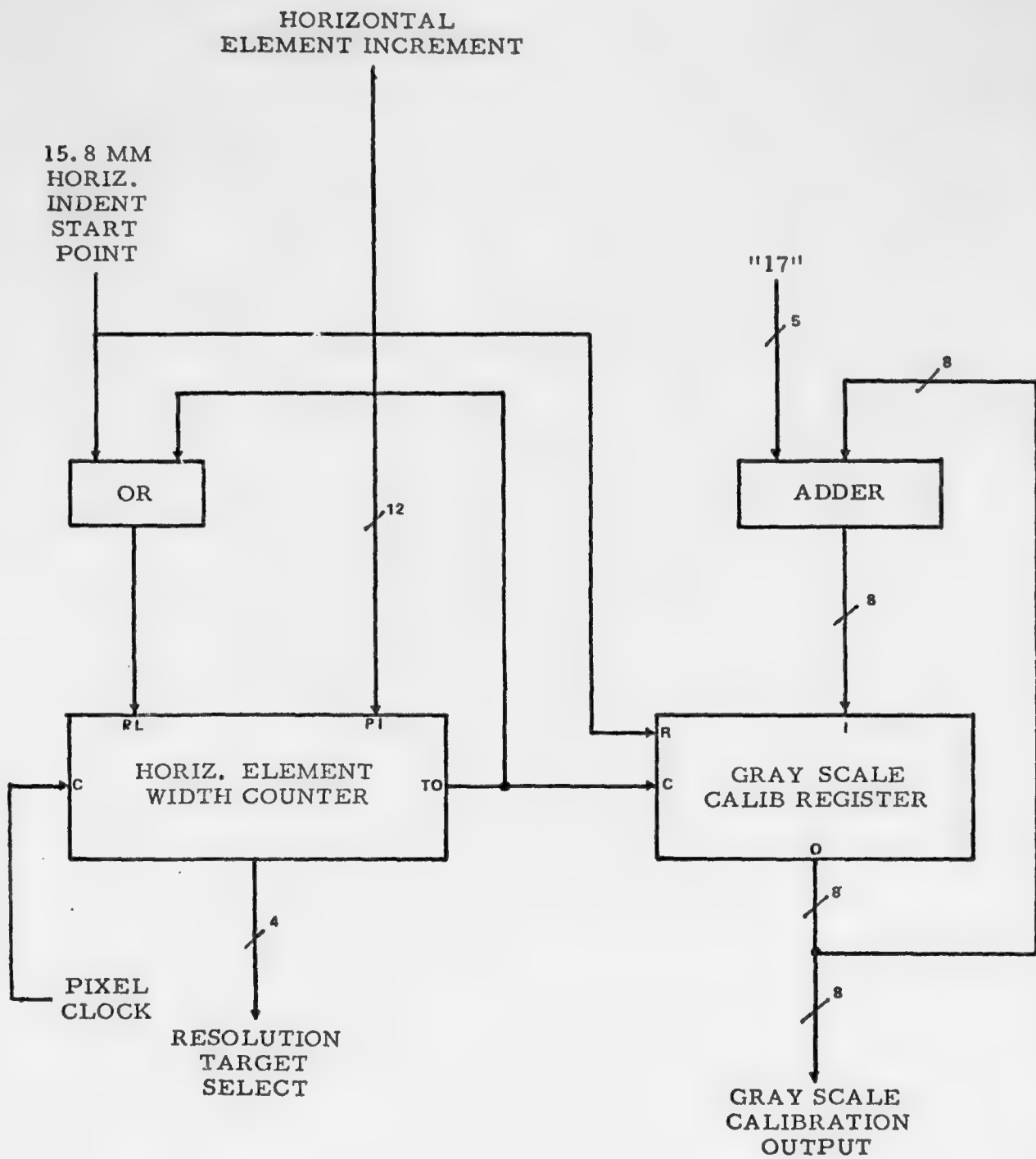
A Gray Scale Test Pattern is provided for calibrating the film imagery intensity levels.

Each image in the band-sequential mode will include a gray scale calibration pattern. The gray scale will consist of 16 steps, sequenced with digital inputs of 0, 17, 34, 51, ....255. Each gray scale step image will occupy about 6.7 mm × 9.55 mm on film, for a total of about 6.7 mm × 153 mm. The location of the gray scale calibration will correspond to that shown on Page 2-36.

The logic for implementing the gray scale data is shown in the diagram. It consists essentially of an +17 adder and accumulator. There is also a counter (used for the resolution targets as well) to create the proper width of each step.

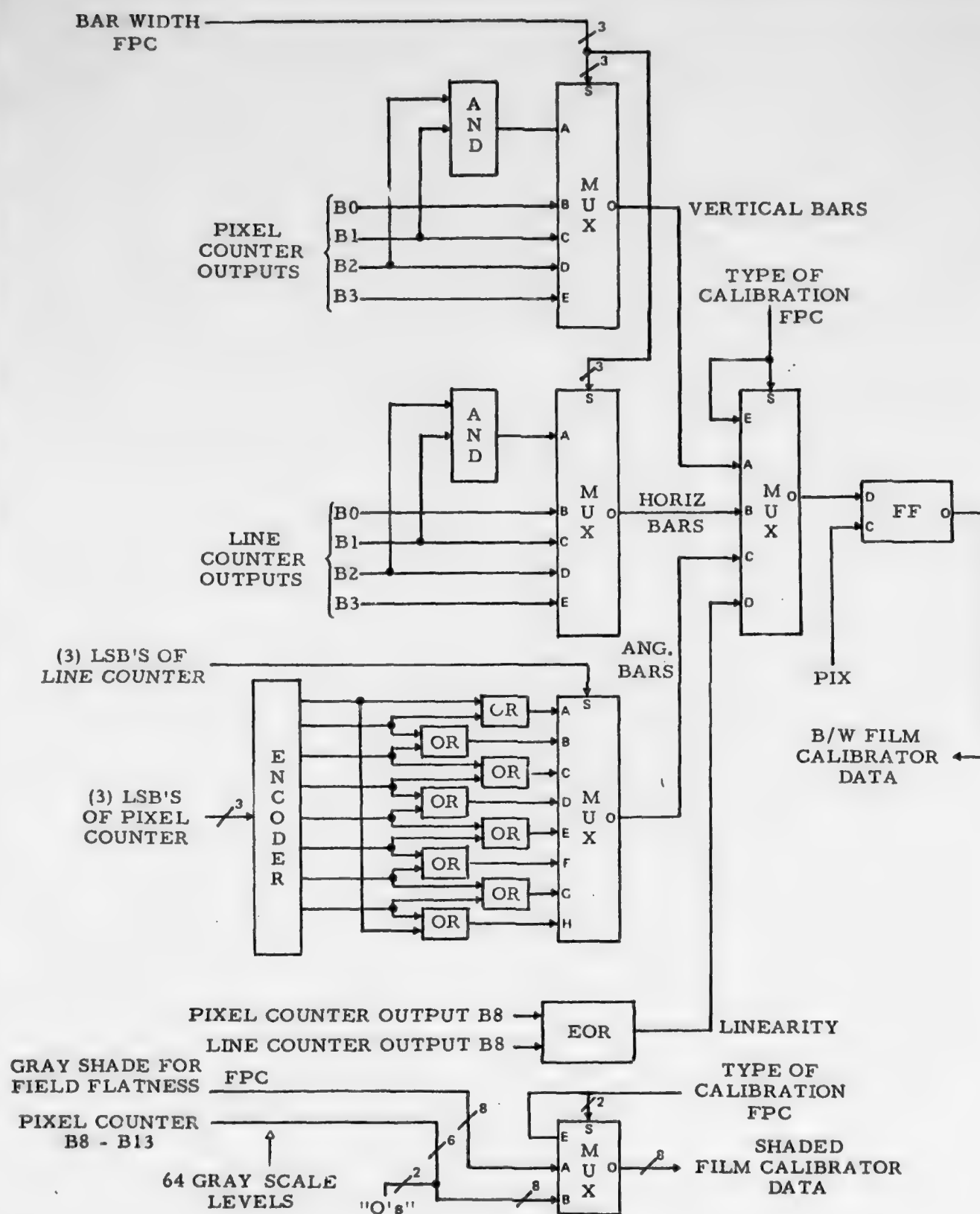


RESOLUTION ANNOTATION LOGIC DIAGRAM



GRAY SCALE LOGIC DIAGRAM





### 5.3 RECORDER-DISPLAY SECTION (UHRRD).

The UHRRD contains the electronic components necessary for processing the input video data, for producing imagery on a recording medium, and for displaying the imagery on a single-operator viewing screen.

The High Resolution Recorder Display section accepts video and control data from the UHRRDC and produces high resolution imagery with a wide range of accurately controlled formats.

The UHRRD contains various optical and electronic systems which are necessary to convert input digital video data into high resolution photographic quality imagery on a real-time recording material.

The UHRRD and the HRRDC are combined and configured as a floor-standing cabinet, with the optical system portion mounted above the electronic components on a self-contained, rigid, optical-mounting structure.

Input signals from the UHRRDC are converted by the video processing system to provide the line-synchronized video image signal. Control signals are provided to the line scan system.

The video image signal is used to intensity modulate the exposure light source.

Operator controls, located at the front panel, are used to set the laser power as well as to provide for normal or special operating procedures such as system alignment and recording material replacement.

#### 5.3.1 UHRRD Data Electronic/System Overview

The electronic circuitry required in the UHRRD is shown in the diagram.

The following digital signals are received from the UHRRDC:

- Video Data (8-bits in parallel)
- Pixel Clock
- Central Pre-Start of Scan (always one pixel clock ahead of 1st pixel data)
- UHRRD Counter Reset (always two clock periods ahead of 1st pixel data)
- Reference Voltage for Scanner Servo Motor
- Reference Frequency for Plotter Drive Stepper Motor
- Switch signals for analog filter selection.



The scanning motor servo electronics provides a tachometer generated pixel clock which is used to clock out the video data. All signals are sent differentially by the UHRRDC for maximum common mode rejection; all lines will be terminated in the recorder to prevent reflections.

The 8-bit video data, after being received, is digitally delayed by an appropriate amount to compensate for start-of-line jitter. The amount of start-of-line positional error is detected by the Start-of-Line Sensor Circuit, which detects the position of the scanner mirror and provides a "crossing-point" signal output. The Start-of-Line correction circuit is used to delay the video stream by the proper amount to eliminate line scan jitter. The video signal is then input to the D/A Converter. The analog output of the D/A Converter is input to an Exponential Circuit. The purpose of the Exponential Circuit is to provide an appropriate non-linear scale factor to the video data so that the video data will be compatible with the recording medium exposure characteristics.

After the video data is scaled by the Exponential Circuit, it is filtered by one of four Filters. The output of the Filter drives the Modulator.

The Scanner Motor Servo Reference signal is received from the UHRRDC through the Data Cable. This reference voltage determines the scanner motor and speed.

The UHRRD can be operated internally without connection to the UHRRDC to provide for certain special operating modes such as system alignment.

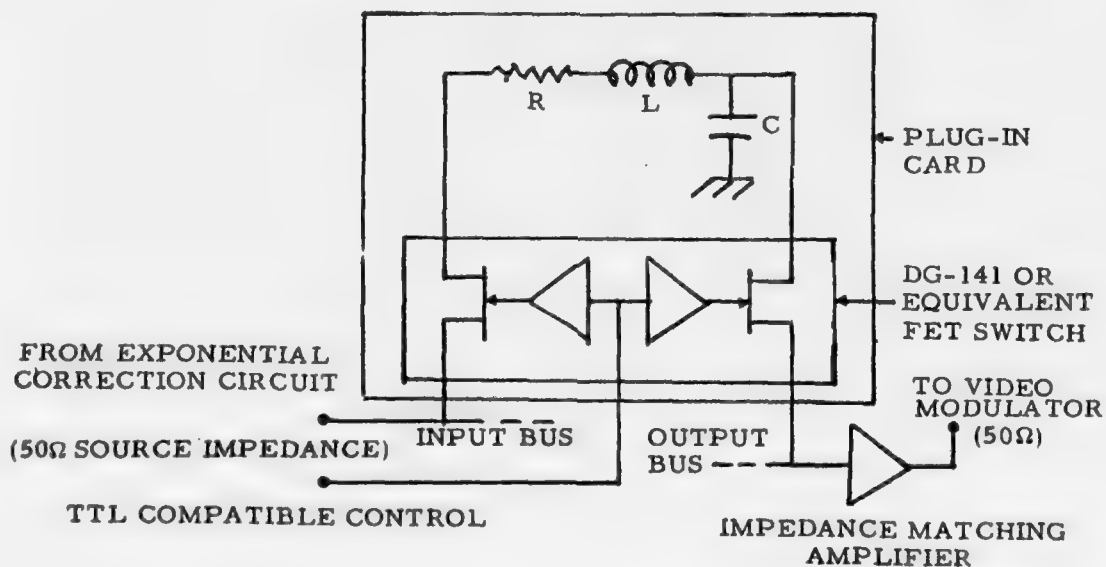
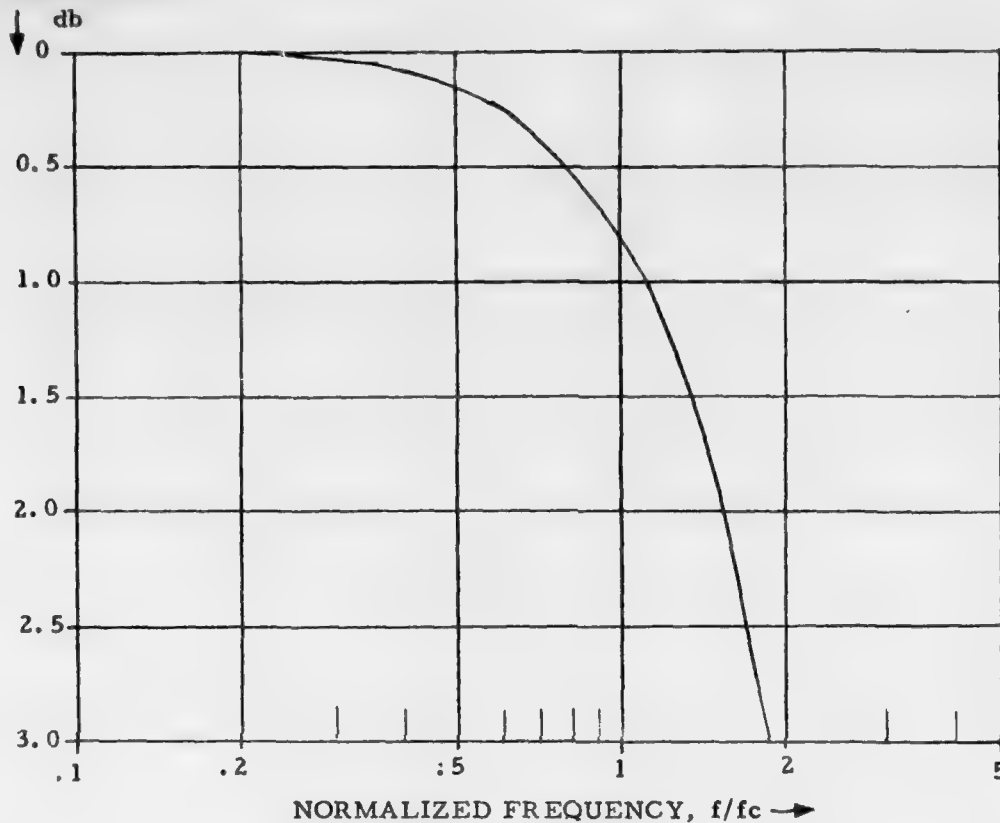
#### 5.3.1.1 Video Filter.

The video low pass filter design is selected for very low overshoot and minimal phase distortion.

##### Requirements

The primary function of the video low pass filter is to reject the high frequency transients caused by non-simultaneous switching of bits in the D/A converter. These transients can be up to half the maximum D/A converter output voltage and may last for up to 5 nanoseconds. The filter should also attenuate any high frequency overshoot generated by the amplifiers in the D/A converter and the exponential correction circuit.

# ATTENUATION



VIDEO FILTER CIRCUIT AND CHARACTERISTICS

While performing this function, the filter must have the following other characteristics to maintain the desired system performance.

- The filter transmission at the video cutoff frequency ( $f_c$ ) must be  $\geq 90\%$  to maintain the system MTF.
- The overshoot from a square wave input must result in  $\leq \pm 0.05$  density unit transient on the film. In a worst case analysis, with no allowance made for the saturation effects of the film and modulator, this requirement translates back to a ringing specification of  $\leq \pm 2.5\%$ . To meet this requirement, the filter must have a very small variation in delay with frequency.

#### Filter Design

The optimum filter for this application is a two pole filter with characteristics similar to those of a Bessel filter. The Bessel filter, also known as a "linear phase" filter, has the minimum variation in time delay with frequency and the least overshoot in its step response. This filter has about 3 db less attenuation at the pixel clock frequency than a Butterworth filter, but since the transient spectrum from the D/A converter will extend to over 50 harmonics of the pixel clock frequency, the amount of energy in the fundamental will be very small. The step response overshoot of this filter is 0.43%. The maximum delay distortion is equivalent to less than 0.01 pixel. The filter attenuation is shown in the figure as a function of frequency normalized to the video cut-off frequency  $f_c$ .

#### 5.3.1.2 Exponential Correction Circuit.

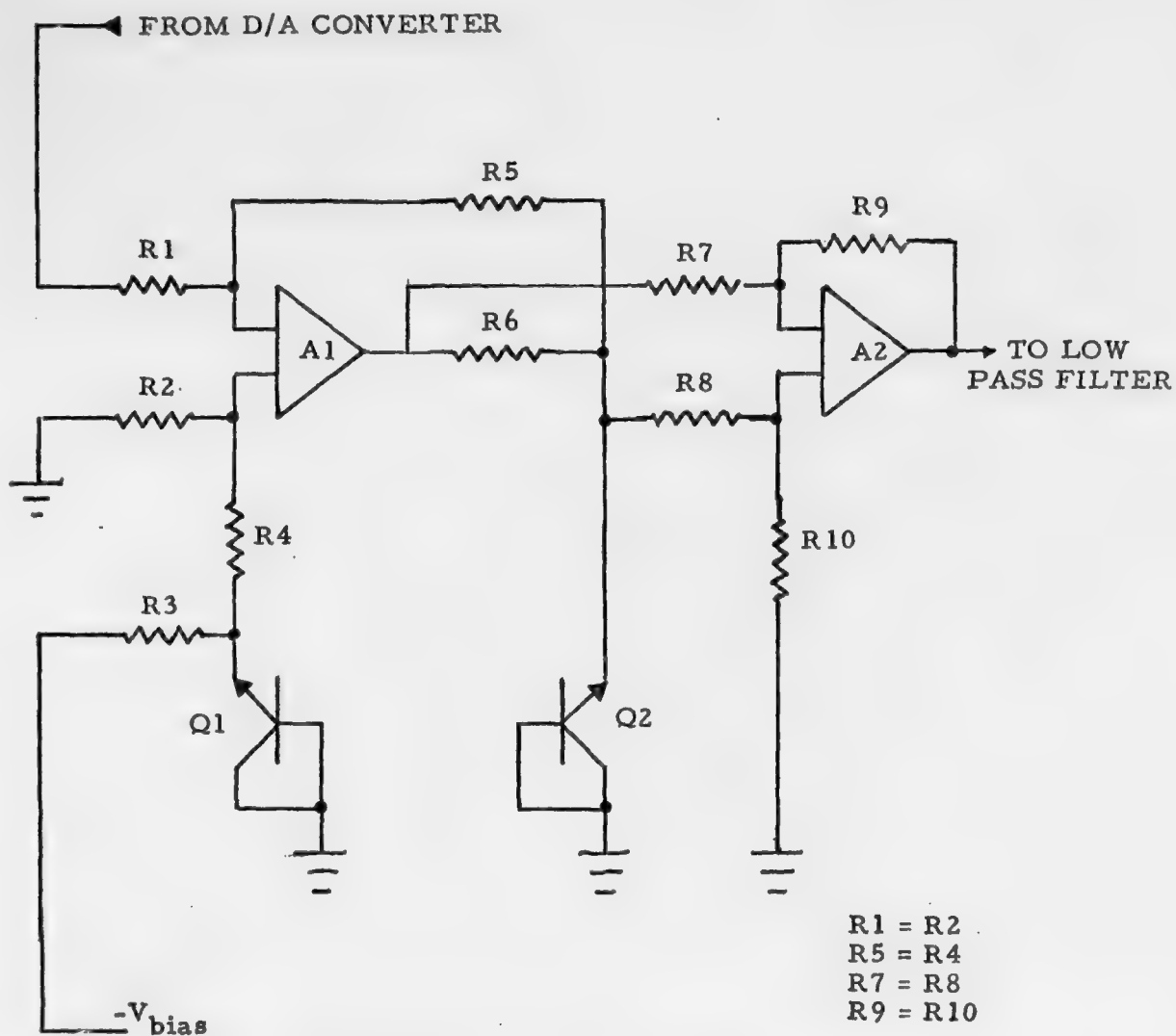
An exponential analog correction circuit allows generation of 64 evenly spaced grey shades without use of an excessively large D/A Converter.

Correction of system non-linearities is simplified by the use of a circuit having an exponential transfer function, i.e.,

$$V_{out} = Ae^{BV_{in}}$$

and the following other characteristics:

- Output Dynamic Range                      20 to 1
- Output Noise                                   $< 0.1\%$  rms
- Long Term Drift                                $< \pm 2\%$



Q1, Q2 are matched transistors in same package

A1, A2 are high speed operational amplifiers, e. g. LM118

### EXPONENTIAL CORRECTION CIRCUIT







A rotating pyramided mirror moves the spot with constant linear velocity across the film plane and creates a line scan.

The position of the mirror facet is monitored by the scanning motor optical tachometer which also provides a start-of-line synchronization signal.

The recording beam is reflected onto the recording plane by means of a beamsplitter located at the bottom edge of the viewing window.

The recording plotter is transparent to enable simultaneous recording and viewing of the imagery.

The moving plotter and line scan combination produces a "waterfall" time history display at the viewing screen in a "B-Scan" format.

The recorded medium is illuminated by the condensing lens and illumination source, and the imagery is rear projected onto the partially diffuse viewing screen. The magnification of the projection optics and the illumination optics can be step-wise varied to vary the field-of-view from full field to one seventh field, while maintaining constant illumination level at the viewing screen.

A CRT beam splitter enables the imagery on the annotation cathode ray tube to be superimposed onto the viewing screen.

#### 5.3.2.1 Laser-Writing Service.

The exposure light service will be a 400mw krypton ion laser which will allow exposure of photodichroic recording material and other real-time recording media.

The calculated power required of the laser is based on the following factors:

1. The required exposure for NaF photodichroic recording material is approximately  $500 \text{ mJ/cm}^2$  for maximum optical density. Dylux film and photochromic film requires slightly less exposure energy.
2. The area scan rate at the recording plane  $\left(\frac{\text{cm}^2}{\text{sec}}\right)$  is the area of a scan line divided by the time required to expose it. The exposure time is the line scan frequency  $\left(\frac{\text{lines}}{\text{sec}}\right)$  divided by the duty factor of the scanner, or the fraction of time it is actually scanning a line.

With a 6 facet mirror and a useable scan angle of 32 degrees, the scan duty factor is

$$\frac{6 \times 32}{360} = .53.$$

A 100mm scan format and a 5 micron exposure spot produces a scan line with area equal to

$$50 \times 10^{-4} \text{ cm}^2.$$

Therefore the area scan rate is

$$50 \times 10^{-4} \times \frac{\text{scan frequency}}{.53} \frac{\text{cm}^2}{\text{sec.}}$$

3. The total optical system transmission is approximately 33%. This transmission results from the following contributions:  
focus lens 68%, scan mirror 90%, miscellaneous optics 90%, acousto-optical modulator 60%.
4. The laser power required to produce a line scan frequency of .5 lines/sec with the previous parameters is:

$$.5 \times \frac{50 \times 10^{-4}}{.53} \times .5 \times \frac{1}{.33} = 7.1 \times 10^{-3} \text{ W}$$

The maximum line scan frequency which can be produced with the 40mW laser is 2.8 lines/sec.

In addition to meeting the power requirement, the laser should have less than  $\pm 1\%$  noise and a long term drift of less than  $\pm 10\%$ .

The laser selected for this application is a 40mW krypton uV ion laser, having the following characteristics:

Power - 350.7nm and 356.4nm, TEM <sub>00</sub> mode	40 milliwatt for warranty period
Short term power variation	<0.5% rms
Power Stability - with optical feedback	< $\pm 1\%$ change over 8 hours
Controls	Remotely controllable
Input Power Requirements	120/208 VAC, 3 phase 20 amp.
Cooling Water Requirements	5.6 liter/min (1.5 GPM) at 70 gm/cm <sup>2</sup> (15lb/in <sup>2</sup> ). Filtered tap water, 35°C maximum temperature.
Warranty Period: System	1 year
Plasma Tube	1 year or 1000 operating hours whichever is less.

#### 5.3.2.2 Video Modulator.

An acousto-optic modulator provides high contrast and allows the modulation stability requirements to be met without stabilizing feedback loops or temperature controlled ovens.

The video modulator will be an acousto-optic unit such as the Zenith Model WBM-20R or equivalent. Such a device uses a glass acoustic medium to carry a 125 MHz acoustic beam. High transmission is achieved by diffracting up to 70% of the incoming light into the first order beam.

Modulators of this type have extinction ratios on the order of 500 to 1. This is far more than is required for this application.

The transfer characteristics of the WBM-20R are shown in Figure a on the opposite page. This curve closely approximates the form  $\sin^2 (V/V_0)$ , where  $V$  is the RF drive voltage.

The frequency response of the WBM-20R is shown in Figure b. Note that at the maximum frequency of interest, the modulation is still 90% of the low frequency response.

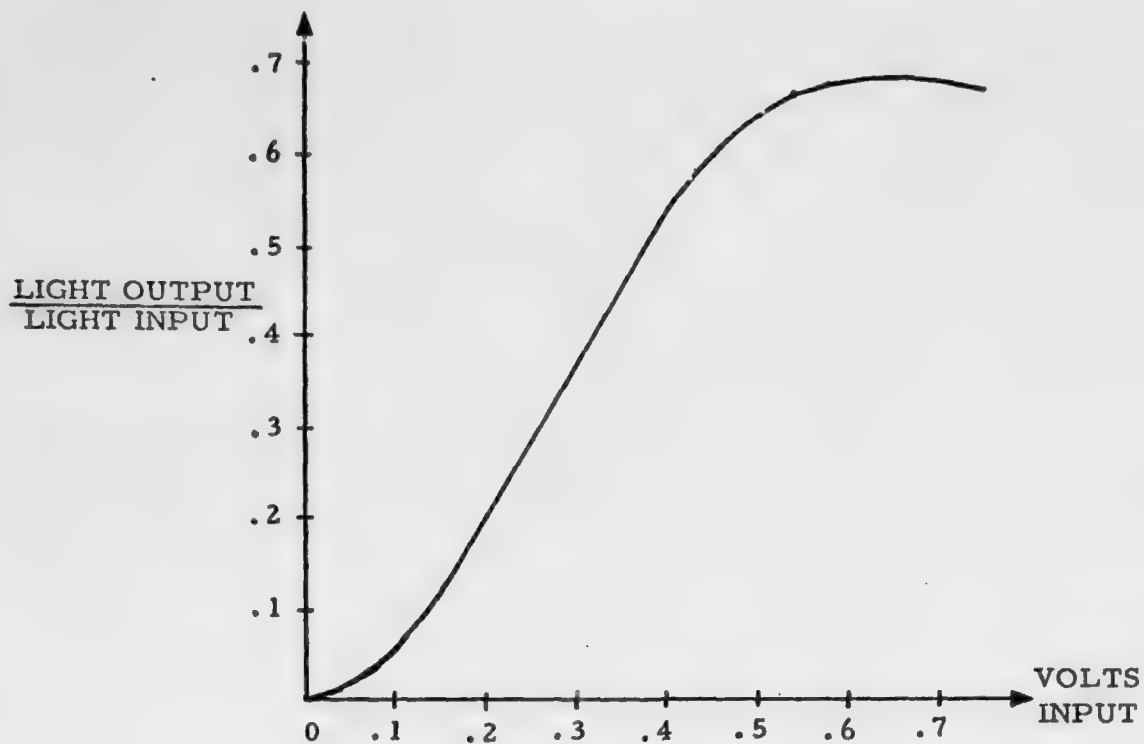
Modulators using other materials, such as lead molybdate ( $\text{PbMoO}_4$ ), are commercially available and give slightly improved frequency response. This is also shown in Figure b. The index of refraction of  $\text{PbMoO}_4$  is 8 to 10 times more sensitive to temperature than that of glass, however, and it is felt that modulation stability is more important here than a slight improvement in frequency response.

Tests run by Zenith show the modulation efficiency of the WBM-20R to change by less than 0.2% when varied over a 7°F temperature range.

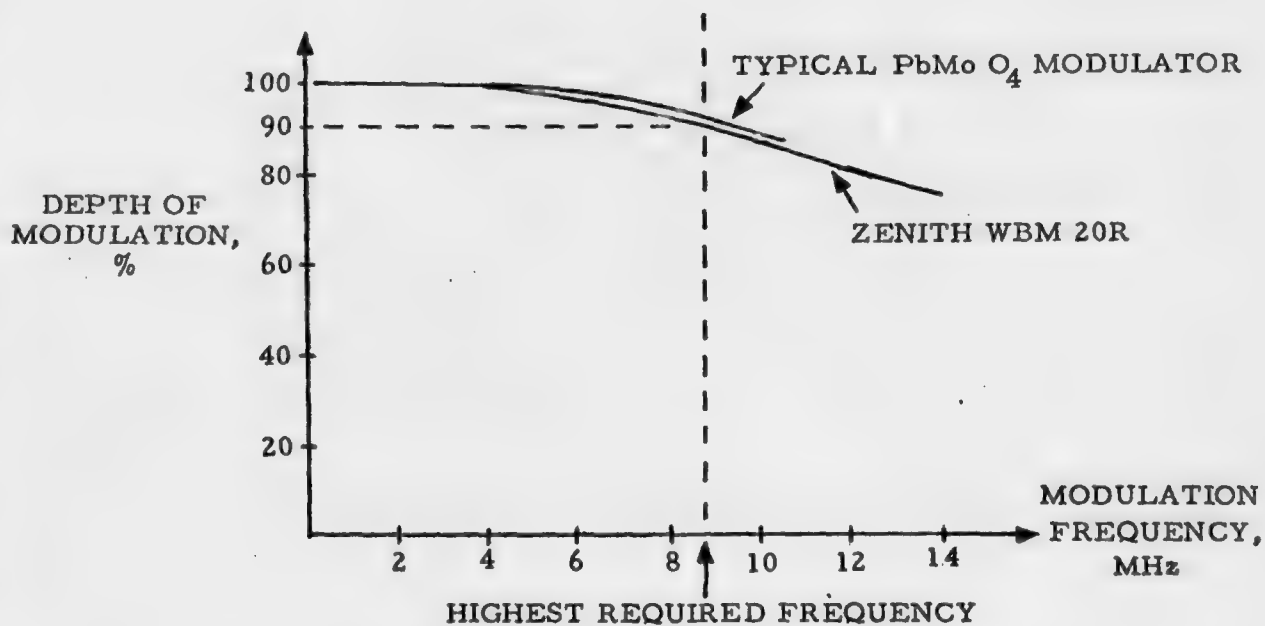
In order to simplify documentation and maintenance procedures, this same model modulator will be used to gate the start-of-line reference beam. In this application, contrast is extremely important while speed is not. The modulator will therefore be used with different beam forming optics to give a large beam waist in the acoustic medium. This will result in slightly higher extinction ratio at the expense of risetime.

#### 5.3.2.3 Line Scan System.

The Line Scan System provides an extremely accurately controlled, constant velocity, scanned input beam to the focus lens.



a) MODULATOR TRANSFER FUNCTION



b) MODULATOR FREQUENCY RESPONSE

The scanner mirror is a front surface, quartz pyramided mirror with a 25mm clear aperture. The scan efficiency can be increased by increasing the number of facets. Four facets will provide a scan efficiency of  $4 \times \frac{50}{360} = .56$  for a  $50^\circ$  mirror scan. The mirror is driven by a D.C. torque motor, which is controlled with a motor servo control system to provide long term stability for the motor speed. An optical tachometer provides an angular position signal to the servo controller.

The motor speed is accurately proportional to the scanner motor servo reference voltage which is provided by an input from the UHRRDC.

Short-term positional errors of the scanner mirror are detected and compensated for by the start-of-line synchronization circuit. Extreme accuracy and reproducibility are accomplished by using the tachometer generated pulse signals to clock-out the pixel video data from the video data buffer.

The scanner mirror assembly consists of a four sided pyramided scanner mirror accurately positioned to a gas bearing assembly. The D.C. torque motor and the optical shaft encoder are precisely coupled to the gas bearing mirror shaft. The scanner mirror assembly is an integral shaft design driven by a servo-controlled DC motor, with an incremental optical shaft encoder on a common shaft.

The scanner mirror is a precision optical element with the following characteristics:

Facet clear aperture	25mm
Number of facets	4
Facet-to-axis angle dynamic apex match error	$< \pm 0.5$ arc sec
Facet-to-axis angle absolute	$0^\circ \pm 15$ arc sec
Surface flatness across clear aperture	$< 1/10\lambda$ @355
Reflectivity through $\pm 12^\circ$ scan angle	784% $\pm 1\%$ @514.5mm

The scanner mirror assembly will be purchased from Speedring Systems, division of Schiller Industries, Inc. or equivalent. The design performance specifications are similar to a model which is currently in production.

In view of the demonstrated confidence in obtaining the required design specifications for the scanner mirror assembly, it is expected that the mirror assembly will cause no imagery banding signatures that exceed the allowed tolerance specifications.

#### 5.3.2.4 Flat Field Recording Lens.

The lens design keeps the linearity error below .05% over the total format. This enables the beam angular scan to be accurately and linearly translated to pixel spot position on the film.

The flat field focus lens has been designed to have the following characteristics:

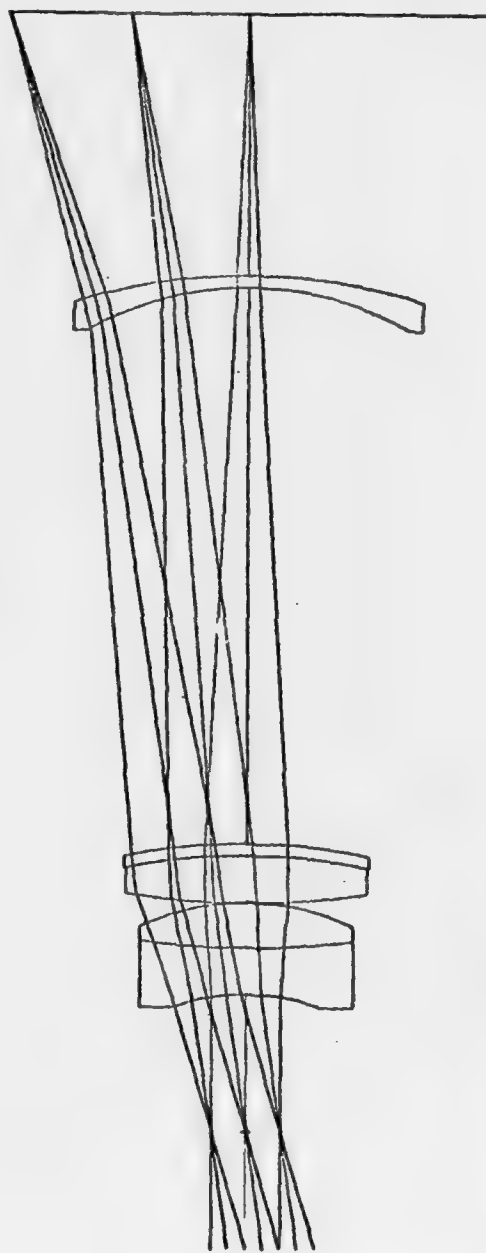
• Equivalent focal length	7.000 in.
• Total field angle	32°
• Format	100mm width
• F Number	12
• Color shift at 350.7nm and 356.4nm	.000007 in
• Back focal length	2.236 in.
• Entrance beam diameter	.583 in.
• Scan linearity error	<.05%
• Transmission	68%

The completed lens design exhibits diffraction limited performance over the entire range of field angle.

A drawing of the lens element configuration is shown on the figure. A ray bundle tracing is shown for the on-axis and extreme off-axis positions.

The table of numbers in the figure describes the wavefront aberrations in the exit pupil of the lens in hundredths of wavelength. The background around the image is filled in with 9's, and being a centered optical system, only half of the wavefront is displayed. The wavefront aberration is shown for the worst case, which occurs at the extreme off-axis position. Note that the maximum wavefront distortion is less than  $0.16\lambda$ , which is considerably better than the  $1/4\lambda$  diffraction limited requirement.





FULL SCALE GRA 11/6/75

SINGER U.V. LASER SCANNER



The modulation transfer function (MTF) for the lens is shown on the opposite figure for on-axis and extreme off-axis positions. Note how closely the actual MTF compares with the actual MTF, demonstrating that the lens is diffraction limited over the entire field of view. The lens exhibits an MTF of 48% at 100 lp/mm.

A quite significant feature of this design is that the linearity error is kept below .05% over the total format. This enables beam angular scan to be accurately linearly translated to pixel spot position on the film.

#### 5.3.2.5 Platen Drive.

The platen drive consists of a lead-screw driven dovetail slide with a one thread per mm pitch lead screw driven by a 200 step/rev. stepper motor, giving a linear motion of .005 mm/step.

Accumulated pitch error of the lead screw is less than .001 in./foot, or .00033 in 4 inches, and the stepper positioning is accurate to  $\pm 3\%$  or .00015 linear travel.

Backlash between the lead screw and travelling nut can be adjusted to zero, but in any case the loading of the lead screw by the slide is always in one direction, so any backlash would have a minimal effect.

Nylatron laminations on the dovetail surfaces provide low friction and long wear. Under normal loading side play may be about .00015 after about 30,000 cycles of operation and an additional .00005 during the next 50,000 cycles. However the unit is mounted so that gravity intimate contact between the slider and the ways in the dovetail "V" so that no side play should occur. Side play translates into a variation in the distance of the platen from the scanning lens which will always be well within the depth of focus.

#### 5.3.2.6 Illumination Source

The illumination source and condensing optics are designed to provide constant viewing screen brightness independent of the projection lens magnification. The screen brightness is sufficient to enable viewing in normal room ambient conditions.

The condensing optics magnification, and position are changed in concert with the projection optics so as to maintain constant illumination of the viewed image area.

The illumination requirement can be calculated based on the known losses throughout the projection path. The optical schematic diagram describes the various elements.

The transmission through the crossed polarizers and the naF crystal in the "on-state" is  $.32 \times .5 \times .82 \times .5 = .0328$ . In addition, the naF transmits approximately 40% of the spectral bandwidth available from the xenon source. Therefore the total transmission through the imaging system is .013.

Viewing under normal room ambient conditions requires a screen brightness of approximately 20 Ft-L, and a screen gain of 2 is adequate for a single viewer at normal reading distance. The 8 x 11" screen size has an area of .6ft<sup>2</sup>. Therefore, the required luminous flux on the screen is

$$F_s = \frac{20 \times .6}{2} = 6 \text{ lumens}$$

To account for the transmission losses, the flux produced by the condensing system is

$$F = \frac{6}{.013} = 462 \text{ lumens.}$$

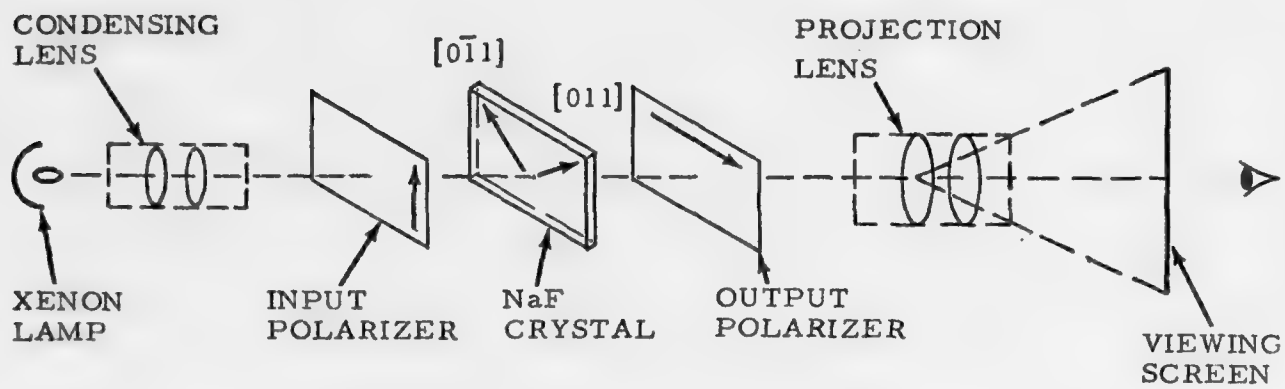
A properly designed xenon lamp and condensing lens will produce 1.5 to 2 lumens output per watt of electrical input.

Assuming a luminous efficiency of 21/w, the lamp power is

$$\frac{462}{2} = 231 \text{ W}$$

#### 5.3.2.7 Projection Lens

A series of projection lenses have been designed to provide a variable range of magnification in equal discrete steps of 2.250 x, 4.304 x, 8.233 x and 15.75 x, while maintaining a fixed relationship between the image plane and object plane.



OPTICAL SCHEMATIC - NaF VIEWING SYSTEM



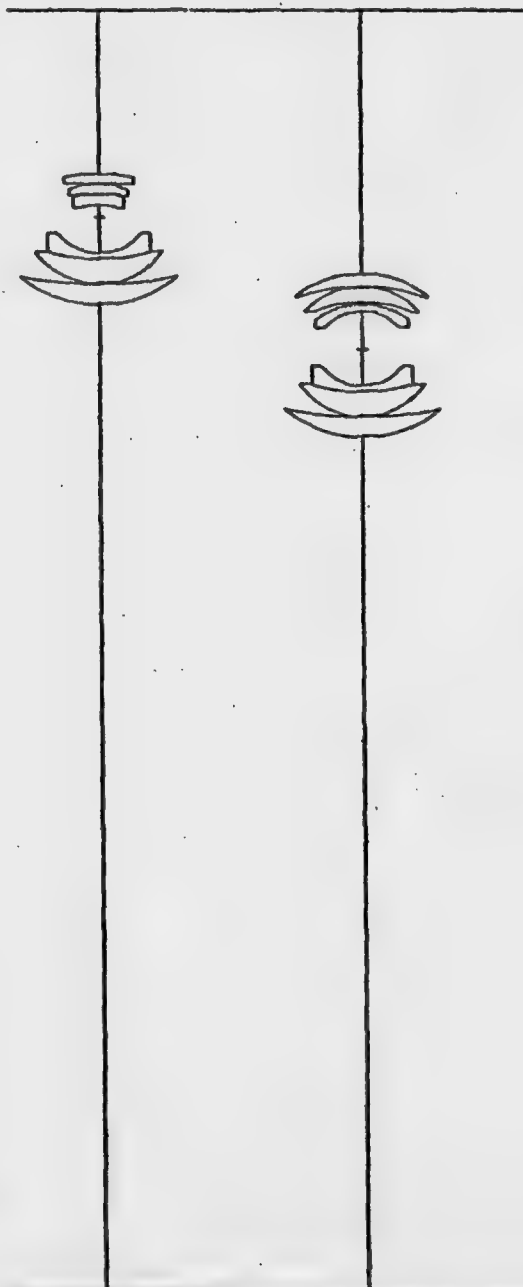
POSITION N. 4  
MAG. = 15.75 X

SCALE 0.50  
11/26/75



POSITION N. 3  
MAG. = 8.233 X

SCALE 0.50  
11/26/75



POSITION N. 2  
MAG. = 4.304 X

SCALE 0.50  
11/26/75

POSITION N. 1  
MAG. = 2.25 X

SCALE 0.50  
11/26/75

o	Magnification	2.250	4.304	8.233	15.75
o	Field of View	$\pm 23.0^\circ$	$\pm 20.4^\circ$	$\pm 18.9^\circ$	$\pm 18.3$
o	Equivalent Local length	4.500	3.157	1.989	1.162
		in			
o	Color correction	Photopic Spectral range, CDF liner			
o	f - number at object	f/7	f/7	f/7	f/5
o	Object to image distance	20.0 in			
o	Transmission	96%			

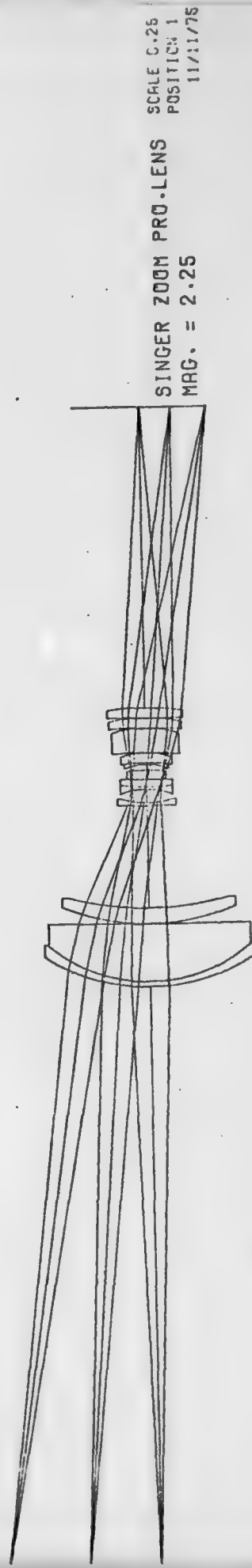
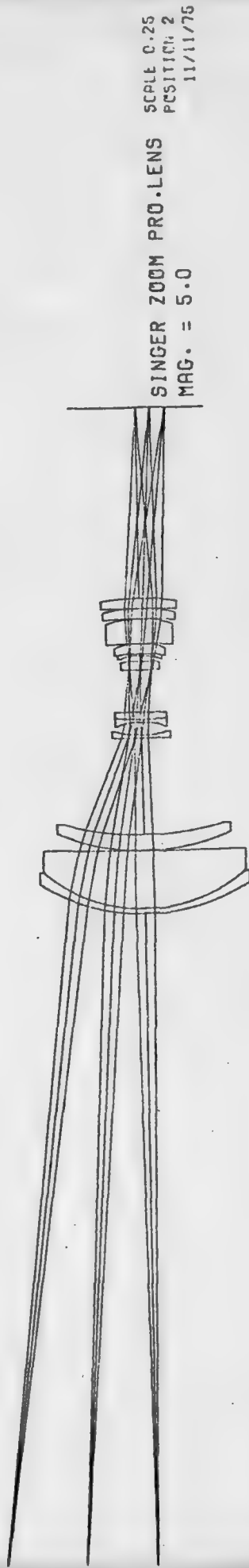
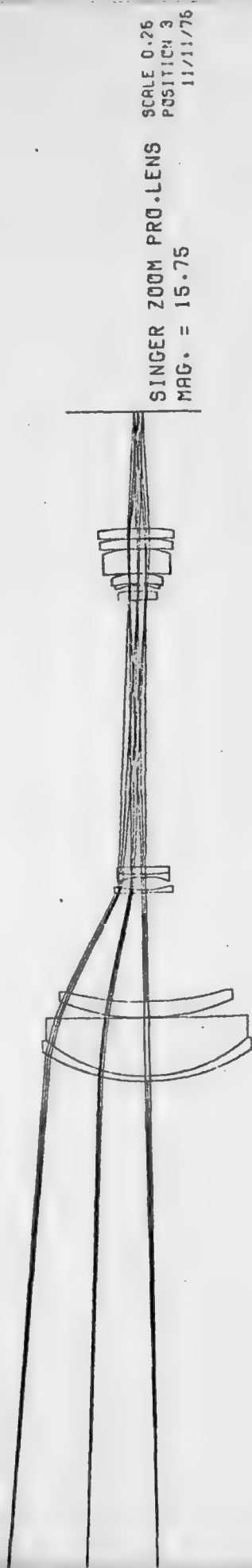
The 6 element projection lenses have been designed to provide a screen resolution adequate to display the smallest object detail in the recording plane at all magnifications. The f/5 lens provides an MTF of 30% at 100 lp/mm at the recording plane. The f/7 lenses provide a limiting resolution of over 100 lp/mm at the recording plane. The projection lenses are all color corrected for use with standard photopic spectral range.

#### 5.3.2.8 Projection Lens - Zoom

A zoom projection lens has been designed as an alternative projection lens for providing a continuously variable projection magnification from 2.250 x to 15.75 x with a fixed image-to-object distance.

- o Magnification - continuously variable 2.250 x to 15.75 x
- o Field of view -  $\pm 23^\circ$  to  $\pm 18^\circ$
- o Equivalent local length range - 12.68 in to 3.938 in  
continuous zoom
- o Color correction - photopic spectral range, CDF lines
- o f - number at object - f/5
- o Object - to - image distance - 50.0 in
- o Transmission - 92%

The 23 elements zoom projection lens has a unique design simplification which uses a fixed spacing between two groups of elements. The spacing of the two fixed groups with respect to the third group is variable with the zoom mechanism. The position of the zoom lens within object-to-image distance is also varied by the zoom mechanism.





#### 5.3.2.9 Multi-lens Turrets

- A. Two turrets are used, one for the condensing optics and the other for the projection optics. Both turrets must have their matching lenses in the appropriate position at the same time, so they are built to operate as a single unit in "X" and "Y". Motor control is by means of a joy stick switching mechanism.
- B. Lens selection is made by blanking all except the active lens in each turret and by moving the active lens to a position at the center of its scanning range.
- C. Translation of a particular portion of the platen format from the field of view of the widest angle lens to a narrower angle lens (small magnification to large) is accomplished by reading the position of the desired format portion in "X" and "Y" from Coordinate Markings on the viewing screen, selecting the desired lens, and moving it to the appropriate X-Y position.
- D. One lead screw driver is used for each turret in "X". Both turrets move together and may be driven by a single motor and timing belt combination or by one stepper motor for each turret, depending upon the ultimate mechanical configuration. Since the "X" positions of each lens are relatively uncritical, some backlash in the screw thread drive can be tolerated, but it can be practically eliminated by traveling nut adjustment.
- E. In order to avoid large cantilever loading of the drive mechanism "Y", 4 head screw driver slides are required; 2 for each turret. All 4 slides are driven by a single motor thru a timing belt or on chain. As in the "X" drive, some backlash can be tolerated but should actually be negligible since the travelling nut can be adjusted and the loading of the nut on the lead screw is unidirectional.

#### 5.4 IMAGE UNIFORMITY CONSIDERATIONS

The uniformity of the imaging on the recording materials is determined by various "image noise" source. The effect of the various noise sources on the resulting imaging is discussed by way of an example calculation based on photographic recording film.

It is specified that the variations of film density for a constant input be no more than 0.02 density units when measured with a square aperture 0.5 to 3.0 mm on a side. Density variation can be the result of any or all of four factors: (1) film granularity and mottle, (2) laser output noise, (3) variations in modulator transfer function, and (4) noise in the analog electronics. Since these sources are uncorrelated, the overall rms density variation will be the square root of the sum of the squares of the individual components. These "noise" sources are discussed in turn.

#### Film Granularity and Mottle

The rms granularity of the 3414, which is the grainier film, is 0.009 density unit when measured with a 48  $\mu\text{m}$  aperture. When this aperture is increased to 500  $\mu\text{m}$ , the granularity scales by the square root of the aperture area to become 0.0009 rms density units.

The film will probably also have a mottle which is a very low spatial frequency density variation. Mottle is dependent on type of film and method of processing, and may vary from lot to lot for the same film type. Kodak will not guarantee that either film will not have more than 0.02 density units of mottle. For the purpose of this analysis, however, the mottle will be assumed to be zero.

For evaluation of the temporal noise sources, the 0.5 to 3.00 mm aperture is equivalent to between 1 and 300 samples of 2.8 to 17 microseconds each. This defines a noise measurement bandwidth that is at most approximately 350 kHz.

#### Laser Noise

The selected laser has an output noise of less than 0.5% rms at 514.5 nm. This noise is the result of plasma variations, mechanical vibration in the resonator, and beats between non-harmonic cavity modes. It is almost entirely within the measurement bandwidth. The resulting rms density variation is  $\gamma \log(1 + 0.5\%)$  where  $\gamma$  refers to the slope of the film characteristic curve. The worst case occurs with the type 3414 film which has a gamma of approximately 2.3. The resultant density variation due to laser noise will then be  $5 \times 10^{-3}$  rms density units.

### Modulator Noise

The only source of short term variations in the modulator is variations in RF oscillator output. The oscillator is a stable crystal oscillator, however, and the balanced mixer that modulates the video onto the carrier is biased in such a way so as to be relatively insensitive to oscillator amplitude. Measurements by Zenith indicate the variations to be less than 1 part in  $10^4$ . The resulting density variations are therefore less than  $\gamma \log (1.0001) = 1.0 \times 10^{-4}$  rms density units.

### Electronic Noise

The noise from operational amplifiers such as the LM118 is approximately  $2 \times 10^{-8}$  V/ $\sqrt{\text{Hz}}$  referenced to the input. Integrated over the measurement bandwidth, this equals  $1.4 \times 10^{-7}$  V. If signal levels in the analog circuitry are approximately 0.1 volt, the noise will be  $10^{-4}$  times the signal. The density variation from this amount of noise is  $\gamma m \log (1 + 10^{-6})$  where  $m$  is slope, on a log scale, of the modulator characteristic. Since the modulator approximates a square law device over the lower half of its range,  $m + 2$ . The resulting variation is  $1.9 \times 10^{-4}$  rms density units. Since there are several electronic noise sources, this number is rounded up to  $5 \times 10^{-4}$  rms density unit.

A comparison of these four noise sources shows that the laser is the most significant noise source and that the density variation will be  $5 \times 10^{-3}$  rms density unit. This variation is considerably less than the allowed peak to peak excursion in density uniformity.

The following factors can limit the repeatability, from run to run, of the grey shades:

- Inconsistency of the film properties
- Variations of processing
- Laser drift
- Non-repeatability of the laser power meter readings.
- Drift of the modulator
- Drift of the exponential correction circuit
- Drift of other electronics

The effect of each component is expressed as  $\Delta D = K \log (1 + q)$  where  $\Delta q$  is variation of each component, and  $K$  equals the film  $\gamma$  for optical components and  $2 \times \gamma$  for electronic components.

The effect of each component is summarized in the following table:

<u>Component</u>	<u>Variation</u>	<u>K</u>	<u><math>\Delta D</math></u>	<u><math>(\Delta D)^2</math></u>
Laser	$\pm 1.0\%$	2.3	$\pm .01$	$\pm 0.0001$
Power Meter	$\pm 1.0\%$	2.3	$\pm .01$	$\pm 0.0001$
Modulator	$\pm 0.5\%$	2.3	$\pm .005$	$\pm 0.000025$
Exponential correction circuit	$\pm 2\%$	4.6	$\pm .04$	$\pm 0.001565$
Other Electronics	$\pm 0.1\%$	4.6	$\pm .002$	$\pm 0.000006$

$$(\text{Total Non-Repeatability})^2 \approx \pm 0.00179$$

## 5.5 RECORDING GRAY LEVEL CONSIDERATIONS

The laser recorder is a highly nonlinear device because of the  $\sin^2$  characteristic of the modulator and the non-linear characteristics of the recording medium. Photodichroic recording material used between crossed polarizers has a  $\sin^2$  transmission characteristic. Real-time recording material such as Dylux film has a linear logarithmic characteristic with a threshold and a saturation region similar to silver halide photographic film. The non-linear transfer characteristics can be linearized by the use of an appropriate non-linear amplifier. A more versatile linearizing element can be made with the combination of a radio-metric look-up table and an exponential circuit.

The radiometric look-up table consists of a programmable RAM which provides an output word for every input word. The input digital word describes the desired grey level on the recording medium. The output word from the look-up table provides the appropriate linearization of the modulator and recording medium transfer characteristics so as to produce at the recording the desired gray level.

An example of a radiometric look-up table to achieve 64 gray levels with Kodak type 3414 recording film is presented to illustrate the principles involved.

If 64 gray shades are to be fit into a density range of approximately 2, the average density step size will be approximately 0.03. Due to restrictions of film granularity and mottle, it is difficult to discriminate shades any closer than this, at least on a microscopic basis. It is therefore necessary to space the shades equally in density, so that the minimum density step is no less than the average value.

This presents a design problem since the output of the D/A converter, which is linear with respect to digital input, passes through a modulator with  $\sin^2(V/V_0)$  response before being recorded on film which is only roughly linear on a logarithmic scale.

Standard procedure in this situation would be to use a digital look-up table and a D/A converter with more than 6 bits, effectively giving 64 voltage increments of varying size such that the resulting density increments are constant. The ratio of voltage step sizes to get constant density steps will be the same as the ratio of density step sizes if the voltage steps are held constant. This ratio of largest to smallest density steps is an upper bound on the multiple of 64 that the resolution of the D/A converter must contain. If step size is equally distributed, i.e., if there are as many big steps as little ones, the required D/A converter size will be half this upper limit.

To determine the required ratio, 1024 equal voltage steps were assumed, and the exposure steps  $\delta \log E$  were calculated as a function of the exposure. This is shown in figure a) on the opposite page. This function was then multiplied by the derivative of the film characteristic curves. These curves may be moved left or right within practical limits by varying the laser power, and are plotted for the required exposure range. The resultant  $\delta D$  curves show the range of density steps for each film. Note that to achieve the desired contrast, the



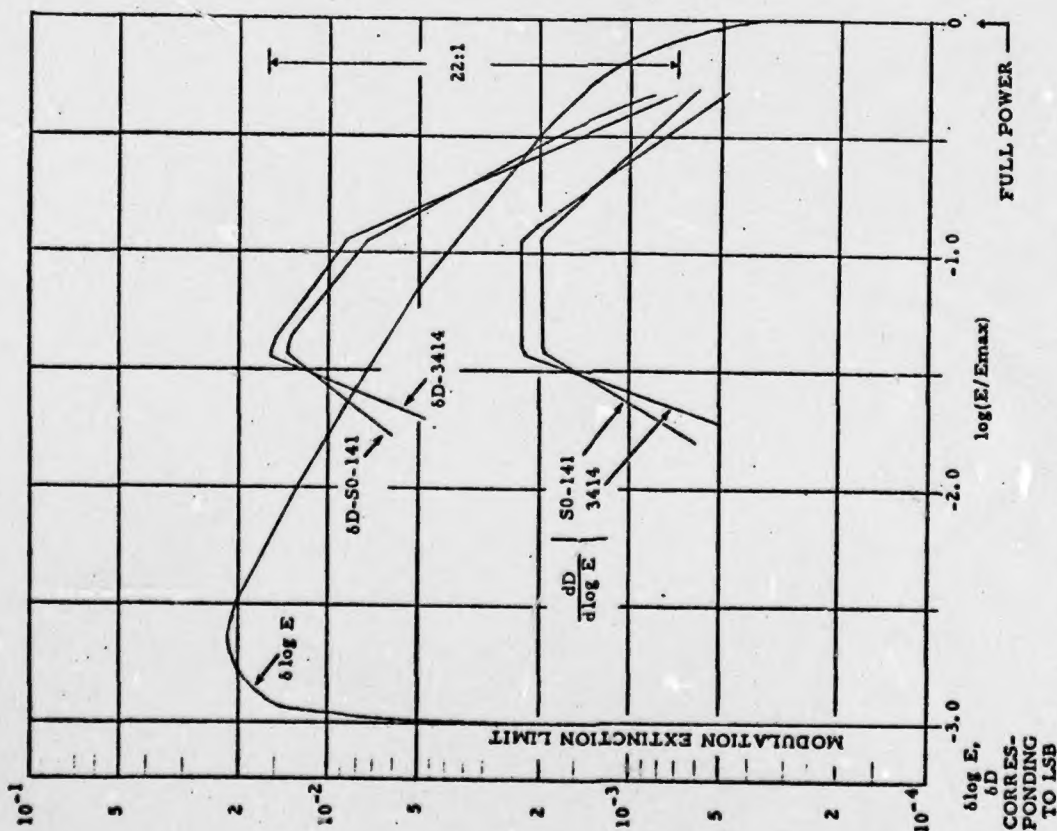
density steps on 3414 film vary by 22 to 1. This correction might be achieved by a 10 bit D/A converter but such a design would be marginal with respect to settling time at the highest video rates.

Higher resolution D/A converters with the required settling times are not known to be commercially available.

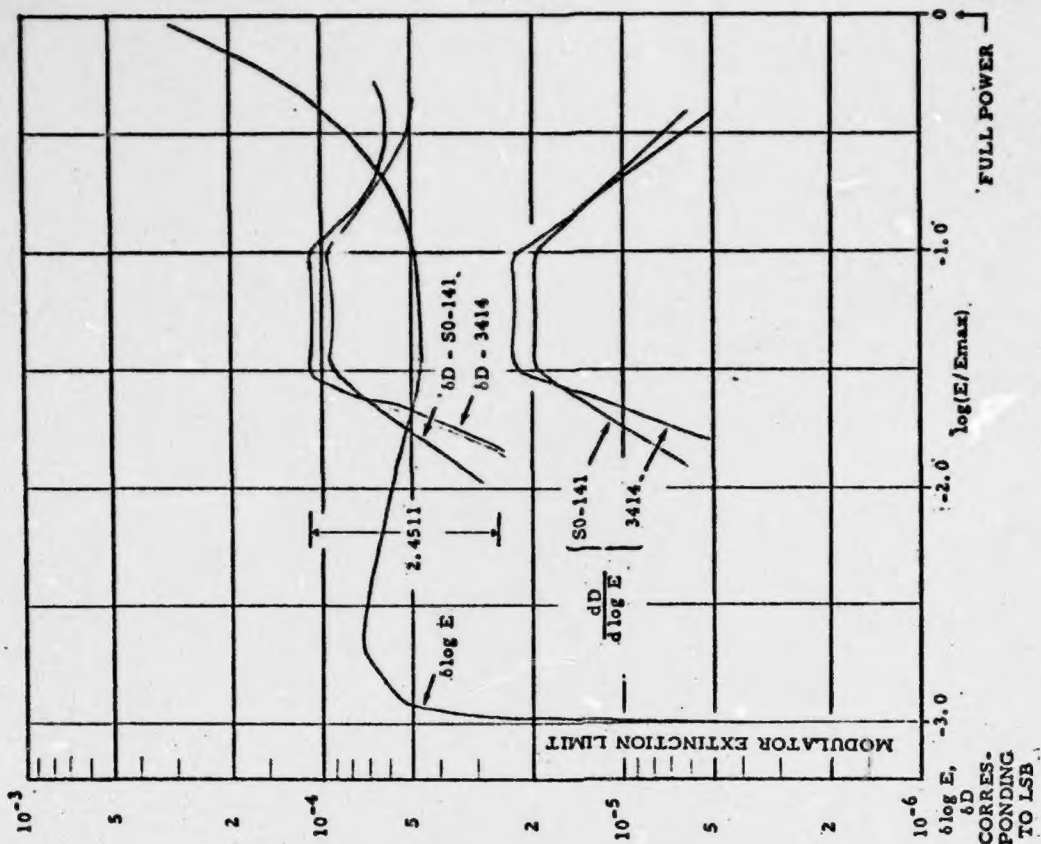
The required resolution of the D/A converter may be substantially reduced if an exponential correction circuit is used between the D/A converter and the modulator. Such a circuit has a transfer function of:

$$V_{out} = A e^{B V_{in}}$$

Figure b) shows the exposure and density step sizes resulting from the use of an exponential correction circuit. In this case the ratio of maximum to minimum step size is only 2.45 to 1. The system may therefore be constructed with an 8-bit look-up table and an 8-bit D/A converter.



a) DENSITY LINEARITY WITHOUT CORRECTION



b) DENSITY LINEARITY WITH EXPONENTIAL CORRECTION CIRCUIT.